

**EVALUATION OF MECHANICAL AND FRACTURE
BEHAVIOUR OF POFA-FA-METAKAOLIN BASED
GEOPOLYMER FIBRE REINFORCED CONCRETE**

IFTEKHAIR IBNUL BASHAR

**FACULTY OF ENGINEERING
UNIVERSITY OF MALAYA
2014**

EVALUATION OF MECHANICAL AND FRACTURE
BEHAVIOUR OF POFA-FA-METAKAOLIN BASED
GEOPOLYMER FIBRE REINFORCED CONCRETE

IFTEKHAIR IBNUL BASHAR

DISSERTATION SUBMITTED IN FULFILMENT OF THE
REQUIREMENT FOR THE DEGREE OF MASTER OF
ENGINEERING SCIENCE

FACULTY OF ENGINEERING
UNIVERSITY OF MALAYA
KUALA LUMPUR

2014

UNIVERSITI MALAYA

ORIGINAL LITERARY WORK DECLARATION

Name of Candidate: IFTEKHAIR IBNUL BASHAR (I.C/Passport No: [REDACTED])

Registration/Matric No: KGA120023

Name of Degree: MASTER OF ENGINEERING SCIENCE

Title of Project Paper/Research Report/Dissertation/Thesis ("this Work"):
EVALUATION OF MECHANICAL AND FRACTURE BEHAVIOUR OF POFA-FA-METAKAOLIN BASED
GEPOLYMER FIBRE REINFORCED CONCRETE

Field of Study: STRUCTURAL ENGINEERING AND MATERIALS

I do solemnly and sincerely declare that:

- (1) I am the sole author/writer of this Work;
- (2) This Work is original;
- (3) Any use of any work in which copyright exists was done by way of fair dealing and for permitted purposes and any excerpt or extract from, or reference to or reproduction of any copyright work has been disclosed expressly and sufficiently and the title of the Work and its authorship have been acknowledged in this Work;
- (4) I do not have any actual knowledge nor do I ought reasonably to know that the making of this work constitutes an infringement of any copyright work;
- (5) I hereby assign all and every rights in the copyright to this Work to the University of Malaya ("UM"), who henceforth shall be owner of the copyright in this Work and that any reproduction or use in any form or by any means whatsoever is prohibited without the written consent of UM having been first had and obtained;
- (6) I am fully aware that if in the course of making this Work I have infringed any copyright whether intentionally or otherwise, I may be subject to legal action or any other action as may be determined by UM.

[REDACTED]

Candidate's Signature

04.09.2014
Date

Subscribed and solemnly declared before,

[REDACTED]

Date 4/Sep/2014

Name: DR. SARAVANAN PICHIAH
Senior Lecturer
Department of Civil Engineering
Faculty of Engineering
University of Malaya
50603 Kuala Lumpur

ABSTRACT

The depletion of natural resources, emission of CO₂ from the cement industries and the waste products from industrial by-products pose irreparable danger to the ecological balance. There have been many attempts to replace ordinary Portland cement (OPC) and the aggregates through the use of industrial by-products and waste materials in recent years.

In Malaysia, the availability of industrial by-products such as palm oil fuel ash (POFA) and fly ash (FA) could be considered as viable binders along with Metakaolin (MK) to develop geopolymer concrete (GC). In addition, other industrial by-products such as manufactured sand (M-sand) and oil palm shell (OPS) could ideally replace the conventional fine and coarse aggregates, respectively.

This dissertation reports the development of POFA-FA-MK-based geopolymer concrete (PFMGC) using M-sand and OPS as fine and coarse aggregates, respectively. The mechanical properties of GC varying different proportion of POFA, FA and MK as binder was investigated. An appropriate mixture design for structural grade PFMGC is also proposed. The effect of steel fibres on the development of mechanical properties and fracture behaviour was investigated for two different aspect ratios (AR 80 and 65) and three different percent of volume as 0.25%, 0.50% and 0.75%. The ratios of M-sand/binder, OPS/ binder, water/ binder and alkaline solution/ binder were kept constant as 1.125, 0.375, 0.18 and 0.4, respectively. The specimens were cured in oven of 65⁰C temperature for 48 hours and then kept in room temperature and relative humidity of 28⁰C and 79%, respectively till the age of testing. The mechanical properties and the fracture behaviour of the fibre-reinforced PFMGC were compared with fibred and non-fibred concrete consisting OPS and crushed granite aggregate.

The results show that the POFA-MK based geopolymer concrete (PMGC) achieved better strength than that of the PFMGC due to presence of the appropriate ratios of Silica/ Alumina, Sodium oxide (and Potassium oxide)/ Silica and Sodium oxide (and Potassium oxide)/ Alumina as 8.73, 0.11 and 0.93, respectively. The corresponding 28-day compressive strengths of concretes having 90% and 80% of POFA with MK as binder were 23.2 and 23.6 MPa, respectively. The highest values of the splitting tensile strength and flexure strength of 2.14 MPa and 3.41 MPa were obtained for the binder consisting 90% of POFA and 10% of MK. The early strength development at the age of 3-day was found above 80% and this is attributed to geopolymerization process at high temperature. The low values of static modulus of elasticity and the Poisson's ratio of 6.36 GPa and 0.176, respectively for PMGC (POFA: MK=90:10) is due to the low stiffness of OPS aggregate. The stress-strain relations of PMGC fit well with the expression developed for OPC concrete. The flexural strength, splitting tensile strength and fracture behaviour were significantly affected by the AR and the volume of steel fibres. The addition of steel fibre with AR of 80 produced higher splitting tensile & flexural strengths and total fracture energy, respectively of 5%, 6% and 50-80% compared to results of the corresponding values with steel fibre with AR of 65.

ABSTRAK

Kekurangan sumber semula jadi, pelepasan CO₂ akibat pengilangan simen dan bahan buangan industri adalah memudaratkan daripada segi keseimbangan ekologi. Banyak percubaan telah dilakukan untuk menggantikan simen Portland biasa (OPC) dan agregat melalui penggunaan bahan buayan sejak kebelakangan ini.

Di Malaysia, kewujudan abu bahan api kelapa sawit (POFA) dan abu terbang (FA) boleh dianggap sebagai pengikat yang berdaya maju bersama-sama dengan metakaolin (MK) untuk membangunkan geopolymer konkrit geopolimer (GC). Di samping itu, bahan buayan industri lain seperti pasir yang dikilong (M- pasir) dan tempurung kelapa sawit (OPS) boleh digunakan untuk menggantikan agregat halus dan halus, masing-masing.

Disertasi ini melaporkan kejian pembangunan konkrit geopolimer penggunaan berasaskan POFA-FA-MK (PFMGC) dengan menggunakan M-sand dan OPS sebagai agregat halus dan kasar, masing-masing. Ciri-ciri mekanikal GC dengan perkadaran bahan pengikat POFA, FA dan MK yang berbeza telah dikaji. Reka bentuk bancuhan yang sesuai untuk mencapai gred struktur PFMGC juga telah dicadangkan. Kesan penggunaan gentian keluli kepada pembangunan sifat-sifat mekanikal dan kelakuan patot telah disiasat untuk dua aspek nisbah yang berbeza (AR 80 dan 65) dan tiga peratuson isipokdu sentian yang berbeza, 0.25%, 0.50% dan 0.75%. Nisbah M-sand/pengikat, OPS / pengikat, air / pengikat dan larutan alkali / pengikat telah dikawal padanisboh 1.125, 0.375, 0.18 dan 0.4 masing-masing. Spesimen telah diawetkan dalam ketuhor pada suhu 65°C selama 48 jam dan kemudian disimpan pada suhu bilik dan kelembapan relatif 28°C dan 79% masing-masing sehingga hari ujian. Sifat-sifat mekanikal dan kelakuan pecah PFMGC bertetulang gentian telah dibandingkan dengan konkrit bertetulang gentian dan torpa sention, yang mengandungi OPS dan agregat granit terhancur.

Keputusan yang didopcti menunjukkan konkrit geopolimer beroskan POFA-MK (PMGC) telah mencapai kekuatan yang lebih tinggi daripada PFMGC akibat daribada nisbah Silika/ Alumina, Natrium oksida (dan Kalium oksida)/ Silika dan Natrium oksida (dan Kalium oksida)/ Alumina yang sesvai sebagai 8.73, 0.11 dan 0.93, masing-masing. Kekuatan mompatan 28 hari yang sepadan bagi konkrit mempunyai 90% dan 80% POFA dengan MK sebagai pengikat adalah 23.2 dan 23.6 MPa, masing-masing . Nilai-nilai tertinggi untuk kekuatan tegangan pecah dan kekuatan lentuan adalah tidak langsung tegangan dan lenturan kekuatan lenturan adalah 2.14 MPa dan 3.41 MPa, masing-masing, yang diperolehi untuk konkrit yang mengadugin 90% POFA dan 10% daripada MK. Pembangunan kekuatan awal pada usia 3 hari didapati melebihi 80% dan ini disebabkan oleh proses pempolimeron-geo pada suhu tinggi. Nilai modulus keanjalan statik dan nisbah Poisson yong rendan, sebanyak 6.36 GPa dan 0.176 masing-masing untuk PMGC (POFA:MK=90:10) adalah disebabkan oleh kekukuhan aggregate OPS rendah. Hubungan tegasan -terikan PMGC juga memafuhi korelasi yong telah dibangunkan untuk konkrit OPC. Kekuatan tegangan lenturan dan tegangan pecah, dan kelakuan patoh juga dipengorul nisbah aspek dan kondung gentian keluli. Penambahan gentian keluli dengan AR 80 menyebobkan kekuatan tegangan pecah dan lentuan donteraga pecah jumlah yang lebih tinggi, masing-masing sebanyak 5% , 6% dan 50-80% berbanding dengan keputusan nilai-nilai yong bersepadanan untuk konkrit dengan gentian keluli dengan AR65.

ACKNOWLEDGEMENT

I would like to thank almighty Allah (swt) for providing me the opportunity to pursue my studies and research work.

I wish to express my sincere thanks and profound appreciation to my supervisors, Dr. Ubagaram Johnson Alengaram and Prof. Ir. Dr. Mohd. Zamin Jumaat for their guidance, encouragement and valuable time spent on the fruitful discussion throughout the work.

I am grateful to the University of Malaya for the financial support through the HIR-MOHE Project UM.C/HIR/MOHE/ENG/02.

I would like to thank the laboratory staffs for their cooperation and assistance.

Finally, I would like to thank the most important people in my life, my parents, sister, wife and son, Abdullah Saaiq Ihtishaam, who have provided their endless support and patience throughout the years.

TABLE OF CONTENTS

Original literary work declaration (English)	ii
Abstract	iii
Abstrak	v
Acknowledgement.....	vii
Table of contents	viii
List of figures	xiii
List of tables.....	xv
List of symbols and abbreviations.....	xvii
List of appendices	xx
CHAPTER 1 Introduction	1
1.1 Background.....	1
1.2 Significance of research work	4
1.3 Aims and objectives.....	4
1.4 Scope.....	5
1.5 Research highlights.....	7
1.6 Structure of the dissertation	7
CHAPTER 2 Literature review	9
2.1 Introduction.....	9
2.2 Geopolymer Technology	9
2.2.1 Geopolymer theory.....	9
2.2.2 Advantages of GC	12
2.3 Pozzolans as source material of geopolymer.....	13
2.3.1 Fly ash (FA)	13
2.3.2 Palm oil fuel ash (POFA)	15
2.3.3 Metakaolin (MK).....	16

2.4	Geopolymer concrete.....	17
2.4.1	Binder proportion	17
2.4.2	Alkaline activator	17
2.4.3	Mechanical vibration.....	18
2.4.4	Heat curing	18
2.4.5	Mechanical properties	19
2.4.6	Toughness.....	20
2.5	Development of geopolymer research.....	22
2.5.1	Invention of first mineral resin.....	22
2.6	Manufactured sand and Quarry dust as fine aggregate.....	23
2.7	Oil palm shell (OPS) as aggregate.....	24
2.8	Previous research works and research gap	25
2.9	Summary.....	25
CHAPTER 3 Materials and Methods.....		27
3.1	Introduction.....	27
3.2	Materials	27
3.2.1	Binding materials (POFA, FA, MK).....	27
3.2.2	Fine aggregates (Conventional mining sand, manufactured sand-M-sand, Quarry Dust-QD).....	28
3.2.3	Coarse aggregates.....	28
3.2.4	Steel fibres.....	29
3.2.5	Water	30
3.2.6	Alkaline solution	30
3.3	Development of geopolymer concrete.....	31
3.3.1	Mixture proportion	31
3.3.2	Casting, specimen preparation, curing and testing age	33

3.4	Testing	36
3.4.1	Fresh concrete tests	36
3.4.2	Mechanical properties of concrete	36
3.4.3	Fracture test	40
3.5	Summary	44
CHAPTER 4 Results and Discussions		45
4.1	Introduction.....	45
4.2	Properties of materials	45
4.2.1	Binding materials	45
4.2.2	Fine aggregates.....	46
4.2.3	Coarse aggregate	49
4.3	Mix Design 1: Effect of molarity, N-sand, M-sand and QD in geopolymer mortar	49
4.3.1	Density	50
4.3.2	Development of compressive strength	51
4.3.3	Failure mode.....	53
4.3.4	Role of POFA-FA on the development of compressive strength.....	54
4.3.5	Effect of particle size of N-sand/ M-sand/QD on geopolymerization	55
4.3.6	Effect of molarity of alkaline activated solution on development of compressive strength	56
4.3.7	Effect of fineness modulus on compressive strength	58
4.3.8	Effect of N-sand, M-Sand and QD on development of compressive strength	59
4.3.9	Comparison of M-sand and QD in geopolymer mortar with published data	63
4.4	Mix Design 2: POFA-FA-MK and POFA-MK based geopolymer concrete	63

4.4.1	Properties of fresh concrete	64
4.4.2	Compressive strength	65
4.4.3	Flexural and indirect tensile strengths	73
4.4.4	Static modulus of elasticity	77
4.5	Mix design 3: Effect of steel fibres on mechanical properties	79
4.5.1	Properties of fresh concrete	79
4.5.2	Compressive strength	80
4.5.3	Flexural strength.....	82
4.5.4	Indirect tensile strength (Splitting tensile test).....	84
4.5.5	Static modulus of elasticity	86
4.6	Mix design 3: Effect of steel fibres on fracture toughness	87
4.6.1	Characteristics of fracture toughness	87
4.6.2	First peak deflection (FPD)	90
4.6.3	Fracture strength.....	91
4.6.4	Fracture toughness.....	93
CHAPTER 5	Conclusion and recommendation.....	95
5.1	Introduction.....	95
5.1.1	Development of appropriate mix proportion (objective 1)	95
5.1.2	Investigation on the mechanical properties of OPSGC (objective 2)	97
5.1.3	Investigation of Mechanical properties of FOPSGC and FNWGC (Objective 3).....	99
5.1.4	Investigation of fracture behaviour of FOPSGC (objective 4)	100
5.2	Recommendation for future work.....	101
	References	102
	List of publications.....	112
	Journal articles	112

Conference papers	112
Appendix A	113
Calculation of Alkaline solution	113
Calculation for Mix design 1.....	114
Calculation for Mix design 2.....	115
Calculation for Mix design 3.....	118
Appendix B	120

LIST OF FIGURES

Figure 2.1: Computer molecular graphics of polymeric $M_n(-Si-O-Al-O-)$ poly(silicate) and $M_n(-Si-O-Al-O-Si-O-)_n$ poly(sialate-siloxo), and related frameworks (Davidovits, 1994b).....	10
Figure 2.2: Chemical structures of geopolymer	11
Figure 2.3: Typical detail of processing of Palm oil fuel ash in industry	16
Figure 2.4: Compressive and flexural strength gain of geopolymers (Duxson et al., 2005)	19
Figure 3.1: Collection of POFA	28
Figure 3.2: Collection of OPS	29
Figure 3.3: Steel fibres of AR 80(above) & 65(below)	30
Figure 3.4: Casting of geopolymer fibre reinforced concrete	34
Figure 3.5: Preparation of specimens	35
Figure 3.6: ELE testing machine of capacity 2000 kN	36
Figure 3.7: Flexural strength test (BS EN 12390-5:2009, 2009).....	37
Figure 3.8: Indirect tensile strength	38
Figure 3.9: Static modulus of elasticity test.....	39
Figure 3.10: Fracture test (ASTM C1609/C1609M-12, 2012)	41
Figure 3.11: Specimens for fracture test	41
Figure 4.1: Particle size distribution of POFA, FA and MK	46
Figure 4.2: Particle shape of manufactured sand (2.36 mm retained)	47
Figure 4.3: Particle shape of quarry dust (2.36 mm retained).....	47
Figure 4.4: Particle size distribution curve for N-sand, M-sand and QD	48
Figure 4.5: Density vs age (days).....	50
Figure 4.6: Relationship between density and compressive strength at different ages...	51
Figure 4.7: Compressive strengths for different mix design.....	53

Figure 4.8: Satisfactory failures (BS EN 12390-3:2009 (2009)).....	53
Figure 4.9: Failure mode of geopolymer mortar.....	54
Figure 4.10: Effect of molarity of alkaline activated solution in compressive strength .	57
Figure 4.11: Development of early age compressive strength.....	57
Figure 4.12: Effect of fineness modulus of composite fine aggregates in development of compressive strength	58
Figure 4.13: Compressive strength (MPa) vs age (days).....	59
Figure 4.14: % Compressive strength development vs age (days)	60
Figure 4.15: N-sand/ M-sand/ QD interlocking in geopolymer mortar (Magnification rate = 5)	61
Figure 4.16: Compressive strength of GC for different mix proportions of (a) POFA, FA & MK and (b) POFA & MK.....	66
Figure 4.17: Compressive strength at age of 3-, 7-, 14- and 28-day.....	67
Figure 4.18: Relationship between compressive strength and oxide compounds.....	72
Figure 4.19: Bond failure of OPSGC.....	74
Figure 4.20: Relationship between $\text{SiO}_2/\text{Al}_2\text{O}_3$ and mechanical properties (f'_c, f'_t, f'_f)..	74
Figure 4.21: Numerical relationship among f_{cube}, f_f and f_t	75
Figure 4.22: Numerical relationship among f_{cube}, E and Poisson's ratio.....	77
Figure 4.23: 28-day compressive strength	81
Figure 4.24: Development of flexural strength for different % volume of steel fibre	84
Figure 4.25: Development of flexural strength for different % volume of steel fibre	85
Figure 4.26: Development of MoE for different % volume of steel fibre	86
Figure 4.27: Fracture failure	88
Figure 4.28: First peak deflection for all mix designs	90
Figure 4.29: First peak load and strength.....	91
Figure 4.30: Residual load and strength.....	92

Figure 4.31: Toughness and equivalent flexural strength ratio.....	93
--	----

LIST OF TABLES

Table 1.1: Mix proportion of N-sand, M-sand and QD in POFA-FA based geopolymer mortar	6
Table 1.2: Mix proportion of POFA, FA and MK	6
Table 1.3: Mix proportion of POFA, FA and MK	7
Table 2.1: Range of chemical composition for low and high-calcium fly ashes (BS EN 450-1:2012)	14
Table 2.2: Phase composition of UK fly ashes Dhir (1986)	15
Table 2.3: The principle phases found in coals and the phases formed after combustion	15
Table 2.4: Chemical composition of POFA Mijarsh et al. (2014)	16
Table 0.1: Previous research work and research gap	26
Table 3.1: Mix design with variables of N-sand, M-sand and QD	32
Table 3.2: Mix design with variables of POFA, FA and MK	32
Table 3.3: Mix design with variables of steel fibre proportion and aspect ratio.....	33
Table 3.4: Specimens for testing of concrete	34
Table 4.1: Chemical composition and physical properties of POFA and FA	45
Table 4.2: Particle size distribution of N-sand, M-sand and QD	48
Table 4.3: Specific gravity and absorption of N-sand, M-sand and QD	49
Table 4.4: Physical properties of coarse aggregate	49
Table 4.5: Development of compressive strength for different mix designs	52
Table 4.6: Percentage of increment of compressive strength	55
Table 4.7: Categorization of fineness of sand, using fineness modulus (Alexander and Mindess, 2005)	59
Table 4.8: Development of compressive strength using N-sand, M-sand and QD	63

Table 4.9: Fresh density and slump value of fresh concrete	64
Table 4.10: Effect of heat curing temperature and time on compressive strength.....	69
Table 4.11: Compressive strength of geopolymer concrete using alkaline activator	70
Table 4.12: Compressive strength (Mix design 2).....	71
Table 4.13: Estimated chemical composition in mix proportions.....	71
Table 4.14: Indirect tensile and flexural strength.....	76
Table 4.15: Young's modulus of elasticity and Poisson's ratio.....	78
Table 4.16: Density (kg/m ³) of FOPSGC and FGGC	80
Table 4.17: Compressive strength.....	81
Table 4.18: Flexural strength	83
Table 4.19: Indirect tensile strength (Mix design 3).....	85
Table 4.20: Modulus of elasticity	86
Table 4.21: Fracture characteristics for different mix designs.....	89

LIST OF SYMBOLS AND ABBREVIATIONS

Symbols Description

AA	Alkaline activator
AIV	Aggregate impact value
AR	Aspect ratio
B	Binder
C_c	Coefficient of curvature
C_u	Uniformity coefficient
E	Young's modulus of elasticity (GPa)
f'_c	Compressive strength (MPa) of mortar
f_{cu}	Cube compressive strength (MPa)
f_{cy}	Cylinder compressive strength (MPa)
f_t	Indirect tensile strength (MPa)
f_f	Flexure strength (MPa)
FA	Fly ash
FM	Fineness modulus
FNWGC	Fibre reinforced normal weight geopolymer concrete
FOPSGC	Fibre reinforced oil palm shell based geopolymer concrete
FPD	First peak deflection

MK	Metakaolin
M-sand	Manufactured sand
M ₂ O	Na ₂ O (Sodium oxide) or K ₂ O (Potassium oxide) or combination of Na ₂ O and K ₂ O
NWGC	Normal weight geopolymer concrete
N-sand	Mining sand
NWC	Normal weight concrete
OD	Oven dry
OPS	Oil palm shell
OPSGC	Oil palm shell based geopolymer concrete
PFMGC	POFA-FA-MK based OPSGC
POFA	Palm oil fuel ash
PMGC	POFA-MK based OPSGC
QD	Quarry dust
S/A	Silica/ alumina ratio
SD	Standard deviation
SH	Sodium hydroxide
<u>SH</u>	Molarity of sodium hydroxide solution
SS	Sodium silicate

SSD Saturated surface dry

ρ Density (kg/m^3)

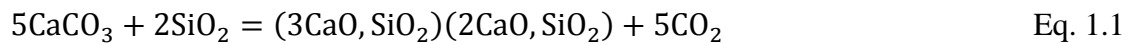
LIST OF APPENDICES

Appendix A	113
Calculation of Alkaline solution	113
Calculation for Mix design 1	114
Calculation for Mix design 2	115
Calculation for Mix design 3	118
Appendix B	120

CHAPTER 1 INTRODUCTION

1.1 Background

The use of ordinary Portland cement (OPC) in concrete as binder and its associated issues in greenhouse gas emissions is well established. The amount of the carbon dioxide (CO₂) released during the manufacture of OPC is mainly due to the calcination of limestone and combustion of fossil fuel. Eq. 1.1 shows the reaction of the constituent materials in cement production and the result of CO₂ emission. The production of 1 tonne of cement directly generates 0.55 tonnes of chemical CO₂ and requires the combustion of carbon fuel to yield an additional 0.4 tonnes of CO₂. In other words, the production of 1 tonne of cement emits 1 tonne of CO₂.



Thus, the enormous amount of CO₂ from cement industry contributes to global warming. Nevertheless, the demand for concrete is on the rise, 11 billion metric tonnes of concrete (Mehta and Monteiro, 2006) is being produced annually, and this leads to exploitation of natural resources. The depletion of natural reserves in alarming phase drew attention of the whole world and the construction industry along with researchers are engaged in research to find alternate materials to replace OPC. There have been research works on the use of alkaline activated materials (Žvironaitė et al., 2012; Noorvand et al., 2013; Tan and Du, 2013; Venkatanarayanan and Rangaraju, 2013; Yusuf et al., 2014) to address some of the issues related to cement industry.

Davidovits (2008) revealed that the geopolymers could be ideal alternate to OPC as in geopolymers the polymeric reaction between silica and alumina could be exploited through the use of alkaline activators. The binder can be produced by a polymeric synthesis of the alkali-activated material from geological origin or by-product materials.

The alkalinity of the activator can be low to mild or high. The main contents to be activated are the silicon and the aluminium present in the by-product material (Palomo et al., 1999). The materials that contain silica and alumina are called pozzolanic materials.

Many researchers (Hussin and Awal, 1996; Awal and Hussin, 1997; Rukzon and Chindapasirt, 2009) reported that fly ash (FA), rice husk ash (RHA) and palm oil fuel ash (POFA) have a potentiality of being pozzolanic material. The abundance and availability of pozzolanic industrial by-product such as POFA, FA and RHA, in the South-East Asia, has created an ideal platform for the researchers to work on this pozzolanic material as source material in the development of geopolymer concrete (GC). Several research publications are available in GC using FA, MK, GGBS and RHA (Autef et al., 2013b; Li et al., 2013; Yost et al., 2013; Yusuf et al., 2013; Abdulkareem et al., 2014); However, research works on POFA-based geopolymer concrete is limited and the incorporation of FA and MK along with POFA is another avenue for research.

Besides the environmental pollution due to the production of cement, consumption of large quantity of concrete leads to depletion of natural resources. Many countries face the shortage of conventional river sand/ mining sand and crushed granite aggregates for fine and coarse aggregates, respectively. The exploitation of the conventional sand and quarrying of rock deposits leads to ecological imbalance globally and its effect has been felt in the construction industry more than any other field. Millions of tons of industrial wastes are generated every year and these wastes cause environmental issue due to shortage of storage facility; this subsequently leads to land and water pollution near factories. In order to ensure sustainable development, researchers all around the world have focused their research on replacing and recycling waste materials to replace conventional materials (Rukzon and Chindapasirt, 2009; Safiuddin et al., 2011a; Safiuddin et al., 2011b; Alengaram et al., 2013a).

Balamurugan and Perumal (2013), Ji et al. (2013) and Raman et al. (2011) reported the potentiality of using quarry fines as a replacement of river/ mining sand. The quarry industries produce millions of tons of wastes in the form of quarry dust (QD); it is produced as waste after crushing granite for the use of coarse aggregates. About 25% QD is produced from the coarse aggregate production by stone crusher (Appukutty and Murugesan, 2009). These wastes are dumped in the factory yards and hence reuse of QD might help in reducing the overuse of mining and quarrying. The sophisticated technology known as Vertical Shaft Impact Crusher System (VSI) allows QD to be centrifuged to remove flaky and sharp edges of QD. The end product is commonly known as manufactured sand (M-Sand) and it is popular in some of the developing countries (Westerholm et al., 2008); the use of M-sand and QD are one of the right direction to achieve sustainable material.

Apart from the use of M-sand to replace conventional sand, another potential local waste from palm oil industry is oil palm shell (OPS). Researchers (Liu et al., 2014; Yap et al., 2014) explored the suitability of OPS as lightweight aggregate and found structural grade lightweight concrete could be produced using OPS as coarse aggregate. During the last three decades, many research works have been carried out using OPS in OPC concrete as lightweight aggregate to replace conventional granite aggregate (Okpala, 1990; Abdullah, 1996; Alengaram et al., 2008; Alengaram et al., 2011a; Alengaram et al., 2013b; Liu et al., 2014; Mo et al., 2014b); Yap et al. (2014) reported the possibility of significant cost saving production of OPS based concrete.

According to ACI 213R-14 (2014), the minimum cylinder compressive strength of structural lightweight concrete is 17.24 MPa (estimated cube compressive strength 21.55 MPa). This research work focusses on the utilization of POFA, FA and MK as a binding material in OPS based geopolymer concrete (OPSGC) of strength 22 MPa. The optimum content of POFA in the development of OPSGC is also being explored in this research.

The investigation on the mechanical properties and fracture behaviour of the hardened OPSGC with and without steel fibres is also carried out and reported.

1.2 Significance of research work

The significance of this research work is due to the usage of 90% of POFA by weight in the structural grade lightweight geopolymer concrete. Though research works on the geopolymer concrete using few other pozzolanic material such as FA, MK and rice husk ash as a binding element have been done, the utilization of POFA in a large volume in geopolymer concrete was investigated for the first time.

The emphasis on POFA is given because of the abundant production of POFA as an industrial by-product in Malaysia, Australia, Thailand and few other countries. The utilization of the POFA in the construction industry will eliminate the problem involving the storage of waste materials. Further, this geopolymer concrete will keep significant effect in the reduction of greenhouse effect.

The fracture analysis of geopolymer concrete incorporating steel fibres has been carried out in this research work. No previous research work was found as published in any journal article on the fracture behaviour of geopolymer concrete. Therefore, this research work could claim its novelty on the analysis of fracture behaviour and utilization of large volume of POFA in geopolymer lightweight concrete.

1.3 Aims and objectives

The main objective of this research work is to utilize local waste materials to develop sustainable structural geopolymer concrete (GC) of grade 20. The variables include different binder and fine aggregate contents; the effect of oil palm shell (OPS) as coarse aggregate in GC is also investigated. In addition, the use of steel fibres in the concrete to

enhance its fracture energy and toughness was investigated. The objectives of the research could be listed as given below:

- (1) To develop an appropriate mixture design for lightweight structural grade (Cube compressive strength 20MPa) POFA-FA-MK based oil palm shell geopolymer concrete (OPSGC).
- (2) To investigate the hardened properties of OPSGC through the measures of compressive strength, flexural strength, splitting tensile strength, static modulus of elasticity and the Poisson's ratio.
- (3) To analyse the effect of steel fibres in the mechanical properties of OPSGC.
- (4) To examine the fracture behaviour of fibre reinforced OPSGC.

1.4 Scope

The scope of the research work is set out based on the objectives of the research and is given under four different aspects namely, materials characterization, variable of mining sand, manufactured sand and quarry dust, binder variation and addition of fibre in the mixes. The different tests conducted in the investigation are given along with the variables in tabular form.

Manufactured sand (M-sand) and quarry dust (QD) to be used in proportion as replacement of mining sand (N-sand) to investigate the effect in POFA-FA-based geopolymer mortar (Table 1.1).

Table 1.1: Mix proportion of N-sand, M-sand and QD in POFA-FA based geopolymer mortar

Variables (% by weight)			Constants	Tests
Fine aggregate			Binder : Fine aggregate = 1 : 1.5 POFA : FA = 1 : 1 Water / Binder = 0.2 Alkaline activator / Binder = 0.4 Molarity of NaOH solution = 12 & 14 NaOH solution : liquid Na ₂ SiO ₃ = 1 : 2.5 Curing temperature 65°C Curing period 24 hours	Fresh and harden density Compressive strength test (3-, 7-, 14- and 28-day)
N-sand	M-sand	QD		
100				
75	25			
25	75			
	100			
	75	25		
	25	75		
		100		
25		75		
75		25		
25	25	50		
25	50	25		
50	25	25		

(b) POFA, FA and MK to be used in proportion for the development of GC of grade 20 (Table 1.2). Since 100% POFA contains very less proportion of alumina, POFA is required to use with another pozzolanic material of high alumina contents. Maximum 90% of POFA was used as binder to develop OPSGC of grade 20.

Table 1.2: Mix proportion of POFA, FA and MK

Variables (% by weight)			Constants	Tests
Binder			Binder : M-sand : OPS = 1 : 1.125 : 0.375 Water / Binder = 0.18 Alkaline activator / Binder = 0.4 Molarity of NaOH solution = 14 NaOH solution : liquid Na ₂ SiO ₃ = 1 : 2.5 Curing temperature 650C Curing period 48 hours	Fresh and harden density Slump test UPV test Compressive strength test (3-, 7-, 14- and 28-day) Flexure test Indirect tensile strength test (Splitting test) Static modulus of elasticity
POFA	FA	MK		
10	85	5		
10	80	10		
10	75	15		
10	70	20		
10	65	25		
90		10		
80		20		
70		30		
60		40		

(c) Effect of steel fibres to be investigated for two aspect ratio with % volume of 0.25, 0.50 and 0.75.

Table 1.3: Mix proportion of POFA, FA and MK

Variables (% by volume)		Constants		Tests
Steel fibres		OPS concrete	Gravel concrete	Fresh and harden density Slump test UPV test Compressive strength test (3-, 7-, 14- and 28-day) Flexure test Indirect tensile strength test (Splitting test) Static modulus of elasticity Fracture test
A.R. = 80	A.R. = 65	Binder:M-sand:OPS		
OPS concrete		1:1.125:0.375	1:0.66:1.33	
0	0	Water / Binder		
0.25		0.11	0.2	
	0.25	Alkaline activator / Binder		
0.50		0.5	0.4	
	0.50	Molarity of NaOH solution = 14		
0.75		NaOH solution : liquid Na ₂ SiO ₃ = 1 : 2.5		
	0.75			
Gravel concrete (control)		Curing temperature 65°C Curing period 48 hours		
0.50				
	0.50			

(d) Material properties to determine to understand the effect of the properties on strength development

POFA, FA, MK	N-sand, M-sand, QD	OPS, Gravel
Specific gravity Particle size distribution XRF test	Particle size distribution Specific gravity Water absorption	Specific gravity Aggregate crushing value Water absorption

1.5 Research highlights

The research highlights could be addressed as follow:

- Up to 90% POFA (by weight) used in the geopolymer concrete.
- All waste materials were used in concrete, such as POFA, FA and MK for binding material and M-sand and OPS as fine and coarse aggregates, respectively.

1.6 Structure of the dissertation

The remainder of the thesis is arranged as follow: Chapter 2 describes the need to find alternatives to make concrete more environmentally friendly, and the availability and the potential use of POFA, FA, MK as binder and M-sand and OPS as fine and coarse

aggregates respectively. This chapter also provides a brief literature review of geopolymer technology.

Chapter 3 describes the experimental program carried out to develop the mixture proportions, the mixing process, and the curing regime of OPSGC and the tests performed to study the engineering properties of the fresh and hardened concrete as well as the fracture behaviour of the hardened concrete.

Chapter 4 presents and discusses the test results. Chapter 5 states the summary and the conclusions of this study, followed by a set of recommendations for future work. The thesis ends with a Reference List and several Appendices.

CHAPTER 2 LITERATURE REVIEW

2.1 Introduction

Energy conservation and protection of environment has become a main concern to the researchers and engineers in the current age and this has led to exploration of alternatives to customary building materials. The challenge to reduction of greenhouse gas emissions and minimize the energy required for materials assert the researchers to find out new material. The conventional construction binding material Ordinary Portland cement (OPC) leads to fulfil the demand of over one and half billion tons annually which is energy intensive and is liable for releasing a significant volume of carbon dioxide (CO₂) to atmosphere (Sumajouw et al., 2004).

The estimation shows that one ton of OPC produces one ton of CO₂ and the production process also involves high temperature, destruction of quarries and emission of CO₂ (Fernandez-Jimenez et al., 2006). Besides on the environmental impact, the costs associated with these energy involved, are significant. This lead to further investigation on new environment friendly binding material. Geopolymer technology is one of them.

2.2 Geopolymer Technology

2.2.1 Geopolymer theory

Geopolymer is a term covering a class of synthetic aluminosilicate materials with potential use in a number of areas, essentially, as a replacement for Portland cement and for advanced high-tech composites, ceramic applications or as a form of cast stone. The name Geopolymer was first applied to these materials by Davidovits (2008) in 1972. The properties and uses of geopolymers are being explored in many scientific and industrial disciplines and in all types of engineering process technologies.

For the chemical designation of geopolymers based on silico-aluminates, poly(silicate) was suggested by (Davidovits, 1994b). Silicate is an abbreviation for silicon-oxo-aluminate. The silicate network consists of SiO_4 and AlO_4 tetrahedra linked alternately by sharing all the oxygens. Positive ions (Na^+ , K^+ , Li^+ , Ca^{++} , Ba^{++} , NH_4^+ , H_3O^+) must be present in the framework cavities to balance the negative charge of Al^{3+} in IV-fold coordination. Poly (silicates) have the following empirical formula (Eq. 2.1).

$$M_n[-(\text{SiO}_2)_z\text{e} - \text{AlO}_2]_n, w\text{H}_2\text{O} \quad \text{Eq. 2.1}$$

Wherein M is a cation such as potassium, sodium or calcium, and “n” is a degree of polycondensation; “z” is 1, 2, 3 (Davidovits, 1979). Poly(silicates) are chain and ring polymers with Si^{4+} and Al^{3+} in IV-fold coordination with oxygen and range from amorphous to semi-crystalline. Some related frameworks are displayed in Figure 2.1.

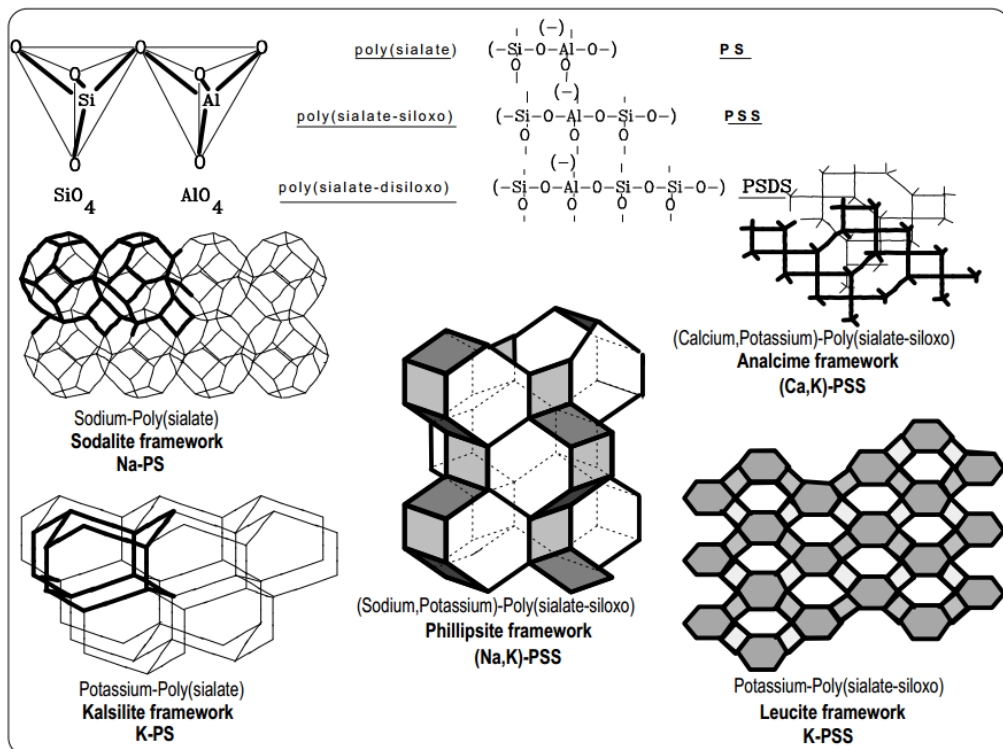


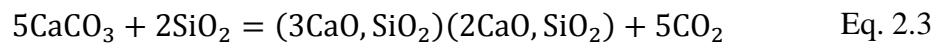
Figure 2.1: Computer molecular graphics of polymeric $M_n(-\text{Si}-\text{O}-\text{Al}-\text{O}-)$ poly(silicate) and $M_n(-\text{Si}-\text{O}-\text{Al}-\text{O}-\text{Si}-\text{O}-)_n$ poly(sialate-siloxo), and related frameworks (Davidovits, 1994b)

Therefore, geopolymers are sometimes referred to as alkali-activate alumina silicate binders (Davidovits, 1994a; Palomo et al., 1999; Roy, 1999; Van Jaarsveld et al., 2002).

Geopolymers can also be made from sources of pozzolanic materials, such as lava or fly ash from coal. Most studies on geopolymers have been carried out using natural or industrial waste sources of metakaolin and other aluminosilicates. Industrial and high-tech applications rely on more expensive and sophisticated siliceous raw materials.

2.2.2 Advantages of GC

In many sense, geopolymer concrete is considered the better solution of Portland cement concrete. Ordinary Portland cement (OPC) results from the calcination of limestones (calcium carbonate) and silica according to the following reaction (Eq. 2.3).



The production of 1 tonne of cement directly generates 0.55 tonnes of chemical CO₂ and requires the combustion of carbon fuel to yield an additional 0.4 tonnes of CO₂. Simply, 1T of Cement = 1T of CO₂.

The elastic properties of hardened geopolymer concrete and the behaviour and strength of reinforced geopolymer concrete structural members are similar to those found in OPC. Therefore, design standards and provisions are similar.

OPC is not fire resistant. It explodes above 300⁰C causing destruction of concrete structures. Geopolymer concrete is a good fire resistant material. It can resist upto 1200⁰C temperature.

2.3 Pozzolans as source material of geopolymer

The pozzolan is a material consisting siliceous or aluminous and silicious material (ASTM C125 - 13b, 2013) and reacts chemically with lime at ordinary temperature in presence of moisture and forms strong-slow-hardening cement. Due to the presence of silica and alumina in pozzolanic material, it is used as a raw material in the geopolymer product (Khale and Chaudhary, 2007).

In the earlier age, the term pozzolana was associated with the naturally formed volcanic ash and calcined earths. Presently, this term covers all silicious and aluminous materials. Pozzolanic material like fly ash (FA), palm oil fuel ash (POFA) and metakaolin (MK) are common in using as a replacement material in cement industry due to its reactivity with calcium hydroxide (CH) which helps in the improvement of durability of concrete (Sabir et al., 2001). The geopolymer technology may apply using this pozzolanic material for a complete replacement of OPC. The source and properties of such well-known pozzolanic material like FA, POFA and MK are reviewed in following clauses.

2.3.1 Fly ash (FA)

Fly ash is produced by the combustion of finely ground coal injected at high speed with a stream of hot air into the furnace at electricity generating power plants. On entry into the boiler, where the temperatures are usually around 1500⁰C, the coal in suspension is burnt instantaneously. The remaining matter present in the coal, such as shales and clays (essentially consisting of silica, alumina and iron oxide), melts whilst in suspension, and then on rapid cooling, as they are carried out by the flue gases, solidifies into fine spherical particles.

About 80% of the coal ash is eventually carried out of the boiler with the flue gases. It must be removed before the flue gases are discharged to the atmosphere. This is the

material, which is called pulverized fuel ash and more commonly fly ash. The remainder of the coal ash falls to the bottom of the furnace where it sinters to form a coarser material called bottom ash (Davidovits, 2008).

Fly ash is divided into two distinct categories:

Class F Low-calcium fly ash: CaO content is less than 10%. This class of fly ash is usually produced from anthracite and bituminous coals (ASTM C618-12a, 2012).

Class C High-calcium fly ash: CaO content is greater than 10%. This type of fly ash is usually produced from sub-bituminous and lignite coals (ASTM C618-12a, 2012). An indication of the composition in oxide values for both low and high-lime is given in Table 2.1: Range of chemical composition for low and high-calcium fly ashes Table 2.1.

Table 2.1: Range of chemical composition for low and high-calcium fly ashes (BS EN 450-1:2012)

	Class F %	Class C Lignite based %
SiO ₂	47.2 to 54	18 to 24.8
Al ₂ O ₃	27.7 to 34.9	12.1 to 14.9
Fe ₂ O ₃	3.6 to 11.5	6.3 to 7.8
CaO	1.3 to 4.1	13.9 to 49
Free lime content	0.11	18 to 25
MgO	1.4 to 2.5	19 to 2.8
SO ₃	0.1 to 0.9	5.5 to 9.1
Na ₂ O	0.2 to 1.6	0.5 to 2
K ₂ O	0.7 to 5.7	1 to 3
Jarrige (1971)		

The fly ash spheres are made of amorphous (glass) and crystalline elements, mostly mullite, haematite, magnetite, quartz and unburned carbon residue.

Table 2.2: Phase composition of UK fly ashes Dhir (1986)

Phase	Mean %	Min %	Max %
Amorphous	59	30	78
Mullite	19	7	46
Haematite	7	2	15
Magnetite	6	2	10
Quartz	5	1	12
Carbon	4	1	13

It appears that the reactivity of the fly ash depends upon the nature and proportion of the glass phase present, which in turn, for a given type and source of coal, is generally determined by the operating temperatures within the boiler (Davidovits, 2008).

Table 2.3: The principle phases found in coals and the phases formed after combustion

Common coal minerals	Phases formed after combustion		
	850 ⁰ C	1500 ⁰ C	1800 ⁰ C
Quartz	Quartz	Cristobalite	Glass
Kaolinite	Metakaolin	Glass + Mullite	Glass
Illite	Illite	Glass + Mullite	Glass
Pyrite FeS ₂	FeS/ FeO	Fe ₂ O ₃ haematite + glass	Glass
Calcite	Lime CaO	Glass	glass
Davidovits (2008)			

It seems that the chemical reactivity depends on the glass content, glass composition and the physical state of the glass (Davidovits, 2008).

2.3.2 Palm oil fuel ash (POFA)

Palm Oil Fuel Ash (POFA) is generally produced in mills due to usage of palm oil shell and fibres as fuel. In practice, POFA produced in Malaysian palm oil mill is dumped as waste without any profitable return (Sumadi and Hussin, 1995). Since Malaysia produces palm oil as a source of national income and the cultivation of palm oil extracted on regular basis and the wastes are burnt more POFA is being produced; hence the utilization of POFA would lead to sustainable development as the storage of POFA in the vicinity of the factories cause land and environmental pollution.

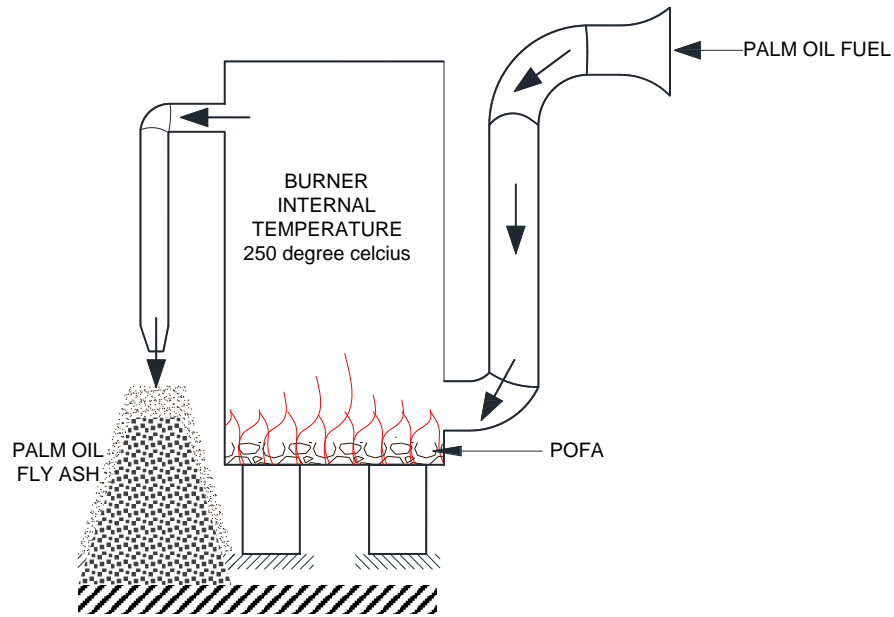


Figure 2.3: Typical detail of processing of Palm oil fuel ash in industry

Mijarsh et al. (2014) reported the chemical composition of POFA as shown in Table 2.4.

Table 2.4: Chemical composition of POFA Mijarsh et al. (2014)

Oxide form	weight (%)	Oxide form	% weight
SiO ₂	65	SO ₃	0.33
Al ₂ O ₃	5.7	TiO ₂	0.25
Fe ₂ O ₃	4.4	MnO	0.11
CaO	8.2	Na ₂ O	0.07
MgO	4.6	C	<1
P ₂ O ₅	4.7	LoI	2.53
K ₂ O	6.5		

2.3.3 Metakaolin (MK)

Metakaolin (Al₂Si₂O₇) is a form of calcined clay blended with lime and it shows the properties of pozzolanic material. Metakaolin is being using for thousands years as a cementitious material. The procedure of producing metakaolin involves the calcination process of kaolinitic clay at high temperature ranging 500⁰ – 800⁰C.

Metakaolin like other pozzolanic materials react with $\text{Ca}(\text{OH})_2$ and produces CSH gel (He et al., 1995; Zhang and Malhotra, 1995). Metakaolin may gain early age strength depending on the calcining temperature and clay type (Sabir et al., 2001).

2.4 Geopolymer concrete

2.4.1 Binder proportion

Geopolymer binding material and the proportion for proper geopolymerization depends on the type, ratios and concentrations of mixing constituents. Each constituent and ratios have significant role in the production of final geopolymer binding material.

2.4.2 Alkaline activator

A mechanically sound cementing material as a product of geopolymerization process depends on the activation of the pozzolans. The activators keep important role during precipitation and crystallization of the silica and alumina compounds in the solution. Hydroxyl ion acts as catalyst in the geopolymeric reaction. The metal cation serves to form a structural element and balance the negative framework carried by the tetrahedral aluminum (Rangan, 2008). The ability of the alkaline solution drives the mechanism of the reaction and assists in releasing silicon and aluminum in solution. The pozzolanic raw material dissolves quickly in this alkaline solution. Amorphous or semi-amorphous structure is formed by micro-crystallization (Khale and Chaudhary, 2007). The various groups of activating agents may be classified as Alkalis (MOH), weak acid salts (M_2CO_3 , M_2SO_3 , M_3PO_4 , MF), silicates ($\text{M}_2\text{O} \cdot n\text{SiO}_3$), aluminates ($\text{M}_2\text{O} \cdot n\text{AlO}_3$), aluminosilicates ($\text{M}_2\text{O} \cdot n\text{Al}_2\text{SO}_3 \cdot (2-6)\text{SiO}_2$) and strong salt Acids (M_2SO_4) where M represents an alkali ion (Pacheco-Torgal et al., 2008). The commonly used activators in geopolymer chemistry are NaOH , Na_2SO_4 , waterglass, Na_2CO_3 , K_2CO_3 , KOH , K_2SO_4 and cement clinker (Khale and Chaudhary, 2007). However, NaOH , KOH and sodium waterglass

($n\text{SiO}_2\text{Na}_2\text{O}$) or potassium waterglass ($n\text{SiO}_2\text{K}_2\text{O}$) are used widely for the availability and economy (Kong and Sanjayan, 2008).

2.4.3 Mechanical vibration

The geopolymeric material is generally highly viscous due to the alkaline material and their reactivity. The air may easily encapsulate into the matrix and proper vibration is mandatory for geopolymer matrix. Mechanical vibrator is useful for reducing substantially trapped air pocket and improves the porosity by proper vibration (Saeed et al., 2010).

2.4.4 Heat curing

The heat curing has an important role in the geopolymerization process. Proper heat curing expedite the geopolymerization process and early age strength development is noticed (Rangan, 2008). Temperature in a range of $50 - 80^\circ\text{C}$ are accepted for a successful geopolymer hydration. Curing time as well as temperature has direct influence in the development of mechanical properties of geopolymer concrete. The research results show that there was a yield of development of compressive strength of 15% over the steam curing method than dry curing (Škvára et al., 2005) and increase of temperature and reaction time has positive effect. The curing temperature may have negative effect if reaction time increases at later age and this attributed a decrease of final strength (Sumajouw and Rangan, 2006).

The basis of the theory of geopolymerization lies within the initial heavy formation of the reaction product and a successive densification of material instantly upon the presence of alkaline solution. The final production may exponentially less over time and increment of temperature serves to degrade previously created aluminosilicate gels within the matrix which may weaken the overall out product (Sumajouw and Rangan, 2006).

Initial 2-5 hours heat curing is important for geopolymer material and strength development beyond 48 hours is insignificant and the research results shew that the compressive strength of 60 MPa could be achieved only after five hours by heat curing at a temperature of 85⁰C (Khale and Chaudhary, 2007).

2.4.5 Mechanical properties

2.4.5.1 Compressive strength

The research works show that compressive strength of about 70% of 28-day strength is developed during the first few hours and the rate of compressive strength is very low afterwards (Duxson et al., 2005; Rangan, 2008). The initial reactivity is highly intense in proper temperature and heating duration and the activation of pozzolanic materials is occurred. But the reactive products eventually goes to unreactive pozzolan that reduce the efficiency of activation as well as the reaction rate (Duxson et al., 2005). Since the activator permeates slowly through the newly formed coating, the rate of reaction slows down and compressive strength continues gradually rise.

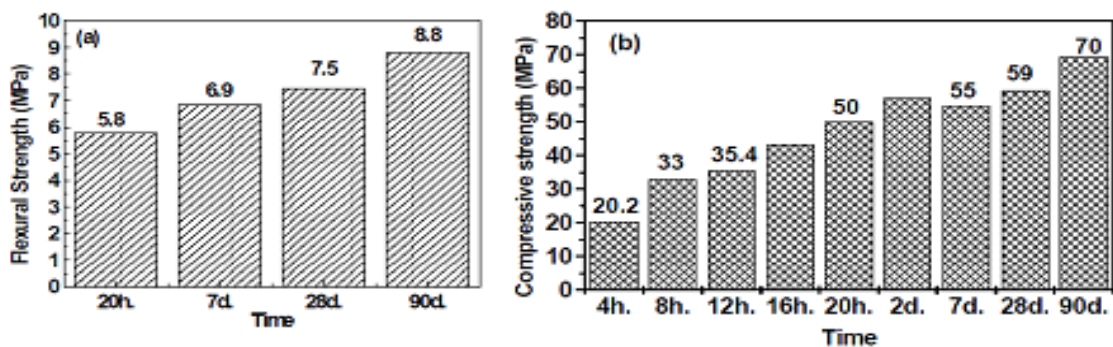


Figure 2.4: Compressive and flexural strength gain of geopolymers (Duxson et al., 2005)

McDonald and Thompson (2003) found the highest compressive strength 100-160 MPa at 28-day age in geopolymer material using fly ash and blast furnace slag mixtures and he concluded that pozzolan mixtures promoted a considerably smaller porosity in the

range of 2-10 % which maximized the strength potentially. Temperature was found beneficially for curing in the range of 70-90⁰C in this experimental work. The added heat increases the viscosity of the material and this develops a higher compressive strength potentially in geopolymer paste (Khale and Chaudhary, 2007).

2.4.5.2 Flexural strength

The flexural strength of geopolymer binding materials is substandard to its compressive strength. McDonald and Thompson (2003) observed that the compressive to tensile strength ratio under flexural loading is in the ratio of 10:5.5. The benefit of such an increased tensile potential suggests a possible reduction in reinforcement quantity for structural elements of identical geometry.

2.4.6 Toughness

This is established now a day that geopolymer mortars and concrete products have capability to develop mechanical strengths and can resist many harsh chemical compounds. The effect of steel fibres in geopolymer concrete was not analysed in detail by the previous research work and the fracture behaviour of fibre-reinforced geopolymer concrete was not clearly identified. There are previous research works on the effect of steel fibre in the normal weight concrete and lightweight conventional concrete (Sivakumar and Santhanam, 2007; Atiş and Karahan, 2009; Hamid et al., 2013; Mo et al., 2014b). The addition of steel fibres in conventional concrete enhances the flexural strength and fracture toughness (İpek et al., 2012; Wang et al., 2013; Mo et al., 2014a).

2.4.6.1 Short fibre

The addition of steel fibre in concrete takes place good role in the development of flexural as well as fracture toughness. The steel fibre improves the ductility of concrete (Wallah and Rangan, 2006). The addition of short polyvinyl alcohol (PVA) fibers reinforced

geopolymer composites and resulted in good flexural strength and reasonable toughness, while adding short basalt fibers reduced the strength of tested specimens and drastically improved the work of fracture element (Hardjito and Rangan, 2005).

The incorporation of short steel fibres increased the flexural strength of geopolymer composite as reported in previous research work (Hardjito and Rangan, 2005). The homogeneity of the fibre material is important and this is ensured by the ultrasonic scattering technology. Short fibres exhibits the advantage of possessing high modulus and strength characteristics and an addition of 3.5 percent of short fiber material increased specimen strength by a magnitude of 4.4, yielding value increases from 16.8 to 91.3 MPa (Hardjito and Rangan, 2005).

The lower aspect ratio as well as the short fibres is directly related to the transmission of load and the cohesion between the fibre and matrix. The larger fibres imparts more restriction on deformation and the shorter fibres create added friction due to the increased number on available fibre ends (Hardjito and Rangan, 2005). The mechanisms that play role in the toughness and flexural strength development in concrete due to the usage of steel fibres are due to the fibre bridging and enhancement of pull-out resistance in matrix (Hardjito and Rangan, 2005).

2.4.6.2 Long fibres

The long fibres provide mechanical stability and toughness from a different perspective than those identified for short fibre material. Long fibres i.e. the fibres with high impact ratio can improve cement functionality as well as toughness due to its sustainability of greater tensile forces prior to the pull out. The ability of the longer steel fibre to withstand additional stress facilitate to enhance the toughness energy. The longer steel fibre can absorb additional tensile load due to its elasticity. The matrix along the tensile side begins to expand under load and the resistance to tensile failure of the matrix acquire additional

stiffness due to the elastic property of longer steel fibre. The longer steel fibre provide higher plasticity prior to final pull out and failure. A fibre length of 7 mm is identified as the critical length, essential for the production of geopolymeric materials with optimum reinforcement and improved toughness (Hardjito and Rangan, 2005).

2.4.6.3 Steel adhesion

An interesting property of geopolymer cements is their ability to form an extremely strong bond with steel products. Pull out testing has concluded that the bond strength between this alkaline concrete mix and steel reinforcement is so great that 8 mm bars embedded in the matrix broke in two prior to experiencing slippage or concrete cracking (Fernandez-Jimenez et al., 2006). Additional samples did not cause steel failure, but the loads being applied to cause bar slippage were 12 MPa and 17 MPa, respectively. This not only surpasses the 9.70 N/mm requirement specified in the Spanish concrete code (EHE) as the minimum load to pass the beam test (Fernandez-Jimenez et al., 2006), but it signifies the intense bonding characteristics of alkali-activated cement systems.

2.5 Development of geopolymer research

2.5.1 Invention of first mineral resin

Since October 1, 1975 Davidovits, J. has been studying the behaviour of metakaolin in Siliface system. The first goal was to find a process for the manufacture of synthetic zeolites (type zeolite A) by reacting metakaolin +NaOH. It was noticed that that mixture was prone to a very important exothermic reaction (t^0 exceeding 100⁰C after 1 hour of storage in a bag) (Davidovits, 2008).

Davidovits (2008) used that exothermic reaction in the manufacturing of insulating blocks consisting entirely of a mineral core made of expanded shale or expanded glass spheres, agglomerated with metakaolin +NaOH. In a panel covered with a siliface facing, the

temperature in the centre of a 15 cm thick core reaches 100⁰C after only 3-4 minutes. The addition of a binder such as Na-Silicate leads to a liquid coating, and allows reducing the quantity of mineral binder used in the process (Davidovits, 2008).

It seemed that metakaolin behaved as a hardener for Na-Silicate. Consequently, a mixture involving Na-Silicate +NaOH + Metakaolin has the following advantages:

- a. Exothermicity (hardening to the heart of thick material);
- b. Reaction with Na-Silicate (very fast hardening of the liquid binder).

Another consequence of that discovery was that one can treat common clays at 500-600⁰C, to obtain a very reactive argillaceous raw material (metakaolin type) being able to be used in the preceding examples in place of pure metakaolin, together with Na-Silicate, or alone. It was a step towards more knowledge on the specific reactions involving mineral polymers, either by using natural raw materials for example standard clay like Clerac B16, dried, ground or by performing the suitable treatment to transform them into reactive raw material. It was the first mineral resin ever manufactured (Davidovits, 2008).

2.6 Manufactured sand and Quarry dust as fine aggregate

The main characteristics of the fine aggregate that affect the compressive strength of fresh and hardened concrete are shape, grade and maximum size. The factors such as shape and texture of the fine aggregate affect the workability of fresh concrete and influence the strength and durability characteristics of hardened concrete. The spherical particles have less surface area than the particles with flat surface and elongated shape. The cubical and spherical shape contributes in good workability with less water (Shilstone, 1999). Flaky and elongated particles have negative effect on workability, producing very harsh mixtures. For given water content, these poorly shaped particles lead to less workable mixtures than cubical or spherical particles. Conversely, for given workability, flaky and

elongated particles increase the demand for water thus affecting strength of hardened concrete. The void content is also affected by angularity.

In fact, the angular particles tend to increase the demand for water as these particles increase the void content compared to rounded particles (Quiroga & Fowler, 2004). The rough aggregate increase the water demand for given workability (Hudson, 1999b). Since natural sand is often rounded and smooth compared to M-sand, natural sand usually require less water than M-sand for given workability (Quiroga & Fowler, 2004). However, workable concrete can be made with angular and rough particles if they are cubical and well graded.

2.7 Oil palm shell (OPS) as aggregate

Besides the mining sand, the usage of conventional granite in a high rate in construction industry, effects on the ecological imbalance. The replacement of conventional coarse aggregate by locally available waste or industrial by-product could reduce the environmental imbalance. The oil palm shell (OPS) which is abundant in Malaysia, Indonesia, Philippine and other few countries worldwide has a potentiality to use as a coarse aggregate.

OPS is the industrial by-product and obtained during extraction of palm oil from the palm oil nut. This is experimented and well known now a day as a lightweight aggregate. The research works show that OPS has comparable mechanical and physical properties like conventional aggregate to produce medium and high strength concrete.

Yew et al. (2014) investigated the effects of heat treatment on OPS aggregates and reported that selection of a suitable temperature and duration of heat treatment for OPS aggregates are potentially usable as a new eco-friendly alternative to enhance concrete

strength. (Shafigh et al., 2013b) found an early age strength development of for initial water curing of OPS lightweight concrete consisting ground granulated blast furnace slug.

2.8 Previous research works and research gap

The geopolymer research work was initiated in 1972 and Davidovits is the pioneer of the geopolymer technology in the practical use. The significant research works on geopolymer concrete and the research gap are shown in Table 0.1.

2.9 Summary

Geopolymer technology has been proved its potentiality to use as a complete replacement of Portland cement in near future. Since the industrial wastes like POFA, FA, RHA, etc are the raw material of developing geopolymer binding material; this could lead to solve the dumping problem of huge production of waste POFA, FA, RHA, etc in Malaysia and other south-Asian countries. Besides the replacement of natural aggregate in the geopolymer concrete by agricultural waste material like OPS and industrial by-product such as M-sand and quarry dust, may contribute resisting the depletion of natural resources as well as the ecological imbalance.

Table 0.1: Previous research work and research gap

Research area	Author	Previous research work	Research gap
Geopolymer concrete	Abdulkareem et al. (2014), Bagheri and Nazari (2014), Phoo-ngernkham et al. (2014), Alida et al. (2013), Li et al. (2013), Pangdaeng et al. (2013)	<ul style="list-style-type: none"> - Effect of elevated temperature on the development of geopolymer concrete - Compressive strength of high strength class C fly ash-based geopolymers - Effect of adding nano-SiO₂ and nano-Al₂O₃ - Effect of Acidic to the Fly Ash Based Geopolymer - Immobilization of simulated radionuclide 133Cs+ by fly ash-based geopolymer - Influence of curing conditions 	<ul style="list-style-type: none"> - Lack of analysis on the mechanical properties of POFA based geopolymer concrete - Fracture analysis on geopolymer concrete was not done - Lack of usage of POFA in large volume with MK for geopolymer concrete - Microstructural analysis of POFA-FA-MK-based geopolymer concrete - Impact resistance of geopolymer concrete - Development of POFA-based geopolymer concrete incorporating nano-alumina
Oil palm shell	Alengaram et al. (2008), Jumaat (2010), Alengaram et al. (2011b), Shafigh et al. (2013a)	<ul style="list-style-type: none"> - Influence of Sand Content and Silica Fume on mechanical properties of OPS concrete - Comparison of mechanical and bond properties of OPSC with NWC - Enhancement and prediction of modulus of elasticity of palm kernel shell concrete 	<ul style="list-style-type: none"> - OPS was not used as a coarse aggregate in geopolymer concrete - Mechanical properties of OPS based geopolymer concrete was not examined before.
Manufactured sand	P.Sravana (2013), Chow et al. (2013)	<ul style="list-style-type: none"> - Effect of Manufacture sand on Strength Characteristics 	<ul style="list-style-type: none"> - Effect of M-sand was not determined in the geopolymer mortar.

CHAPTER 3 MATERIALS AND METHODS

3.1 Introduction

This chapter discussed on the preparation of materials, proportions of mix designs and procedure of casting, curing and testing. All these are described in detail below.

3.2 Materials

3.2.1 Binding materials (POFA, FA, MK)

The palm oil fuel ash (POFA), fly ash (FA) and metakaolin (MK) were collected locally from Jugra Palm Oil Mill, Lafarge Malayan Cements and a local supplier, respectively. All binding materials were tested for its mineral contents and the loss of ignition using X-ray Fluorescence (XRF) analysis. The average particle size distribution was determined by laser particle analyser with obscuration 16% and beam length of 2.40 mm. The density of POFA, FA and MK was determined in the laboratory according to ASTM C188-09 (2009). The raw POFA was sieved through 300 μm size sieve and then dried in an oven and ground 30,000 times in a grinding machine. FA and MK were stored in airtight containers.



Figure 3.1: Collection of POFA

3.2.2 Fine aggregates (Conventional mining sand, manufactured sand-M-sand, Quarry Dust-QD)

The manufactured sand (M-sand), quarry dust (QD) and the conventional mining sand (N-sand) were collected locally. The N-sand, M-sand and QD were dried, sieved through 5 mm sieve and retained on 300 μm sieve were used in the preparation of geopolymer mortar and concrete. The sieve analysis and fineness modulus of fine aggregate were conducted according to ASTM C136-06 (2006) while the specific gravity as well as absorption tests were done in accordance with ASTM C128-12 (2012).

3.2.3 Coarse aggregates

The oil palm shell (OPS) and crushed granite aggregates were collected from local oil palm and quarry industry, respectively. . The OPS was washed, dried and crushed before

casting. The particle sizes used for casting were in between 5 and 9 mm. The specific gravity, water absorption (ASTM C127-12 (2012)) and aggregate impact values (ASTM C131-06 (2006)) for both aggregates were determined based on ASTM specifications. The OPS was soaked in water 24 hours and used in saturated surface dry (SSD) condition for casting.



Figure 3.2: Collection of OPS

3.2.4 Steel fibres

Hooked-end type steel fibres of length 60 mm and 35 mm with aspect ratio 80 and 65, respectively, were used as shown in Figure 3.3. The steel fibres used had minimum tensile strength of 1100 MPa as specified by the manufacturer.

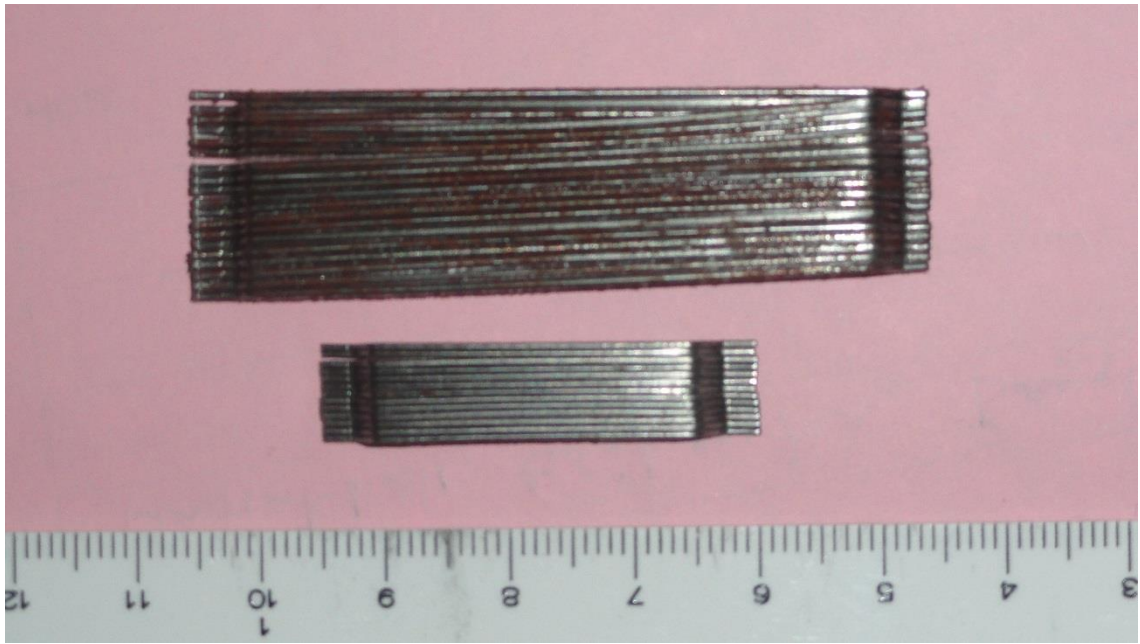


Figure 3.3: Steel fibres of AR 80(above) & 65(below)

3.2.5 Water

Potable water was used for casting. The water was free from organic materials and suspended solids.

3.2.6 Alkaline solution

The alkaline activator using sodium hydroxide (NaOH) and sodium silicate (Na_2SiO_3) was prepared at least 24 hours before the casting. The sodium hydroxide (NaOH) solution of molarity 14 M was prepared for each mix proportion. The modulus of sodium silicate (i.e. ratio of $\text{SiO}_2/\text{Na}_2\text{O}$) was 2.5. The sodium silicate liquid was mixed with NaOH solution by weight proportion of 1: 2.5 (NaOH solution: liquid Na_2SiO_3).

3.3 Development of geopolymer concrete

3.3.1 Mixture proportion

The mixture design was carried on in three different aspects as follows to fulfil the objectives of this research project. The purpose of the first mix design governs the investigation of the effect of the replacement of mining sand by two industrial by-product such as quarry dust and manufactured sand in the development of compressive strength of geopolymer mortar. The best mix proportion for the replacement of mining sand was used in the second stage of the mix design to determine an appropriate mix proportion of POFA, FA and MK as a binding material by the study of the mechanical properties of lightweight geopolymer concrete. The mix proportion that satisfy the minimum compressive strength of 20MPa as mentioned in the objective, was chosen for further improvement of tensile strength by using two types of steel fibre with varying volume as shown in mix design 3. Normal weight geopolymer concrete of similar compressive strength of the lightweight geopolymer concrete was designed by trial mixes as a control for the comparison purpose of mechanical properties as well as fracture behaviour.

Mix design 1: The variables of this mixture design were N-sand, M-sand and QD as shown in Table 3.1. The quantities of POFA, FA, alkaline activator and water used in the mixes were respectively 343, 343, 274 and 137 kg/m³. The binder content (POFA: FA) was kept constant at 50:50 with the variable of different proportions of fine aggregate contents.

Table 3.1: Mix design with variables of N-sand, M-sand and QD

Mortar Designation*	Mix Proportions by weight (kg/m ³)		
	Fine Aggregates		
	N-Sand	M-Sand	QD
M 1	1029 (100**)	0	0
M 2	771 (75)	257 (25)	0
M 3	257 (25)	771 (75)	0
M 4	0	1029 (100)	0
M 5	0	257 (75)	771 (25)
M 6	0	771 (25)	257 (75)
M 7	0	0	1029 (100)
M 8	257 (25)	0	771 (75)
M 9	771 (75)	0	257 (25)
M 10	514 (50)	257 (25)	257 (25)
M 11	257 (25)	514 (50)	257 (25)
M 12	257 (25)	257 (25)	514 (50)
* Legend: N100 Normal mining sand 100% N25-Q75 Normal mining sand 25% and quarry dust 75% ** Proportion in percent in bracket ()			

Mix design 2: The proportion of POFA, FA and MK was varied as shown in Table 3.2. The ratios of M-sand/ binder, OPS/ binder, alkaline activator/ binder and water/ binder were 1.125, 0.375, 0.4 and 0.18, respectively. Alkaline solution was prepared using 14 M NaOH solution and liquid Na₂SiO₃ with a proportion of 1:2.5.

Table 3.2: Mix design with variables of POFA, FA and MK

Concrete Designation	Binder (kg/m ³)		
	POFA	FA	MK
P10-F85-M05	60 (10*)	507 (85)	30 (5)
P10-F80-M10	60 (10)	478 (80)	60 (10)
P10-F75-M15	60 (10)	448 (75)	90 (15)
P10-F70-M20	60 (10)	418 (70)	119 (20)
P10-F65-M25	60 (10)	388 (65)	149 (25)
P90-M10	537 (90)	-	60 (10)
P80-M20	478 (80)	-	119 (20)
P70-M30	418 (70)	-	179 (30)
P60-M40	358 (60)	-	239 (40)
* Proportion in percent in bracket ()			

Mix design 3: The effect of steel fibres on the mechanical properties and fracture behaviour was investigated for two different aspect ratios. The volume proportions of the steel fibres were 0.25, 0.50 and 0.75% (Table 3.3). The mixes OG-65/0.25 to OG-80/0.75, GG-65/0.5 and GG-80/0.5 had fibre contents varying between 0.25 and 0.75% of total volume of concrete; the mixes OG and GG were designed as control mixes without fibres for comparison. The proportions of alkaline solution and water are shown in Table 3.3.

Table 3.3: Mix design with variables of steel fibre proportion and aspect ratio

Concrete designation	POFA	MK	M-sand	OPS	Gravel	Steel Fibre-65/35	Steel fibre-80/60	Alkaline/binder	Water/binder
	Proportion (kg/m ³) by weight								
OG	508	56	636	212	-	-	-	0.5	0.11
OG-65/0.25	508	56	636	212	-	19.75 (0.25*)	-		
OG-80/0.25	508	56	636	212	-	-	19.75 (0.25)		
OG-65/0.5	508	56	636	212	-	39.50 (0.5)	-		
OG-80/0.5	508	56	636	212	-	-	39.50 (0.5)		
OG-65/0.75	508	56	636	212	-	59.25 (0.75)	-		
OG-80/0.75	508	56	636	212	-	-	59.25 (0.75)		
GG	510	57	380	-	753	-	-		
GG-65/0.5	510	57	380	-	753	39.50 (0.5)	-		
GG-80/0.5	510	57	380	-	753	-	39.50 (0.5)		
* Proportion in percent in bracket ()									

3.3.2 Casting, specimen preparation, curing and testing age

The binders were mixed with the aggregates and steel fibres (for mixture design 3) in the drum mixture of capacity 0.2 m³ (Figure 3.4). The alkaline activator was then added and mixed properly. It was taken around 15 minutes to mix all with alkaline solution properly. The water was then added to the mixture. The slump and fresh density were then tested

for fresh concrete. Prior to casting, the moulds were cleaned and coated with oil. The dimensions and numbers of specimens prepared are shown in Table 3.4.



Figure 3.4: Casting of geopolymer fibre reinforced concrete

Table 3.4: Specimens for testing of concrete

Test (age)	Specimens and dimensions (mm)	Remarks
Compressive strength test (3-, 7-, 14- and 28-day)	Cubes 100 mm (concrete) 50 mm (mortar)	Mechanical properties tests were conducted for both OPSGC and NWGC with fibres and without fibres; special arrangement was made for fracture toughness test based on ASTM C1609/C1609M-12 (2012).
Indirect tensile strength test (28-day)	Cylinders ϕ 100 mm x 200 mm height	
Flexural strength test (28-day)	Prisms 100 mm x 100 mm x 500 mm	
Static modulus of elasticity (28-day)	Cylinders ϕ 150 mm x 300 mm height	
Fracture toughness test (28-day)	Prism of 100 mm x 100 mm x 500 mm with 30 mm groove	

The concrete was poured into the moulds in three consecutive layers (Figure 3.5). After each pour, the vibrating table was set to run for 10 seconds and this vibration was kept consistent for all the mix proportions. Since a minimum quantity of water used, segregation was not noticed during the vibration. The minimum amount of water was determined by the trial mix design. After the vibration, the top surface was trowelled to give a smooth surface. Specimens were then covered and kept into the oven for 48 hours at a temperature of 65⁰C after 3 to 5 hours. Hardjito and Rangan (2005) reported that a delay in starting heat curing up to five days had no noticeable degradation in the compressive strength. The specimens were demoulded after 48 hours and kept in a room temperature and relative humidity of 28⁰C and 79%, respectively.



Figure 3.5: Preparation of specimens

3.4 Testing

3.4.1 Fresh concrete tests

The slump test was conducted according to ASTM C143/C143M-12 (2012) for evaluating workability and consistency of concrete. The fresh density was tested in compliance with ASTM C1688/C1688M-13 (2013).

3.4.2 Mechanical properties of concrete

3.4.2.1 Compressive strength test

The compressive strength test was carried out according to BS EN 12390-3:2009 (2009). The specimens were tested at the age of 3-, 7-, 14- and 28-day. An ELE testing machine (Figure 3.6) of capacity 2000 kN was used. The loading pace was 2.4 kN/sec. The compressive strength (MPa) was calculated based on Eq. 3.1.

$$\sigma = \frac{\text{Failure load}}{\text{Area}} \quad \text{Eq. 3.1}$$



Figure 3.6: ELE testing machine of capacity 2000 kN

3.4.2.2 Flexural strength test

The flexural test was conducted on 100 x 100 x 500 mm prisms following BS EN 12390-5:2009 (2009) at the age of 28-day. The flexural strength was calculated by the maximum moment arisen due to two-point loading from ELE testing machine with a pace rate 0.06±0.04 N/(mm².s). The flexural strength, f_f was calculated using Eq. 3.2.

$$f_f = \frac{P \times l}{b \times d^2} \quad \text{Eq. 3.2}$$

Where, P = breaking load, N

l = distance between supporting rollers, mm

b = width of cross section, mm

d = depth of cross-section, mm

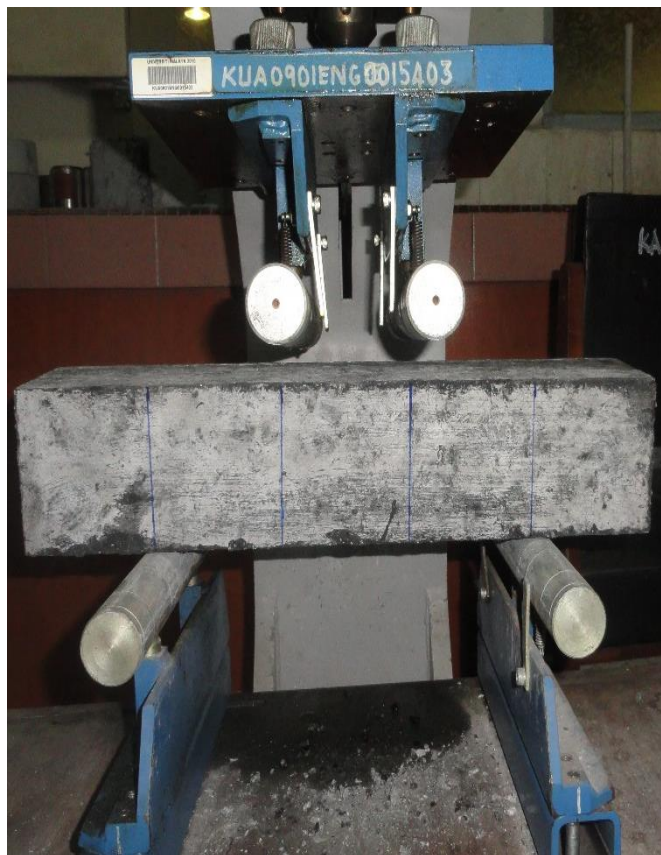


Figure 3.7: Flexural strength test (BS EN 12390-5:2009, 2009)

3.4.2.3 Splitting tensile strength test

The indirect tensile strength test was done as prescribed in BS EN 12390-6:2009 (2009). Cylinders of dimension 200 mm x ϕ 100 mm were used for the indirect tensile strength test at 28-day age. The arrangement of specimen in the apparatus is shown in the Figure 3.8. Eq. 3.3 shows the calculation of the indirect tensile strength.

$$\sigma_{ct} = \frac{2P}{\pi \times l \times d} \quad \text{Eq. 3.3}$$

Where, P = maximum load, N

l = length of the specimen, mm

d = cross-sectional dimension of the specimen, mm



Figure 3.8: Indirect tensile strength

3.4.2.4 Static modulus of elasticity test

The static modulus of elasticity was carried out in accordance with ASTM C469 - 14 . Two cylinders of dimension 300 mm x ϕ 150 mm were tested at the age of 28-day. The compressometer was attached axially to the specimen (Figure 3.9) and placed centrally in the ELE compression machine. The pace of loading was fixed to 4.418 kN/sec. An initial stress of 0.5 MPa was applied and the strain gauge readings were recorded. Final stress was applied at the one-third cylinder compressive strength of concrete. The stress was maintained 60 seconds in both the initial and final stress. The static modulus of elasticity (E, GPa) is determined by the Eq. 3.4.

$$E = \frac{(\text{Final stress}-\text{Initial stress}) \times 2 \times 200}{(\text{Final gauge reading}-\text{Initial gauge reading}) \times 0.01} \times 10^{-3} \quad \text{Eq. 3.4}$$



Figure 3.9: Static modulus of elasticity test

3.4.3 Fracture test

The fracture and flexural toughness were determined from the test prescribed by ASTM C1609/C1609M-12 (2012) and ASTM C1018-97 (1997).

ASTM C1609/C1609M-12 (2012) evaluates the flexural performance of fibre reinforced concrete from the load-deflection curve obtained by third-point loading (Figure 3.10).

The modulus of rupture can be determined from the Eq. 3.5.

$$f = \frac{PL}{bd^2} \quad \text{Eq. 3.5}$$

Where,

f = modulus of rupture (MPa)

P = load (N)

L = span length (mm)

b = the average width of the specimen at the fracture, as oriented for testing, (mm)

d = the average depth of the specimen at the fracture, as oriented for testing (mm)

First peak, peak loads, corresponding stresses, residual loads at specified deflection and the corresponding residual strength are also required to determine from this test for the modulus of rupture calculation by Eq. 3.5. Specimen toughness obtained by the load-deflection area is an expression of the energy absorption capability of that particular specimen.



Figure 3.10: Fracture test (ASTM C1609/C1609M-12, 2012)



Figure 3.11: Specimens for fracture test

The definition and calculation of the terminologies used in the fracture test is given in the following clauses.

3.4.3.1 End point deflection: The deflection value on the load-deflection curve equal to $1/150$ of the span length, or a larger value as specified at the option of the specifier of tests.

3.4.3.2 First peak load, P_1 : The load value at the first point on the load-deflection curve where the slope is zero.

3.4.3.3 First-peak deflection, δ_1 : The net deflection value on the load-deflection curve at first-peak load.

3.4.3.4 First-peak strength, f_1 : The stress value obtained when the first-peak load is inserted in the formula for modulus of rupture given in Eq. 3.5.

3.4.3.5 Load-deflection curve: The plot of load versus net deflection of a flexural beam specimen loaded to the end-point deflection.

3.4.3.6 Net deflection: The deflection measured at mid-span of a flexural beam specimen exclusive of any extraneous effects due to seating or twisting of the specimen on its supports or deformation of the support and loading system.

3.4.3.7 Peak load, P_P : The maximum load on the load-deflection curve.

3.4.3.8 Peak-load deflection, δ_P : The net deflection value on the load-deflection curve at peak load.

3.4.3.9 Peak strength, f_P : The stress value obtained when the peak load is inserted in the formula for modulus of rupture given by Eq. 3.5.

3.4.3.10 D: Nominal depth of the beam specimen in mm. To simplify nomenclature, the nominal beam depth is shown in units of mm for both the SI and inch-pound version of this test method.

3.4.3.11 L: Span length or distance between the supports.

3.4.3.12 Residual load, P^D_{600} : The load value corresponding to a net deflection of $L/600$ for a beam of nominal depth D.

3.4.3.13 Residual load, P^D_{150} : The load value corresponding to a net deflection of $L/150$ for a beam of nominal depth D.

3.4.3.14 Residual strength, f^D_{600} : The stress value obtained when the residual load P^D_{600} is inserted in the formula for modulus of rupture given in Eq. 3.5.

3.4.3.15 Residual strength, f^D_{150} : The stress value obtained when the residual load P^D_{150} is inserted in the formula for modulus of rupture given in Eq. 3.5.

3.4.3.16 Specimen toughness, T^D_{150} : Toughness of beam specimen of nominal depth D at a net deflection of $L/150$.

3.4.3.17 Equivalent flexural strength ratio, $R^D_{T, 150}$: The value obtained when the specimen toughness T^D_{150} is inserted in Eq. 3.6.

$$R^D_{T,150} = \frac{150 \cdot T^D_{150}}{f_1 \cdot b \cdot d^2} \cdot 100\% \quad \text{Eq. 3.6}$$

3.5 Summary

The main focus was given to the usage of POFA in large quantity in geopolymer lightweight concrete. The compressive strength of 20 MPa was considered as a benchmark for the minimum compressive strength for the structural lightweight concrete. The mix designs does not reflect the optimum mix design. The steel fibres were used to improve the tensile properties of OPSGC.

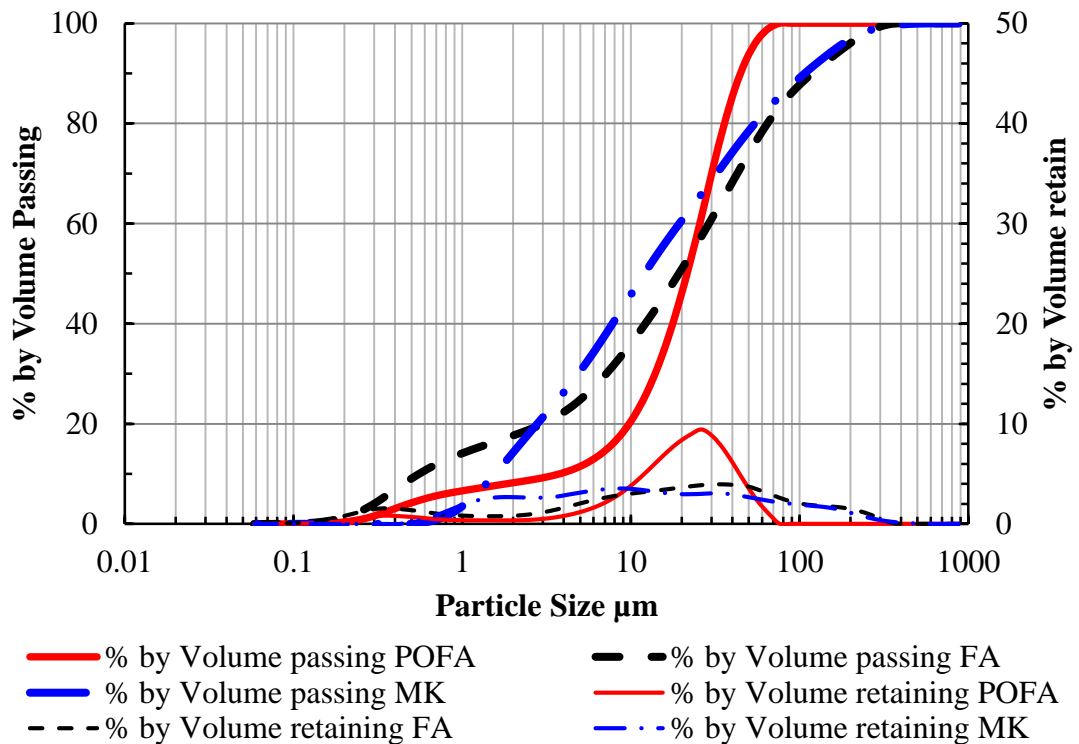


Figure 4.1: Particle size distribution of POFA, FA and MK

4.2.2 Fine aggregates

The main characteristics of the fine aggregate that affect the compressive strength of fresh and hardened concrete are shape, grading and maximum size. The factors such as shape and texture of the fine aggregate affect the workability of fresh concrete and also influence the strength and durability characteristics of hardened concrete. The spherical particles have lesser surface area than the particles with flat surface and elongated shape. The cubical and spherical shape contributes in good workability with less water (Shilstone, 1999). Flaky and elongated particles have negative effect on workability, producing very harsh mixtures. For given water content, these poorly shaped particles lead to lesser workable mixtures than cubical or spherical particles. Conversely, for given workability, flaky and elongated particles increase the demand for water thus affecting strength of hardened concrete. The void content is also affected by angularity.

In fact, the angular particles tend to increase the demand for water as these particles increase the void content compared to rounded particles (Quiroga and Fowler, 2004). The rough aggregate increase the water demand for given workability (Hudson, 1999b). Since N-sand is often rounded and smooth compared to M-sand, N-sand usually require less water than M-sand for given workability (Quiroga and Fowler, 2004). However, workable concrete can be made with angular and rough particles if they are cubical and well graded. The effect of M-sand and QD in the development of compressive strength of geopolymer mortar and concrete are related to these angularity, flaky and smoothness properties. The detail discussion of the effects is narrated in clause 4.3 .

The particle size distribution for N-sand, M-sand and QD were carried out in accordance with BS 882-1992. The particle size distribution for N-sand, M-sand and QD is shown in Figure 4.4 and Table 4.2. According to BS 882-1992, fine aggregates are divided into three grades based on the percentage of passing through standard sieves. It is found that all three types of fine aggregates fall into the category of Grade C sand. The particle size distribution curves for M-sand and QD are overlapped as they have similar particles.



Figure 4.2: Particle shape of manufactured sand (2.36 mm retained)

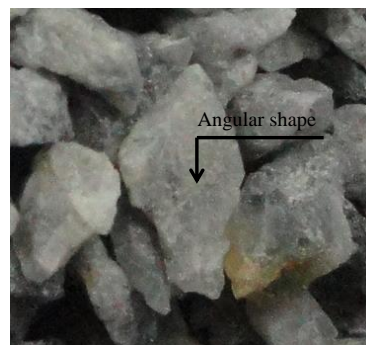
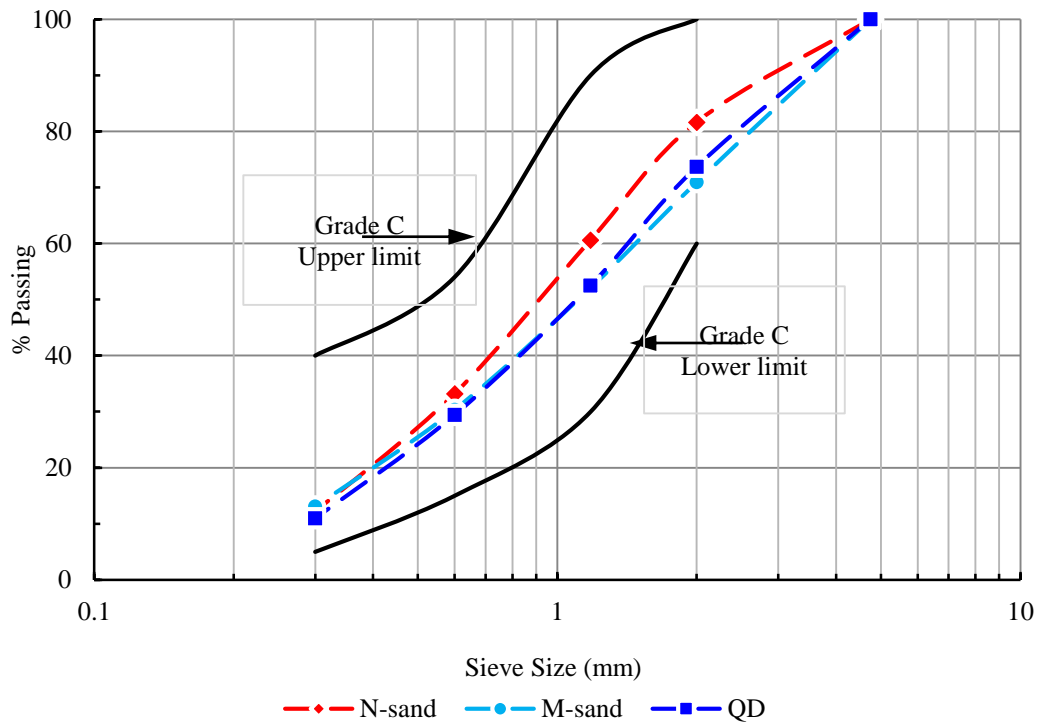


Figure 4.3: Particle shape of quarry dust (2.36 mm retained)

Table 4.2: Particle size distribution of N-sand, M-sand and QD

Sieve size	Percentage of passing		
	N-sand	M-sand	QD
5 mm	99.99	100.00	99.98
2.36 mm	81.63	70.91	73.66
1.18 mm	60.60	52.09	52.52
600 μm	33.18	30.34	29.41
300 μm	12.16	13.12	11.01
Fineness modulus	2.88	2.66	2.67
D ₁₀ , mm	0.27	0.30	0.31
D ₃₀ , mm	0.50	0.55	1.41
D ₆₀ , mm	1.24	1.42	0.57
$C_u = D_{60} / D_{10}$	4.53	4.80	4.56
$C_c = D_{30}^2 / (D_{10} \times D_{60})$	0.74	0.73	0.74
C_u = Uniformity coefficient; C_c = Coefficient of curvature			



Grade C based on BS EN 933-8-2012

Fineness Modulus: 2.88, 2.66, 2.67 for N-sand, M-sand & QD respectively

Figure 4.4: Particle size distribution curve for N-sand, M-sand and QD

The Specific gravity, and absorption of N-sand, M-sand and QD were measured (Table 4.3) according to ASTM C29/29M & ASTM 128.

Table 4.3: Specific gravity and absorption of N-sand, M-sand and QD

	N-sand	M-sand	QD
Specific gravity			
OD	2.77	1.97	2.09
SSD	2.79	2.63	2.61
Absorption (%)	0.81	0.91	0.92
OD Oven Dry SSD Saturated Surface Dry			

4.2.3 Coarse aggregate

The fineness modulus, specific gravity, water absorption and aggregate impact value (AIV) of crushed granite and OPS were determined according to ASTM C127-12 (2012), ASTM C131-06 (2006) and ASTM C136-06 (2006). Table 4.4 shows the physical properties of granite and OPS. It is noticed that the water absorption of OPS is higher than granite and the AIV is lower than granite.

Table 4.4: Physical properties of coarse aggregate

Coarse aggregates	Fineness modulus	Specific gravity	Water absorption, %	Aggregate impact factor, %
Granite	7.43	2.67	<1	11.9
OPS	6.25	1.32	24.74	3.93

4.3 Mix Design 1: Effect of molarity, N-sand, M-sand and QD in geopolymer mortar

The following discussions focus on the mortar mix developed using POFA and FA with three different types of fine aggregates, namely N-sand, M-sand and QD. The fresh and hardened densities, compressive strength, effect of molarity, fineness modulus etc. are analyzed and reported in the subsequent sections.

4.3.1 Density

The fresh and hardened densities of mortar for different mix proportions at the ages of 3-, 7-, 14- & 28-day are shown in Figure 4.5. The fresh densities of the 12 mixes are shown along the X-axis for zero compressive strength. The fresh and hardened densities vary in the range of 2060 - 2154 kg/m³ and 1981- 2069 kg/m³, respectively. The apparent density increases with the ratio of Si:Al (Davidovits, 2008). Since the main variables for different mix proportions in geopolymer mortar are N-sand, M-sand & QD, and the specific gravity of these materials influence the variation of densities. Thus the influence of fresh densities of mixes M1 (100% NS), M4 (100% M-sand) and M7 (100% QD) of 2146, 2060 and 2060 kg/m³, respectively could be related to the respective specific gravities of fine aggregates of 2.79 (NS), 2.63 (M-sand) and 2.61 (QD).

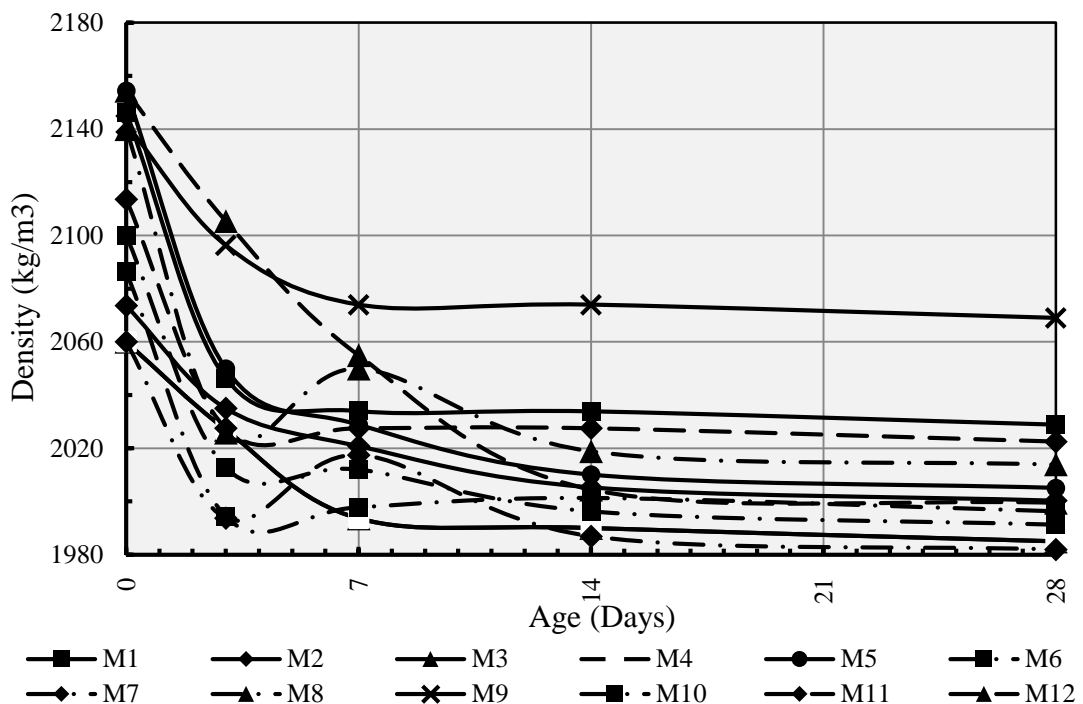


Figure 4.5: Density vs age (days)

The changes in density at different ages are influenced by the geopolymerization and curing condition as these undergo several dehydroxylation and crystallization phases at

a certain phase (Davidovits, 2008). Three types of water release takes place during heating from geopolymer concrete namely, physically bonded water, chemically bonded water and hydroxyl group (OH⁻) (Davidovits, 2008). The rate of reduction of water from the hardened geopolymer causes the density reduction and it can be seen that this reduction varies from 3.41 to 7.19 %. The correlation between the density and compressive strength at different ages of geopolymer mortar is shown in Figure 4.6. The gradient of compressive strength/density varies between 0.12 and 0.34.

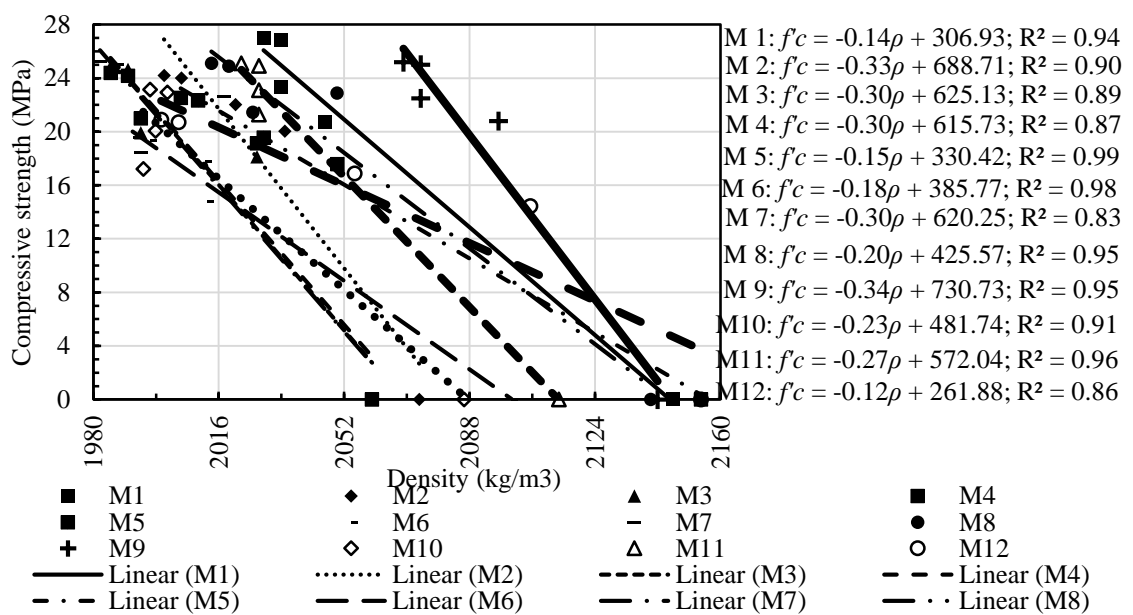


Figure 4.6: Relationship between density and compressive strength at different ages

$f'c = 0.0315\rho - 39.558$, where $f'c$ and ρ represent compressive strength (MPa) and density (kg/m^3)

4.3.2 Development of compressive strength

The compressive strengths for different mix proportions at the ages of 3-, 7-, 14-, and 28-day are shown in Table 4.5. The 28-day compressive strength for the mixes varied between 21 and 28 N/mm². The standard deviations as shown in Table 4.5 were measured from the results found for 3 specimens. The bold values refer to the compressive strength

of mortar with 100% N-sand, M-sand and QD. The average 3-day compressive strength of all mixes was found to be 76% of the 28-day strength. The pattern of early age strength development supports the findings reported by previous researchers (Davidovits, 2008; Lloyd and Rangan, 2009).

Figure 4.7 shows the comparison of the compressive strengths for different mortar mixtures with varying proportion of N-sand, M-sand and QD. Though the mortar with 100% N-sand produced the highest 28-day strength, the combination of N-sand with M-sand and QD reduced the strength. The shape, texture and particle size distribution affect the compressive strength (Quiroga and Fowler, 2004) that might have attributed to the variation of the compressive strength as seen in Figure 4.7. The packing density is another factor that influences the workability as well as the compressive strength. Fung et al. (2009) cited from Powers (1969) that for a constant volume of binder paste, higher packing density lead to higher workability.

Table 4.5: Development of compressive strength for different mix designs

Designation	Compressive strength (N/mm ²)							
	3 day	SD	7 day	SD	14 day	SD	28 day	SD
M 1	20.8	0.6	23.3	0.3	26.8	0.2	27.8	0.4
M 2	20.0	0.3	22.0	0.9	24.0	0.4	25.1	0.5
M 3	18.1	0.2	19.9	0.2	24.7	0.1	25.7	0.2
M 4	19.1	1.0	21.0	0.2	24.2	0.5	25.2	0.6
M 5	17.6	1.1	19.6	0.5	22.3	0.9	23.4	0.8
M 6	14.8	1.2	17.8	0.6	19.4	0.3	20.5	0.7
M 7	21.6	0.1	23.0	0.4	25.0	0.2	26.1	0.2
M 8	21.5	1.0	22.9	1.2	24.9	0.9	26.0	1.0
M 9	20.8	0.3	22.5	0.3	25.0	1.1	26.1	0.6
M 10	17.2	0.3	20.1	0.3	22.9	0.8	24.0	0.4
M 11	21.3	0.6	23.1	0.7	24.9	0.8	26.0	0.6
M 12	14.5	0.7	16.9	0.7	20.7	0.7	21.8	0.7

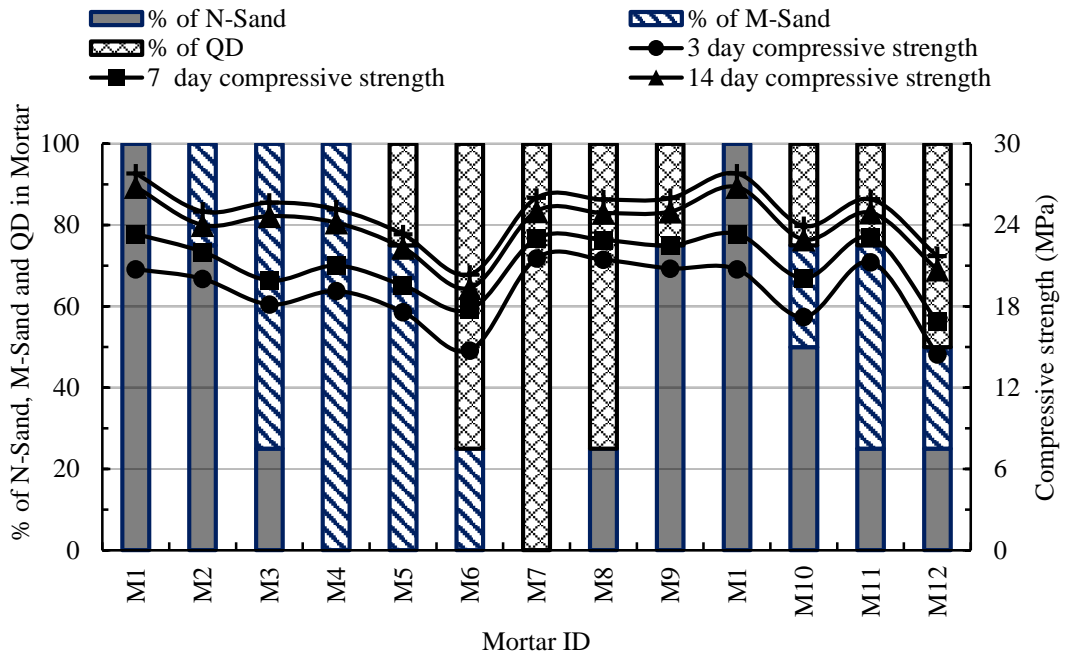


Figure 4.7: Compressive strengths for different mix design

4.3.3 Failure mode

The failure mode of N-sand/ M-sand/ QD based geopolymer mortar was found similar to the N-sand based cement mortar. Also, the mode of failure was found satisfactory as specified in BS EN 12390-3:2009 (2009) (Figure 4.8 and Figure 4.9).

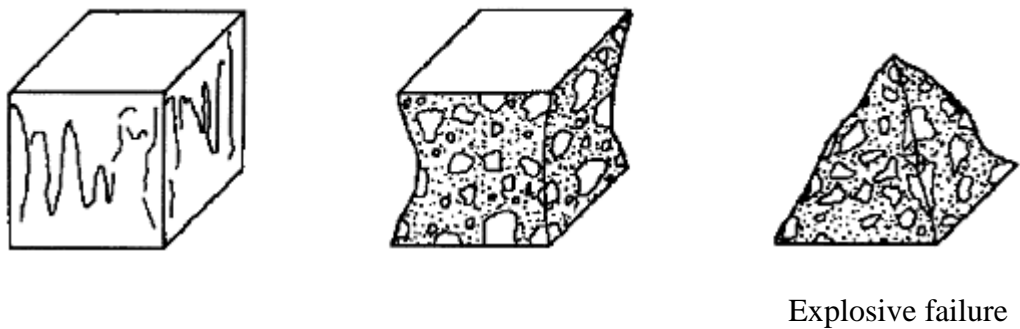


Figure 4.8: Satisfactory failures (BS EN 12390-3:2009 (2009))

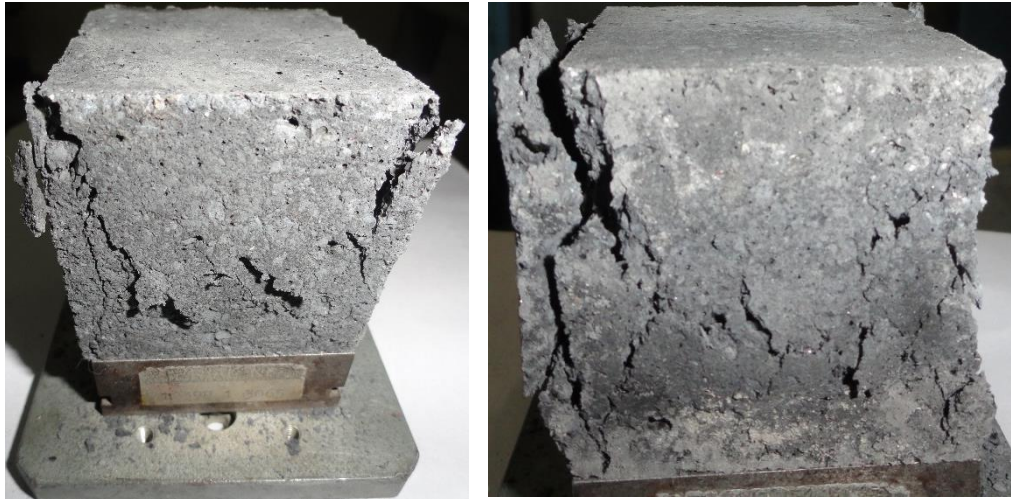


Figure 4.9: Failure mode of geopolymer mortar

4.3.4 Role of POFA-FA on the development of compressive strength

The high content of pozzolanic silica and alumina in POFA and FA causes the silica-based geopolymerization in presence of alkaline solution. The silica/ alumina ratio, total content of silica, alumina and Fe_2O_3 affect the strength development (Davidovits, 2008). It is to be noted that the binders, POFA and FA were kept at equal proportion for all the mixes. The silica/alumina ratio and the total contents of silica, alumina and Fe_2O_3 in the POFA-FA mixture were found to be 3.95 and 82%, respectively and Autef et al. (2013a) reported that high amount of silica content increased the rate of geopolymerization.

As seen from Table 4.1, 90% of the particles of POFA and FA were found below 38.27 and 101.74 μm , respectively. The finer particles decrease the volume of capillary pore effectively (Chindaprasirt et al., 2007). The angular and irregular shaped QD particles create voids within the mortar. The filler effect of the fine FA and POFA might reduce the voids and Ashtiani et al. (2013) reported that higher packing factor enhanced the compressive strength.

The effect of oven curing on the strength development also plays significant role in geopolymer mortar as seen from the 3-day compressive strength; as seen from Table 4.6,

the achievement of 76% of 28-day compressive strength at the age of 3-day is attributed to the heat curing in oven at 65⁰C temperature for 24 hours. However, the rate of strength increment from 3-day to 7-day was found between 12 and 16% and beyond 7-day, it is much lower as reported in Table 4.6. Similar finding on high early strength development due to heat curing at elevated temperature was reported elsewhere (Davidovits, 2008; Pangdaeng et al., 2013). The fineness of POFA and FA also have significant effect on the development of early age strength at 3-day. The finer particles have larger surface area that may increase the reactivity in the geopolymerization process (Somna et al., 2011).

Table 4.6: Percentage of increment of compressive strength

Equations		Mortar ID											
		M1	M2	M3	M4	M5	M6	M7	M8	M9	M10	M11	M12
3 to 7 day	$\frac{S7 - S3}{S3} \times 100$	12.5	9.9	9.8	9.8	11.2	20.4	6.8	6.8	8.1	16.6	8.6	16.8
7 to 14 day	$\frac{S14 - S7}{S7} \times 100$	14.9	9.0	23.9	15.1	14.2	9.0	8.8	8.8	11.1	14.3	7.9	22.7
14 to 28 day	$\frac{S28 - S14}{S3} \times 100$	3.7	4.2	4.1	4.1	4.5	5.2	4.0	4.0	4.0	4.4	4.0	4.8
S3, S7, S14, S28 are the compressive strengths at 3-, 7-, 14-, and 28-day, respectively													

4.3.5 Effect of particle size of N-sand/ M-sand/QD on geopolymerization

The volume of fine particles (below 600 μm) of N-sand is slightly higher than that of M-sand and QD (Table 4.2). The fine particles may have positive effect on the geopolymerization process and therefore a slightly higher 28-day compressive strength (27.8 MPa) was noticed for N-sand than that of M-sand (25.2 MPa) and QD (26.1 MPa). Tasong et al. (1998) reported that a wide range of chemical interactions is anticipated within the interfacial transition zone between aggregate and cement paste matrix. Isabella et al. (2003) found a positive effect on the addition of soluble silicates into leaching solution by promoting significant structural breakdown of sand & metakaolin; they also reported that larger surface area of the aggregate interacted with soluble silicates releasing a greater amount of Si. It is conceivable that the fine particles of N-sand/ M-sand/ QD may interact with the alkaline solution in mortar; the rate of interaction with N-sand, M-

sand and QD surfaces may be related to their particle surface area. A strong bonding between geopolymer matrix and the aggregate surface by the ionic interaction may exist (Lee and van Deventer, 2007) and this could enhance the development of compressive strength of N-sand/ M-sand/ QD based geopolymer mortar.

4.3.6 Effect of molarity of alkaline activated solution on development of compressive strength

The effect of molarity of alkaline activated solution (NaOH solution) on the 28-day compressive strength is shown in Figure 4.10. As shown in Figure 4.11 the early age compressive strength at the age of 3-day for the mix with 14 M was found between 55 and 77% of the 28-day strength and this is higher than the corresponding strength of mixes with 12M. The use of low concentrated alkaline solution causes a weak reaction (Puertas et al., 2000). The compressive strength increase in the mixes with high molarity based alkaline solution was due to the leaching of silica and alumina (Chindapasirt et al., 2009). The NaOH concentration performs the dissolution process and bonding of solid particles in the geopolymeric environment (Álvarez-Ayuso et al., 2008). The use of high concentration of NaOH solution leads to greater dissolution and increases the geopolymerization reaction (Guo et al., 2010) and this is supported by various studies (Kovalchuk et al., 2007; Hardjito et al., 2009; Somna et al., 2011; Memon et al., 2013).

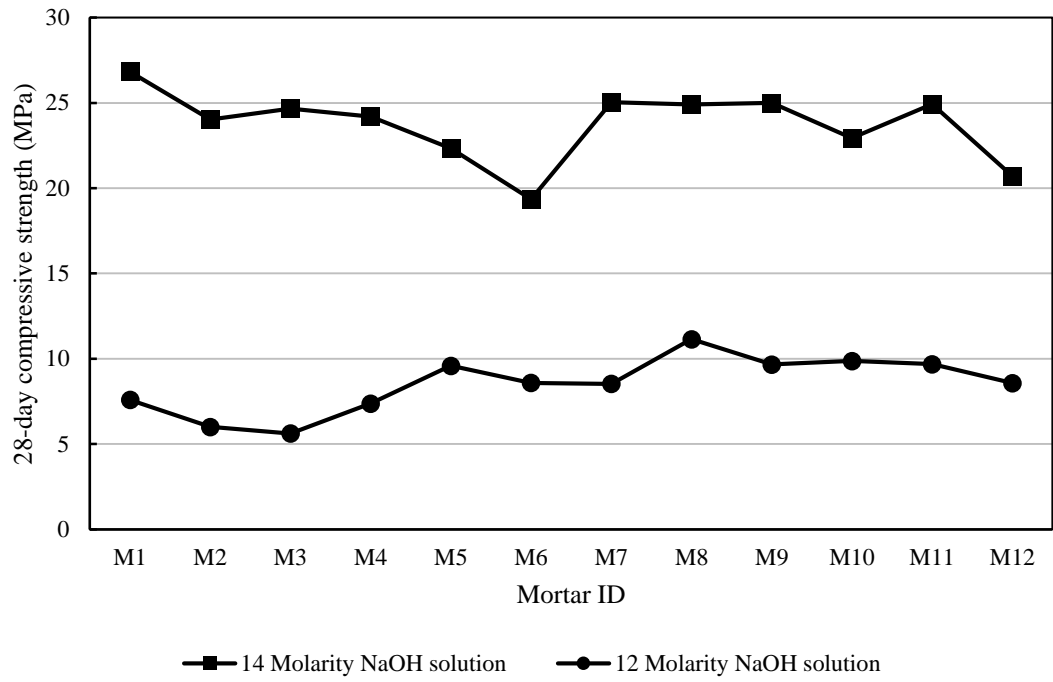


Figure 4.10: Effect of molarity of alkaline activated solution in compressive strength

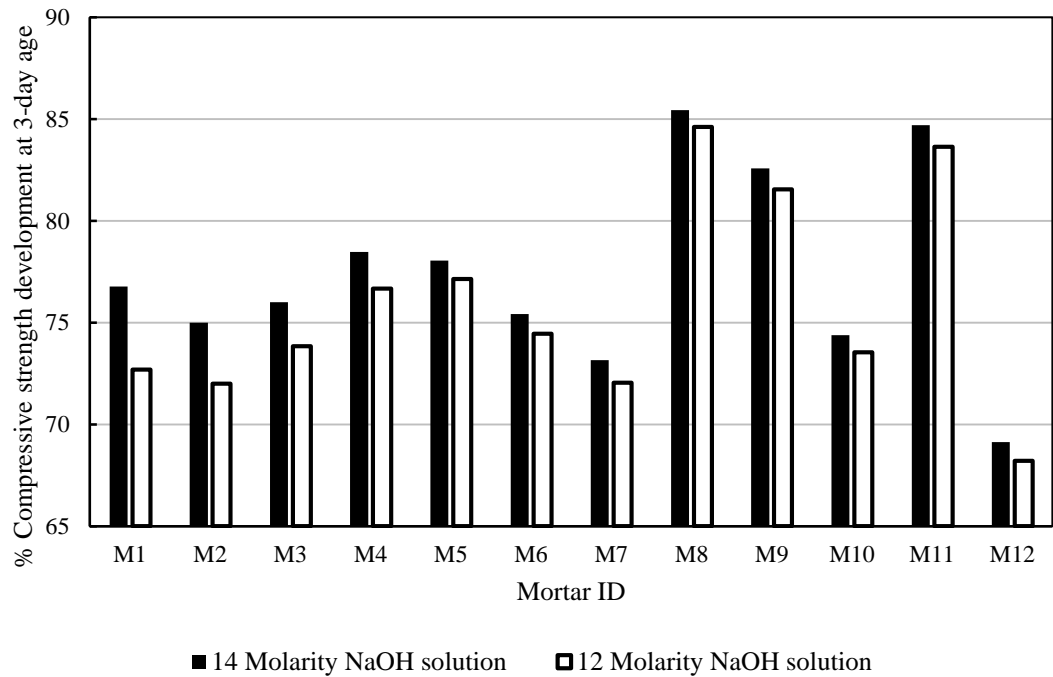


Figure 4.11: Development of early age compressive strength

4.3.7 Effect of fineness modulus on compressive strength

Figure 4.12 shows the variation of fineness modulus due to the different mix proportion of N-sand, M-sand and QD. The fineness modulus for the composite mix proportion was calculated by arithmetic proportion (Alexander and Mindess, 2005). For example, mortar ID M11 represents N-sand: M-sand: QD = 25: 50: 25.

Fineness modulus (FM) for M11 = $FM_{N\text{-sand}} \times 0.25 + FM_{M\text{-sand}} \times 0.50 + FM_{QD} \times 0.25 = 2.72$

Hence, the fineness moduli of the various combination of the fine aggregates using N-sand, M-sand and QD vary from 2.66 to 2.88. The values of fineness modulus of the combined fine aggregates in this investigation fall in the medium range based on the classification as proposed by Alexander and Mindess (2005) which is shown in Figure 4.7. It is to be noted that the binder content is kept constant for all the mixes; The mixes with more fine particles need large volume of paste as the surface area is more. The variation in the compressive strength of the mortars between 20.36 and 26.03 MPa could be attributed to the paste volume and the fineness or coarseness of the fine aggregates.

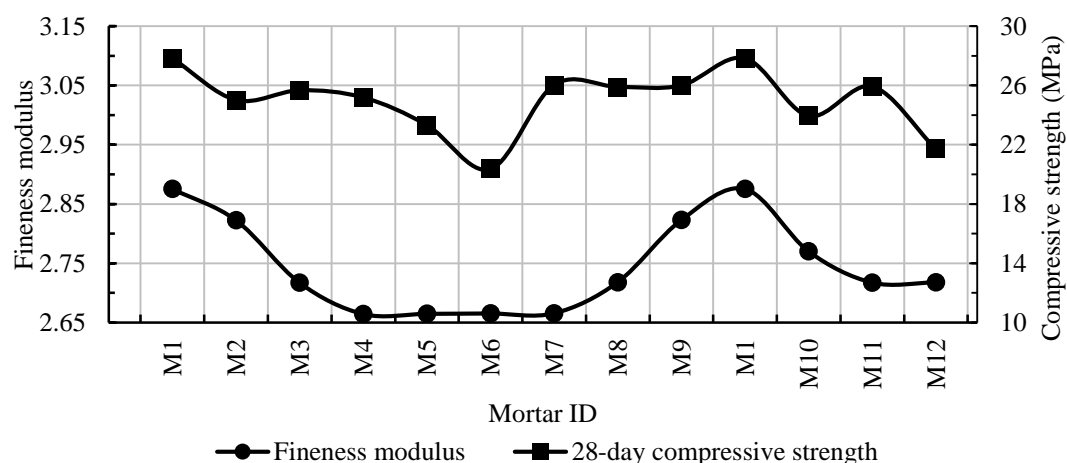


Figure 4.12: Effect of fineness modulus of composite fine aggregates in development of compressive strength

Table 4.7: Categorization of fineness of sand, using fineness modulus (Alexander and Mindess, 2005)

Fineness modulus	Sand fineness
<1.0	Very fine
1.0 – 2.0	Fine
2.0 – 2.9	Medium
2.9 – 3.5	Coarse
>3.5	Very coarse

4.3.8 Effect of N-sand, M-Sand and QD on development of compressive strength

The compressive strengths at different ages along with their respective percentages with age are shown in Figure 4.13 and Figure 4.14. The mortar using 100% N-sand shows better compressive strength performance than the mix with M-sand. The replacement of N-sand by M-sand reduces compressive strength.

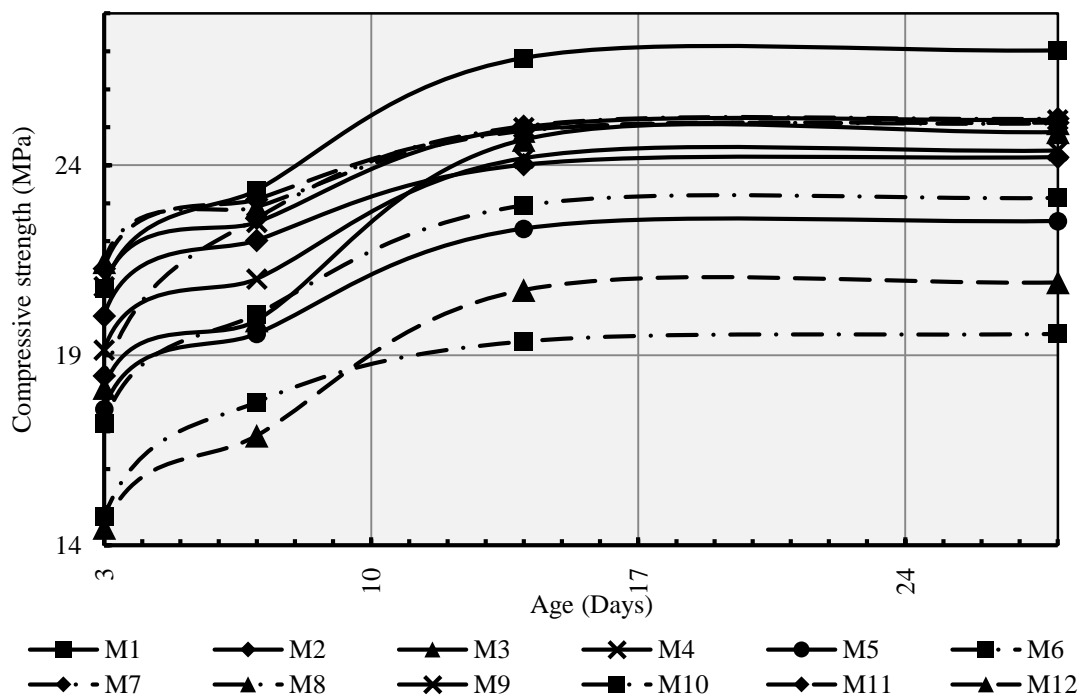


Figure 4.13: Compressive strength (MPa) vs age (days)

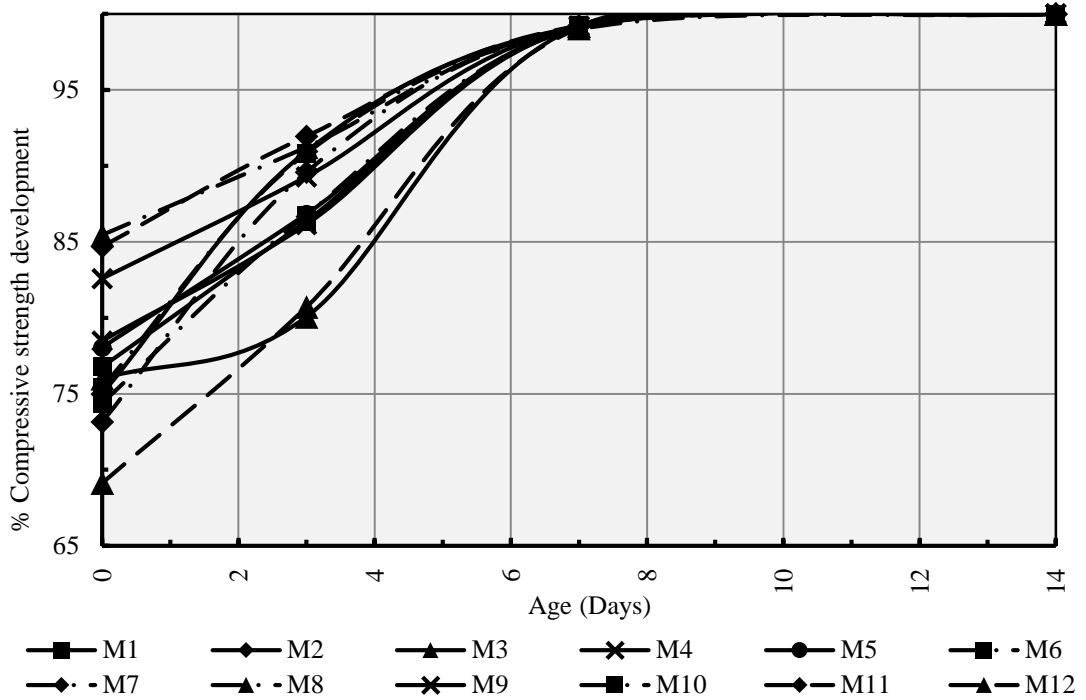


Figure 4.14: % Compressive strength development vs age (days)

The N-sand contains rounder and smoother particle than M-sand (Quiroga and Fowler, 2004). Hudson (1999a) reported that rough aggregates have a propensity for increasing water demand for a given workability. Thus, for a given water content, the N-sand is more workable than M-sand (Quiroga and Fowler, 2004). The rough surfaces of M-sand particles demand more water than N-sand. In this study, the water and binder content was kept constant. This could lead to absorption of water from the alkali-solution and this might have affected the reactivity of binder in alkali solution. Thus, the reduction of the compressive strength due to the replacement of N-sand by M-sand could be attributed to absorption of water by the rough surfaces of M-sand.

The 28-day compressive strengths of about 28 MPa and 25 MPa were obtained for specimens with 100% N-sand and 100% M-sand, respectively. The reduction of strength between these two mixes was found only 3 MPa and similar finding on the strength difference for M-sand and N-sand was reported by Dumitru et al. (1999).

The mortar using 100% QD shows better performance than the mix with M-sand in Figure 4.13 and Figure 4.14. The presence of high percentage of QD in composite fine aggregate mixture of M-sand & QD reduces the strength (M5, M6). The particle shape and texture may influence the strength reduction.

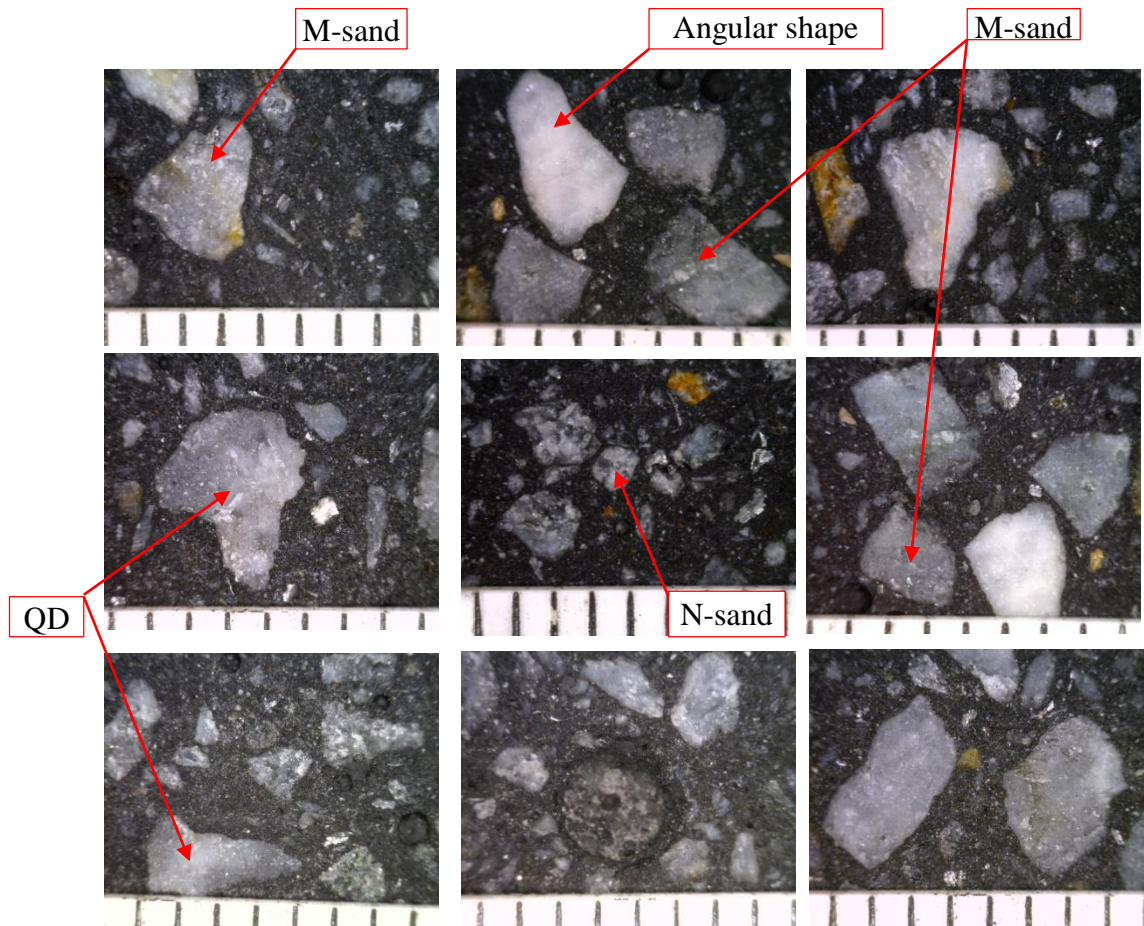


Figure 4.15: N-sand/ M-sand/ QD interlocking in geopolymer mortar (Magnification rate = 5)

The QD has sharp angular particles as shown in Figure 4.3. According to Quiroga and Fowler (2004) and Kaplan (1960), the angularity of aggregates has a positive effect on the compressive strength. Further, the angularity of the aggregates enhances the bond between the matrix and the aggregates due to its surface texture. Galloway (1994) also reported the effect of surface texture on the strength significantly as rough surface

increase bonding between the aggregate surface and the paste. Figure 4.15 shows the interlocking of N-sand/ M-sand/ QD in geopolymer mortar.

The combination of M-sand and QD might tend to create voids due to the combination of semi-rounded particles and the sharp angular particles. Further, the increase in voids demands more water for a given workability and hence decreases the strength (Quiroga and Fowler, 2004). Since the water-binder ratio was maintained constant for all the mixes, the composite mixes that contained both M-sand and QD might have absorbed more water that could influence the geopolymerization process. This might reduce the strength for mixes with high percentage of QD in the mixes that contained both the M-sand and QD. Nevertheless, the strength reduction between the mixes with 100% QD and 100% M-sand was negligible and similar finding was reported by Dumitru et al. (1999).

Figure 4.13 and Figure 4.14 shows that there is not much significant difference in the compressive strength due to the replacement of N-sand by QD either partially or fully. The mixes with N-sand developed better strength due to its well-graded and round particles. As mentioned the angularity of QD particles enhances the compressive strength and for a given workability, the rough surface increases water demand (Quiroga and Fowler, 2004).

The 28-day compressive strength of mixes with N-sand and QD were 28 MPa and 26 MPa, respectively. Again, the strength difference between these two mixes was about 2 MPa and negligible. Raman et al. (2011) found the similar effect of QD in rice husk ash based concrete and reported that inclusion of QD as partial replacement for sand slightly decreases the compressive strength of concrete. Dumitru et al. (1999) reported that the replacement of N-sand by QD produces comparable strength and hence QD is viable replacement to conventional N-sand for sustainable material.

4.3.9 Comparison of M-sand and QD in geopolymer mortar with published data

Dumitru et al. (1999) investigated the effect of river sand, manufactured quarry fines and unprocessed quarry fines, that are comparable to the research materials N-sand, M-sand and QD, respectively used in this research work.

Table 4.8: Development of compressive strength using N-sand, M-sand and QD

Age	3-day		7-day		14-day		28-day	
Fine aggregate	NC	GM	NC	GM	NC	GM	NC	GM
N-sand (100%)	22	21	28	23	33	27	37	28
M-Sand (100%)	15	19	23	21	26	24	32	25
QD (100%)	19	21	28	23	32	25	37	26
NC results from [Dumitru et al. (1999)] experiment on OPC concrete								
GM results from this experiment on geopolymer mortar								

The development of 3-, 7-, 14- and 28-day compressive strength is quite similar to the outcome from this investigation; as seen from the Table 4.8. The effect of QD, M-sand and N-sand in both normal concrete (NC) and geopolymer mortar (GM) between the 3- and 14-day shows similar trends, albeit these are different kinds of concretes. As known, the geopolymer concrete develops high early strength due to geopolymerization and hence the strength difference between the 14- and 28-day strength was not much different, unlike normal concrete where the strength development continues beyond 14-day.

4.4 Mix Design 2: POFA-FA-MK and POFA-MK based geopolymer concrete

After developing appropriate mortar, the next stage of work aimed at developing structural grade geopolymer concrete using OPS as coarse aggregate; in addition, the use of POFA-FA-MK and POFA-MK as combined binders was investigated and reported in the subsequent sections. Since M-sand was found to produce equivalent strength as that of N-sand in the mortar, it was used to replace conventional N-sand in the development

of geopolymer concrete. The binder combination that produced structural grade concrete was used for further investigation.

4.4.1 Properties of fresh concrete

The fresh density and the slump value are shown in Table 4.9. The changes of fresh density in this experiment were due to the specific gravity of binding material since all other proportions were kept constant. The specific gravity of POFA, FA and MK were measured as 2.2, 2.34 and 2.5, respectively. The specific gravity of the mix proportions were calculated by arithmetic proportion as shown in Table 4.9. The fresh density of concrete increases with the replacement of POFA/ FA by MK since the specific gravity of MK is higher than POFA and MK. The arithmetic calculation for the composite binding material also reflects the increment of specific gravity due to the replacement of POFA/ FA by MK.

Table 4.9: Fresh density and slump value of fresh concrete

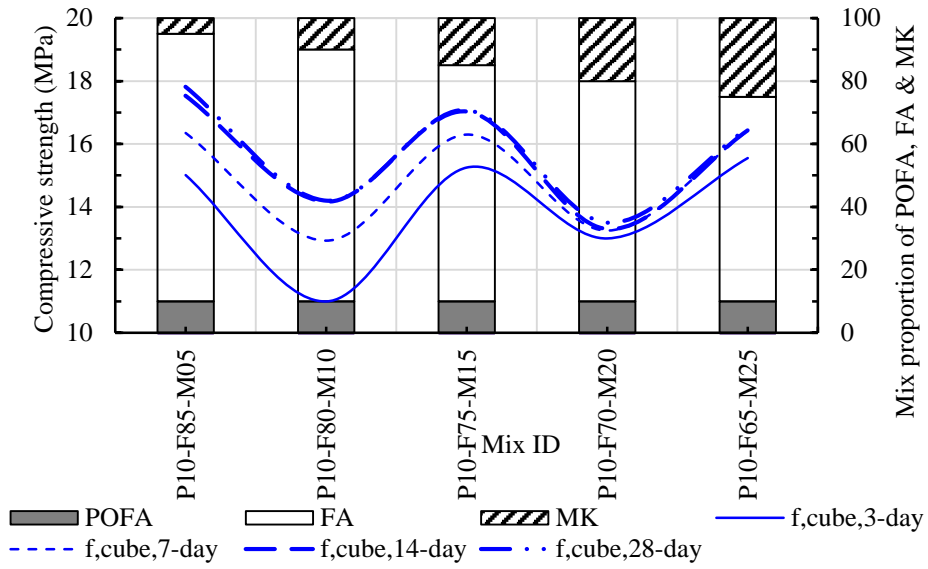
Properties of fresh concrete	P10-F85-M05	P10-F80-M10	P10-F75-M15	P10-F70-M20	P10-F65-M25	P90-M10	P80-M20	P70-M30	P60-M40
Fresh density, kg/m ³	1856	1857	1859	1860	1862	1833	1839	1845	1851
Slump, mm	120	75	50	42	30	0	0	0	0
Specific gravity of binders	2.33	2.34	2.35	2.36	2.37	2.23	2.26	2.29	2.32

The slump is an important factor of measuring the workability of fresh concrete. However, no standard or limit has yet been established for geopolymer concrete. Generally, water or superplasticizer is added in normal Portland cement concrete to achieve good workability. Nevertheless, usage of excessive water decreases the strength of geopolymer concrete. Excessive quantity of water is not recommended for proper

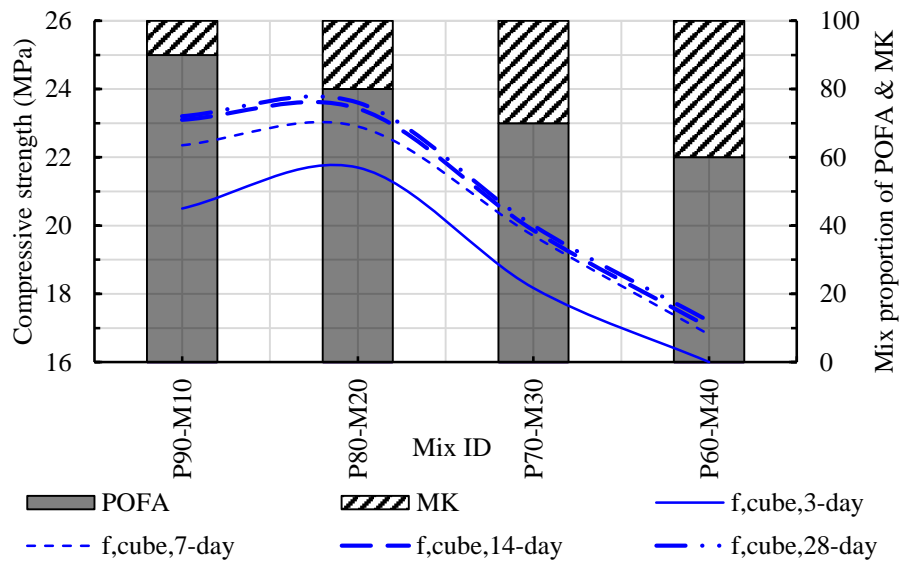
geopolymerization (Davidovits, 1991, 1994b). Therefore, minimum required water was used in consistent rate for all mix proportions; however, this resulted in zero slump for POFA-MK based concrete. Extended vibration (10 second/ layer casting) was provided during the casting of specimens into the moulds to overcome low or zero workability. Segregation was not noticed for the extended vibration. On the other hand, the mixes with POFA-FA-MK based binding materials produced higher slump values of 30-120 mm. It is well established that FA with spherical particles produce high workability in concrete; however, the replacement of FA with MK reduces the slump values due to viscous mixes. As the additional water was kept constant for all the mixes, the effect of adding more MK for the replacement of FA has negative effect on the workability.

4.4.2 Compressive strength

The variation of compressive strength of oil palm shell geopolymer concrete (OPSGC) consisting of different proportion of pozzolanic binding materials such as POFA-FA-MK and POFA-MK is shown in Figure 4.16 and Figure 4.17. Table 4.12 also shows the development of compressive strength at the ages of 3-, 7-, 14-, and 28-day. The ratios of aggregate/ binder, water/ binder, alkaline activator/ binder and the curing condition were kept constant for all OPSGC. The physical and chemical properties of materials as well as activators and the curing condition have significant effect on the development of compressive strength as reported by many researchers (Shafiq et al., 2013a; Abdulkareem et al., 2014; Bagheri and Nazari, 2014; Liu et al., 2014; Yew et al., 2014; Yusuf et al., 2014).



(a)



(b)

Figure 4.16: Compressive strength of GC for different mix proportions of (a) POFA, FA & MK and (b) POFA & MK

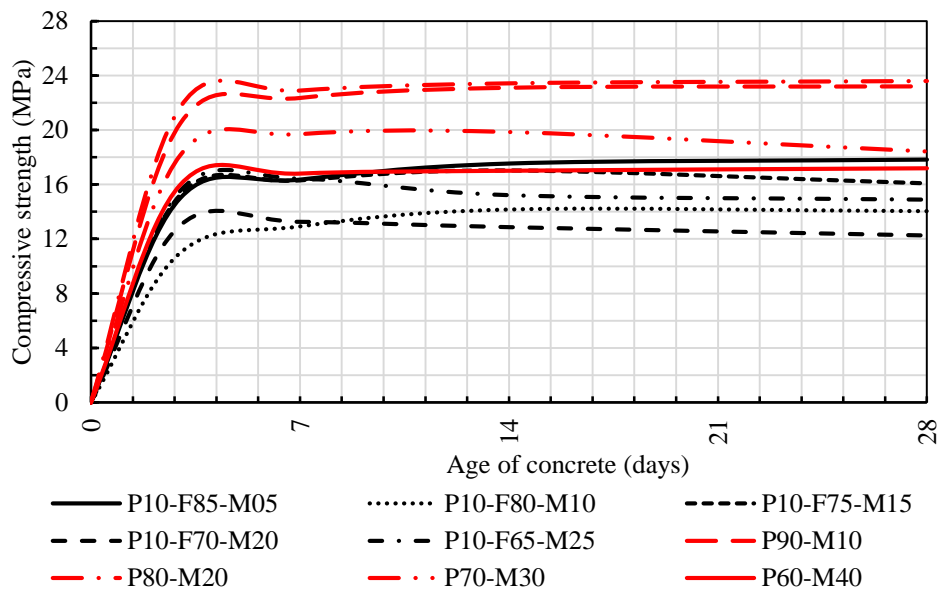


Figure 4.17: Compressive strength at age of 3-, 7-, 14- and 28-day

The compressive strength varies (Figure 4.16) between 11 and 18 MPa for the mixes with FA, MK and POFA; it should be noted that in these mixes, the FA was replaced with MK from 5-25% keeping POFA constant at 10%. Among these mix proportions of POFA-FA-MK, the maximum 28-day compressive strength of about 18 MPa was obtained for the mix with 5% of MK and 85% of FA. There was no consistent variation in the compressive strength due to the gradual replacement of FA. A decrease of compressive strength (14 MPa, 28-day) was found for the replacement of FA with MK; however, an enhancement in the compressive strength (16 MPa, 28-day) was found for 15% FA replacement with MK. The inconsistent strength development might be due to the variation of the combination of chemical compounds of binding materials. The binder combination of FA-MK-POFA did not produce the desired compressive strength due to the required silica-alumina proportion.

The change of the binder contents by omitting the FA and replacing it with POFA produced the highest strength. The highest 28-day compressive strength of about 24 MPa was obtained for the mix with the combination of POFA and MK; this mix consisted of 90% of POFA and 10% of MK. POFA, which has a major compound of silica reacts with

MK due to the presence of alumina compounds in MK. The reactivity also depends on the curing condition, alkaline solution and additional water. The curing condition, alkaline solution and water content were kept constant for all the mixes. The effects of these factors as well as the variables such as POFA and MK on the development of compressive strength are described in the following sub-clauses.

4.4.2.1 Selection of curing temperature

The mix proportions of the POFA-FA-MK and POFA-MK based binding materials as investigated in this research work are a combination of low-calcium based geopolymer solid materials (Table 4.13) according to the definition of ASTM C618-12a (2012). The heat curing was adopted due to proper geopolymeric reaction as recommended by Rangan (2008). Both curing time and temperature have substantial effect on the development of strength (Hardjito and Rangan, 2005). Bagheri and Nazari (2014) specified the curing temperature as the most effective factor on the compressive strength and the proportion of pozzolans (i.e. the quantity of the reactive granulated blast furnace slag with fly ash), the concentration of sodium hydroxide (NaOH) and oven curing time as other relevant parameters that affect the compressive strength albeit with less significance.

The curing temperature of 40 – 75⁰C is normally required to obtain a reasonable strength development in fly ash-based i.e. alumino-silicate based geopolymer concrete (Bakharev, 2006; Pangdaeng et al., 2013). The higher curing temperature may enhance compressive strength of conventional geopolymer concrete (Hardjito and Rangan, 2005); on the contrary, light-weight-aggregate-geopolymer-concrete (LWAGC) loses the compressive strength at a very low rate with increasing elevated temperature after 70⁰C (Abdulkareem et al., 2014).

Table 4.10: Effect of heat curing temperature and time on compressive strength

Research Work	Mix proportion	Binding Material	AA/binder	SS/SH(M)	Heat curing condition	f_c , MPa (age-day)
1	1:1.16:2.72 (Binder:Sand:Granite)	FA	0.35	2.5 (14)	48 hours (30°C)	49 (7)
					24 hours (60°C)	68 (28)
2	1:3:0 (Binder:Sand)	MK	0.83	-	4 hours (60°C)	50 (7)
3	1:2.41:1.42	FA	0.60	1 (12)	24 hours (70°C)	18.75 (28)
4	1:1.125:0.375 (Binder:M-sand:OPS)	POFA-FA-MK, POFA-MK	0.40	2.5 (14)	48 hours (65°C)	12.25 – 23.60 (28)

Legend:

1	Hardjito and Rangan (2005)	3	Abdulkareem et al. (2014)
2	Rovnaník (2010)	4	This research work

AA/binder Alkaline activator/ binder
SS/SH(M) liquid Sodium Silicate/ Sodium hydroxide solution (molarity of NaOH solution)
FA = Fly ash M-sand= Manufactured sand
MK = Metakaoline
POFA = Palm oil fuel ash OPS = Oil palm shell

(Yusuf et al., 2014) Generally, the development of compressive strength takes place up to 48 hours with a high temperature curing condition (Hardjito et al., 2005). Thus based on the recommendation from previous research work for light-weight concrete, a temperature of 65°C for a period of 48 hours was selected. After the removal of the specimens from the curing chamber, these were kept in laboratory condition of 28°C and relative humidity of 79%.

4.4.2.2 Effect of alkaline solution and water content on the development of compressive strength

The combination of sodium hydroxide (NaOH) and sodium silicate (Na₂SiO₃) or potassium hydroxide and potassium silicate is used for geopolymer concrete, mostly (Palomo et al., 1999; Barbosa et al., 2000; Rangan, 2008; Memon et al., 2013). Previous researchers found liquid Na₂SiO₃ in combination with NaOH as an effective activator due to the reactivity and the cost of the alkaline solutions (Palomo et al., 1999; Xu and Van Deventer, 2000; Fernández-Jiménez et al., 2005). Hardjito et al. (2005) observed an insignificant effect on the compressive strength due to the increase of Na₂O/SiO₂ ratio

and recommended higher concentration (in terms of molar) of sodium hydroxide (NaOH) solution that could enhance the compressive strength. Table 4.11 shows a comparison of compressive strength with the previous research works due to the effect of alkaline solution and water content.

Table 4.11: Compressive strength of geopolymer concrete using alkaline activator

Research works	SS/SH (SH)	AA/B	M ₂ O/SiO ₂ (M ₂ O/Al ₂ O ₃)	SiO ₂ / Al ₂ O ₃ (H ₂ O/M ₂ O)	<i>f_c</i> , MPa (Specimen)	Remarks
1	-	0.25 & 0.30	1.23	-	52.7 & 62.6 Concrete with NWA	65°C curing for 24h
2	1.5 (15)	0.66	0.26 (1.08)	4.14 (10.40)	32 (mortar)	Sand/binder=2 65°C curing for 48hrs
3	2.5 (14)	0.4	0.06 – 0.13 (0.13 – 1.19)	2.08 – 9.26 (4.12 – 9.89)	12.25 – 23.60 (OPSGC)	OPS/binder=0.375 M-sand/binder=1.125 65°C curing for 48hrs

Legend:
 1 Palomo et al. (1999)
 2 Chindaprasirt et al. (2009)
 3 **Present research work**
 SS/SH liquid Na₂SiO₃/NaOH solution; SH NaOH molarity
 AA/B - Alkaline activator/binder; *f_c* Compressive strength
 M₂O - Na₂O or K₂O or combination of Na₂O and K₂O

In this work, the ratios of liquid Na₂SiO₃/NaOH solution (14M) and alkaline solution/binder were kept constant as 2.5 and 0.4; the compressive strength of the mixes was found in range of 12 to 24 MPa. Palomo et al. (1999) obtained the highest compressive strength using the ratio of alkaline activator to FA of 0.25 to 0.30. The higher compressive strength of their work could be attributed to NWA used in their work compared to OPS that has less stiffness. Xu and Van Deventer (2000) achieved the maximum compressive strength of 19 MPa by a geopolymeric reaction with alkaline activator to alumino-silicate powder ratio of 0.33 by mass. Bakharev (2005) prepared low-calcium (Class F) FA-based geopolymers with a proportion of 0.3 of activator to FA and activated FA using either water glass (sodium silicate) or with NaOH solution. Hardjito and Rangan (2005) used two different concentration of NaOH solution and prepared FA-based geopolymer applying activator/ FA ratio as 0.35. Rangan (2008) recommended the activator/ FA mass

mixing ratio as 0.30 to 0.45 though Chindaprasirt et al. (2009) carried on an experiment on high calcium FA based geopolymer with an activator/ FA ratio 0.66.

Table 4.12: Compressive strength (Mix design 2)

Mix Designation	Compressive strength, f_{cu} (MPa)				Flexural strength, f_f (MPa)	Splitting tensile strength, f_t (MPa)	Young's modulus elasticity, E (GPa)	Poisson's ratio
	3-day	7-day	14-day	28-day				
P10-F85-M05	15.0	16.4	17.5	17.8	2.98	1.24	5.20	0.247
P10-F80-M10	11.0	12.9	14.2	14.1	2.02	1.18	4.37	0.202
P10-F75-M15	15.3	16.3	17.0	16.1	2.21	1.09	4.90	0.251
P10-F70-M20	13.0	13.3	12.9	12.3	1.76	0.87	3.38	0.197
P10-F65-M25	15.6	16.4	15.2	14.9	1.79	1.11	4.13	0.573
P90-M10	20.5	22.4	23.1	23.2	3.41	2.14	6.36	0.176
P80-M20	21.7	22.9	23.4	23.6	3.32	1.75	7.06	0.125
P70-M30	18.2	19.7	19.9	18.4	2.35	1.43	6.47	0.179
P60-M40	16.0	16.8	17.0	17.2	1.94	1.27	6.47	0.179

4.4.2.3 Effect of chemical compounds on development of compressive strength

The variables of this investigation was the proportion of POFA, FA and MK; therefore, the variation of strength development was mainly due to the physical and chemical properties of POFA, FA and MK (Table 4.1). The proportion of oxide compositions is shown in Table 4.13 and the effect on compressive strength in Figure 4.18. The POFA-MK-based OPSGC (PMGC) mixes show better performance than POFA-FA-MK-based OPSGC (PFMGC). As shown in Figure 4.16 (b), the compressive strengths of PMGCs are in a range of 17.2 to 23.2 MPa for the proportion of POFA/ MK 1.5 to 9, respectively.

Table 4.13: Estimated chemical composition in mix proportions

Mix Designation	Oxide composition, %											
	CaO	SiO ₂	Al ₂ O ₃	MgO	Na ₂ O	SO ₃	K ₂ O	Fe ₂ O ₃	SiO ₂ /Al ₂ O ₃	M ₂ O/SiO ₂	M ₂ O/Al ₂ O ₃	H ₂ O/M ₂ O
P10-F85-M05	5.07	55.92	25.61	1.34	0.39	0.97	1.64	4.95	2.34	0.07	0.15	9.38
P10-F80-M10	4.81	55.82	26.37	1.30	0.37	0.92	1.60	4.79	2.27	0.07	0.15	9.51
P10-F75-M15	4.55	55.71	27.14	1.25	0.35	0.87	1.57	4.64	2.20	0.06	0.14	9.63
P10-F70-M20	4.28	55.61	27.90	1.20	0.33	0.82	1.54	4.48	2.14	0.06	0.14	9.76
P10-F65-M25	4.02	55.51	28.66	1.15	0.31	0.78	1.50	4.32	2.08	0.06	0.13	9.89
P90-M10	5.02	66.21	7.59	3.65	0.15	0.97	6.93	4.44	9.26	0.13	1.19	4.12
P80-M20	4.46	64.71	11.46	3.26	0.14	0.87	6.20	4.17	6.00	0.12	0.72	4.49
P70-M30	3.91	63.20	15.33	2.86	0.14	0.76	5.47	3.90	4.38	0.11	0.49	4.93
P60-M40	3.36	61.70	19.20	2.47	0.13	0.66	4.74	3.63	3.42	0.10	0.35	5.47

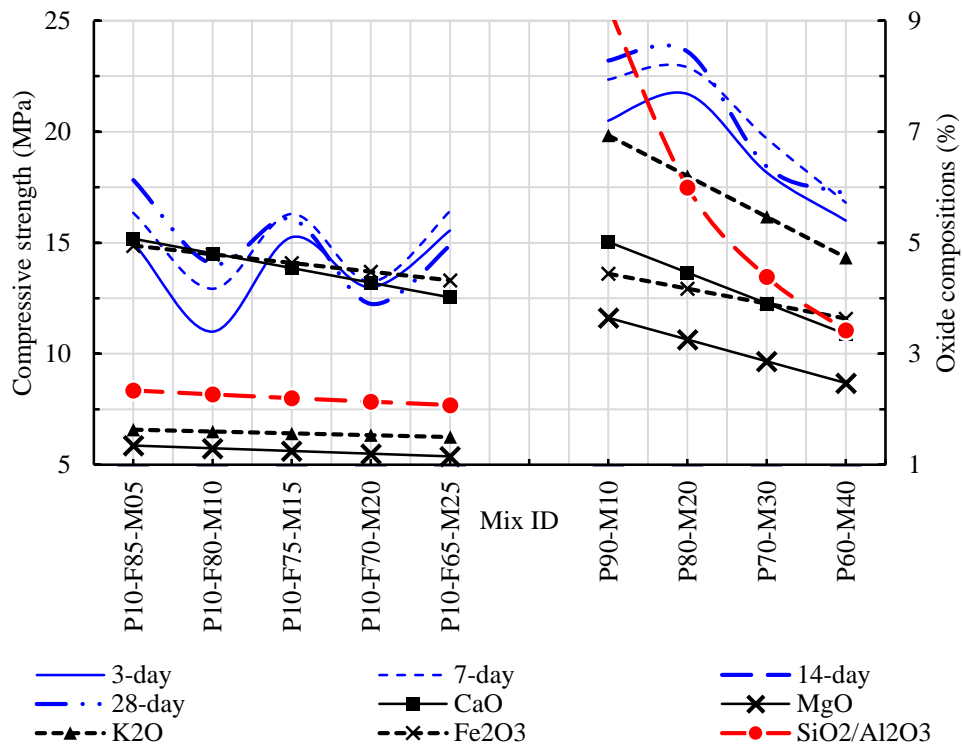


Figure 4.18: Relationship between compressive strength and oxide compounds

It is seen from Figure 4.18 that the proportion of silica and alumina has an important role in the development of compressive strength. Other oxide compounds in this research work have not shown much variation. P90-M10 shows the compressive strength of about 23 MPa due to the high silica/alumina ratio; a gradual reduction of compressive strength is noticed with lower silica/alumina ratio in the mixes (Figure 4.19). Rashad (2014), cited from Zhang et al. (2009), reported that appropriate addition of MK improved the compressive strength. Wu and Sun (2010) investigated the FA/MK-based geopolymer concrete by replacing FA in different proportion with MK and reported the effect of MK in the development of geopolymer concrete due to the presence of silica, alumina and calcium oxide (CaO). Since the replacement of POFA with MK varies between 10 and 40%, the quantity of CaO in these composite binders is less than 6%, which may have less effect in building geopolymer in these types of concrete. Since alumina proportion in POFA is very less, replacement of 10% POFA by MK could contribute to the required proportion of silica and alumina in the development of structural grade concrete.

4.4.3 Flexural and indirect tensile strengths

Figure 4.20 shows the relationship among compressive strength, indirect tensile strength, flexure strength and silica/ alumina ratio (S/A). This proportion may be applicable for silica and alumina based geopolymer concrete. The reason of the variation of compressive strength is explained in the sub-clause 4.4.2 . The relationship of flexural and indirect tensile strength with S/A ratio is graphically represented in Figure 4.20. It should be noted that the only variable in this experimental analysis is the proportion of binding materials as well as S/A ratio. Table 4.13 shows the estimated chemical composition computed from the raw material chemical analysis. Hence, the relationships of compressive, indirect tensile and flexure strength with S/A ratio as listed in Figure 4.20 could be appropriate only for the S/A variable.

Table 4.13 shows that there is a very slight difference in the oxide composition of POFA-FA-MK based binding materials and it has insignificant effect on the results of indirect tensile strength. On the other hand, the S/A ratio for the mix P90-M10 as shown in Table 4.12 of about 9.26 has significant effect on both the flexural and indirect tensile strengths (Figure 4.20). Further, the achievement of indirect tensile strength between 1.27 and 2.14 MPa for the S/A ratio of 3.42 to 9.26 (Table 4.13) could be attributed to the higher S/A ratio compared to the PFMGC mixes.

The structural grade concrete mix, P90-M10 with a cube compressive strength of 23 MPa mix also fulfills the minimum requirement of 2MPa for splitting tensile strength. The failure mode of the specimens as shown in Figure 4.19 shows bond failure between the OPS and the matrix.

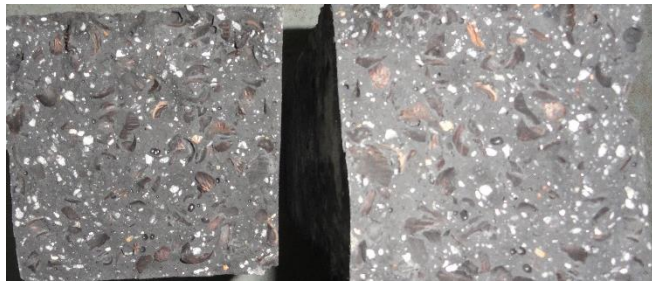


Figure 4.19: Bond failure of OPSGC

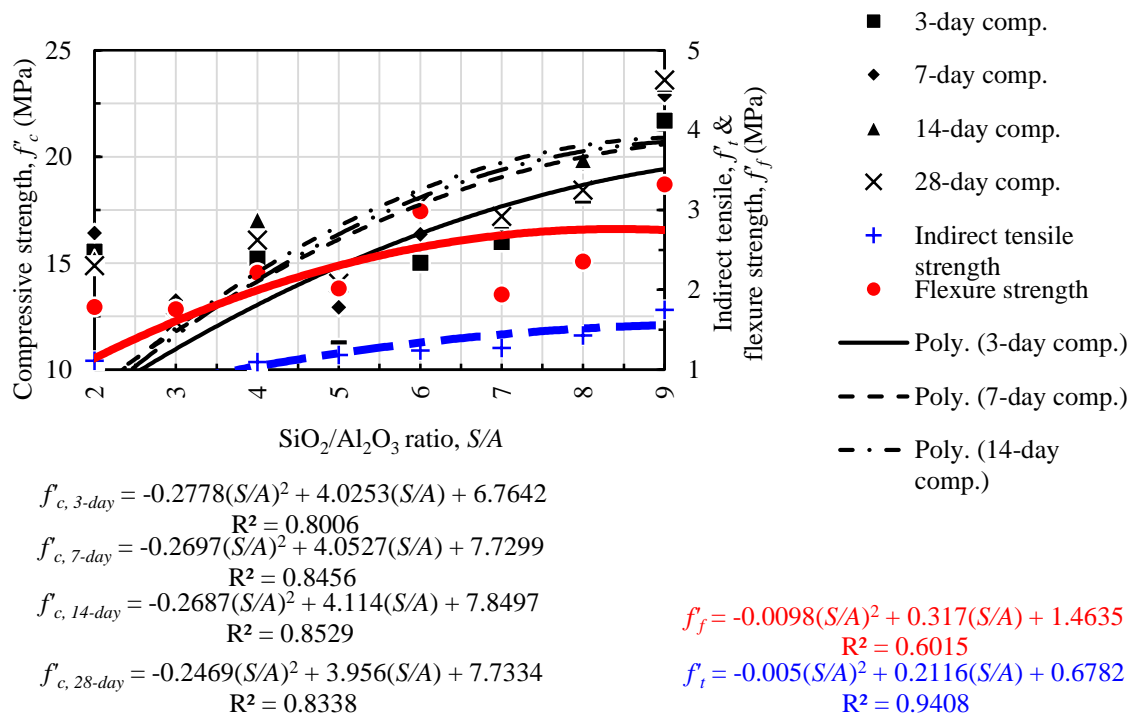


Figure 4.20: Relationship between $\text{SiO}_2/\text{Al}_2\text{O}_3$ and mechanical properties (f'_c, f'_t, f'_f)

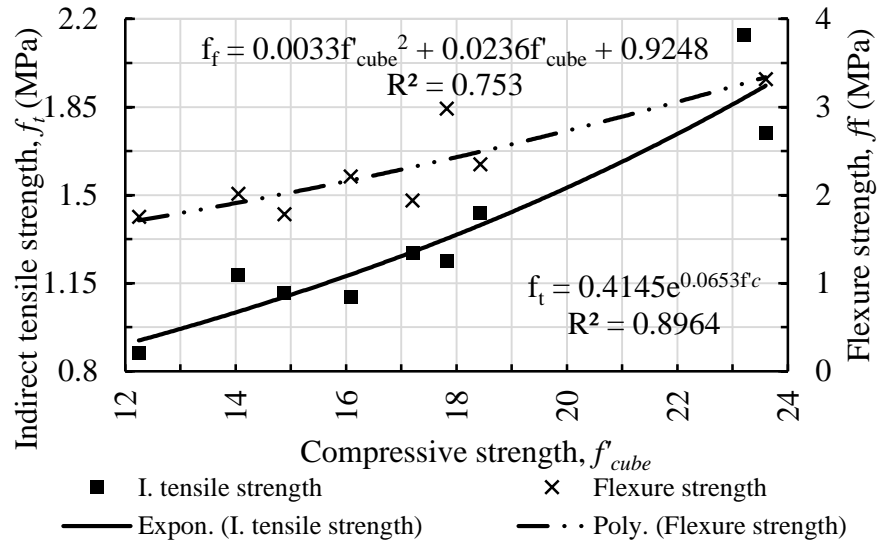


Figure 4.21: Numerical relationship among f_{cube} , f_f and f_t

The experimental correlation between the compressive, indirect tensile and flexure strengths is shown in Figure 4.21. Ryu et al. (2013) recommended Eq. 4.1 for the estimation of indirect tensile strength of fly ash based geopolymer normal weight concrete.

$$f_t = 0.17(f_{cy})^{\frac{3}{4}} \quad \text{Eq. 4.1}$$

Short and Kinniburgh (1978) cited Eq. 4.2 for the lightweight aggregate concrete (LWC).

$$f_t = Kf_{cy}^{\frac{1}{2}} \quad \text{Eq. 4.2}$$

Where, K varies from 0.37 – 0.5, in average to consider 0.42.

Table 4.14 shows the comparison of experimental data with the Eq. 4.1 and Eq. 4.2. The present research work falls in between the equations proposed by Ryu et al. (2013) and Short and Kinniburgh (1978) due to the geopolymer paste and lightweight aggregate used. However, the prediction of the splitting tensile strength by these two equations seems to be in the range of the experimental value.

Table 4.14: Indirect tensile and flexural strength

Mix Designation	Compressive strength (MPa)		Indirect tensile strength (MPa)			Flexural strength (MPa)		
	28-day cube strength	28-day cylinder strength	Experimental data (LWGC)	Eq. 4.1 (NWGC)	Eq. 4.2 (LWC)	Experimental data (LWGC)	Eq. 4.3 (NWC)	Eq. 4.4 (LWC)
P10-F85-M05	17.82	13.19	1.24	1.18	1.53	2.98	2.83	2.05
P10-F80-M10	14.05	10.40	1.18	0.98	1.35	2.02	2.51	1.75
P10-F75-M15	16.08	11.90	1.09	1.09	1.45	2.21	2.69	1.91
P10-F70-M20	12.25	9.07	0.87	0.89	1.26	1.76	2.35	1.59
P10-F65-M25	14.88	11.01	1.11	1.03	1.39	1.79	2.58	1.81
P90-M10	23.20	17.17	2.14	1.43	1.74	3.41	3.23	2.44
P80-M20	23.60	17.46	1.75	1.45	1.75	3.32	3.25	2.47
P70-M30	18.43	13.64	1.43	1.21	1.55	2.35	2.88	2.09
P60-M40	17.20	12.73	1.27	1.15	1.50	1.94	2.78	2.00
LWGC	Lightweight geopolymers concrete							
NWC	Normal weight concrete							
LWC	Lightweight concrete							

The flexural strength was also significantly affected by the S/A ratio like indirect tensile strength. Short and Kinniburgh (1978) proposed Eq. 4.3 for the estimation of flexural strength from the cube strength of NWC.

$$f_t = 0.67 f_{cu}^{1/2} \quad \text{Eq. 4.3}$$

Alengaram et al. (2008) reported following Eq. 4.4 to determine the flexural strength of OPS based lightweight concrete.

$$f_f = 0.3 f_{cu}^{2/3} \quad \text{Eq. 4.4}$$

The comparison of the experimental flexural strength with the proposed Eq. 4.3 and Eq. 4.4 are shown in Table 4.14.

It is noticed from Table 4.14 that the experimental data were found to in close range to that of the predicted by these two equations, Eq. 4.1 and Eq. 4.2. The effect of both the binding material and the OPS could be attributed to the flexural strength. Similar to the indirect splitting strength, the mix with 90% of POFA and 10% of MK produced the

highest flexural strength of 3.41 MPa. The failure mode was found similar to that of the splitting tensile strength with bond failure visible in the broken specimens.

4.4.4 Static modulus of elasticity

The Young's modulus of elasticity (MoE) is graphically represented in Figure 4.22 and the values are shown in Table 4.12.

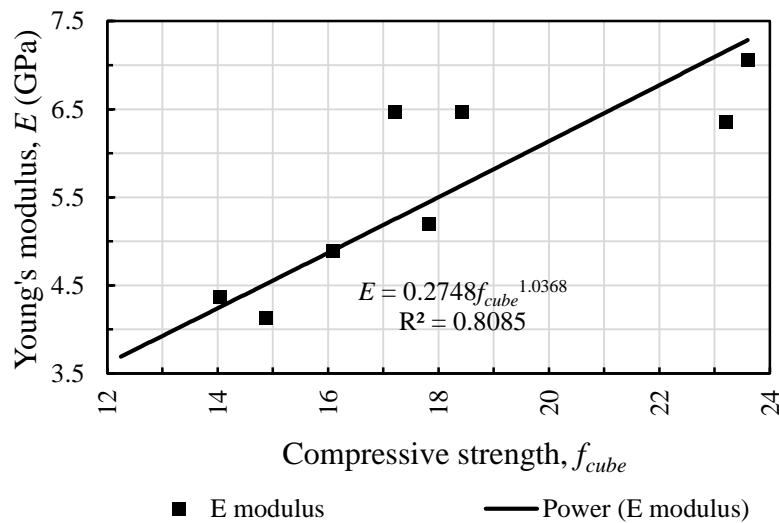


Figure 4.22: Numerical relationship among f_{cube} , and E

The E-value was measured as 27 to 38% of the compressive strength while the Poisson's ratio was determined from 0.12 to 0.57 (Table 4.15). Short and Kinniburgh (1978) reported that MoE is considerably lower in LWC than NWC and ranges between 1/3 to 2/3rd of the corresponding NWC. Alengaram et al. (2011b) recommended Eq. 4.5 for the OPS based lightweight concrete.

$$E = \left(\frac{\rho}{2400} \right)^2 \times 5f_{cube}^{1/3} \quad \text{Eq. 4.5}$$

Where, ρ refers to the density (kg/m^3)

A comparison with the recommended equations to the experimental data is shown in Table 4.15.

Table 4.15: Young's modulus of elasticity and Poisson's ratio

Mix Designation	Density, kg/m ³	Compressive strength (MPa)	Modulus of elasticity				Poisson's ratio
	28-day	28-day cube strength	Experimental data	Eq. 4.5	Eq. 4.6	Eq. 4.7	
P10-F85-M05	1779	17.8	5.20	7.18	4.59	Not applicable	0.247
P10-F80-M10	1728	14.1	4.37	6.25	4.00		0.202
P10-F75-M15	1738	16.1	4.90	6.62	4.24		0.251
P10-F70-M20	1748	12.3	3.38	6.11	3.91		0.197
P10-F65-M25	1722	14.9	4.13	6.33	4.05		0.573
P90-M10	1782	23.2	6.36	7.86	Not applicable	7.08	0.176
P80-M20	1784	23.6	7.06	7.92		7.13	0.125
P70-M30	1787	18.4	6.47	7.32		6.59	0.179
P60-M40	1790	17.2	6.47	7.18		6.46	0.179

Short and Kinniburgh (1978) reported that MoE depends on the aggregate. The quantity of OPS used in all the mixes was 212 kg/m³; as the stiffness of OPS is lower compared to the NWA, the MoE of the OPSGC is very much lower than the conventional concrete. The effect of variation of the binder material used in this investigation cannot be underestimated; as stated the S/A ratio of the different mixes contribute to the strength development. Thus, both the stiffness of OPS and the S/A ratio of the mixes influence the MoE of the concrete.

The constant 5 as used in Eq. 4.5 may not be appropriate for the geopolymer concrete and hence the modification factor of 5 was changed to predict the MoE and the equations are proposed via Eq. 4.6 (POFA-FA-MK) and Eq. 4.7 (POFA-MK).

$$E = \left(\frac{\rho}{2400} \right)^2 \times 3.2 f_{cu}^{1/3} \quad \text{Eq. 4.6}$$

$$E = \left(\frac{\rho}{2400} \right)^2 \times 4.5 f_{cu}^{1/3} \quad \text{Eq. 4.7}$$

Where, ρ = density (kg/m³)

4.5 Mix design 3: Effect of steel fibres on mechanical properties

Based on the mix design for OPSGC in the previous section, P80-M20 shows the highest compressive strength. Though P90-M10 achieved slightly lower compressive strength than P80-M20, P90-M10 was chosen as the structural grade concrete for further investigation in the effect of fibres in the OPSGC due to the usage of higher volume of POFA and better performance in the development of tensile strength. Two different steel fibres with aspect ratio (AR) of 65 and 80 were used and the mechanical properties were investigated and reported. The second variable in this investigation is the use of different volume of fibres (0.25%, 0.5% and 0.75%) of concrete volume. The results were compared with geopolymer concrete prepared using normal weight aggregate (NWGC) as mentioned in the methodology for 0.5% of steel fibre volume. Only one NWGC with 0.5% was chosen for comparison as the main focus was the effect of fibres in the OPSGC.

4.5.1 Properties of fresh concrete

The fresh concrete properties include slump and densities. The slump test was conducted using conventional slump test used for normal concrete. The geopolymer concrete is cohesive and sticky and slump test may not be suitable to test the workability. At present, there are no standard tests available for measuring the workability of geopolymer concrete. Thus using the slump test, the workability was measured and all mixes produced zero slump; this could be due to the cohesive mix and low amount of additional water; further, no superplasticizer was used in the mixes. The fresh densities of all mixes including normal weight geopolymer concrete (NWGC) are shown in Table 4.16.

The difference in fresh densities of OPSGC and FOPSGC is mainly due to the proportion of additional steel fibres as all other material proportions were kept constant. The concretes, NWGC and FNWGC with crushed granite as coarse aggregate was used for comparison with lightweight FOPSGC. As known, the higher fresh density of NWC compared to FOPSGC is due to the higher specific gravity of aggregate. All the fresh densities of FOPSGC were found to fulfill the requirement for LWC and the slight increase in the density among the mixes could attributed to the increase in the steel fibre volume.

Table 4.16: Density (kg/m^3) of FOPSGC and FGGC

Age	OPSGC	FOPSGC						NWGC	FNWGC	
	OG	OG-65/0.25	OG-80/0.25	OG-65/0.5	OG-80/0.5	OG-65/0.75	OG-80/0.75	GG	GG-65/0.5	GG-80/0.5
Fresh density, kg/m^3	1830	1845	1845	1880	1860	1890	1875	2046	2084	2084
Slump, mm	Zero slump									
OPSGC	Oil palm shell geopolymer concrete									
FOPSGC	Fibre reinforced oil palm shell geopolymer concrete									
NWGC	Granite geopolymer concrete									
FNWGC	Fibre reinforced granite geopolymer concrete.									

4.5.2 Compressive strength

The compressive strengths development at the ages of 3-, 7-, 14- and 28-day are shown in Table 4.17. The early strength development was found 82 – 97% and 85 - 98% of the 28-day compressive strength at the ages of 3-day and 7-day, respectively for all geopolymer concrete with or without fibre and this could be attributed by geopolymerization process during heat curing (Hardjito and Rangan, 2005). The volume of steel fibre and the aspect ratio (AR) did not have any significant influence on the compressive strength.

Table 4.17: Compressive strength

Mix Designation	f_{cu} (MPa)			
	3-day	7-day	14-day	28-day
OG	28.7	29.0	30.0	30.0
OG-65/0.25	28.3	30.6	29.4	31.4
OG-80/0.25	28.0	29.4	28.5	29.9
OG-65/0.5	26.8	29.0	30.2	30.9
OG-80/0.5	26.1	27.2	31.9	31.9
OG-65/0.75	30.5	30.9	26.8	31.3
OG-80/0.75	29.2	28.5	30.5	30.5
GG	26.4	27.0	27.6	27.6
GG-65/0.5	27.9	28.2	29.1	29.2
GG-80/0.5	30.3	30.5	31.1	31.7

The 28-day compressive strength of OPSGC varies between 30.9 to 31.35 MPa and 29.96 to 31.86 MPa for % volume of 0.25, 0.50 and 0.75 of steel fibre of AR65 and AR80, respectively; the addition of 0.5% volume of steel fibre with AR80 shows the highest compressive strength for both OPSGC and NWGC (Figure 4.23).

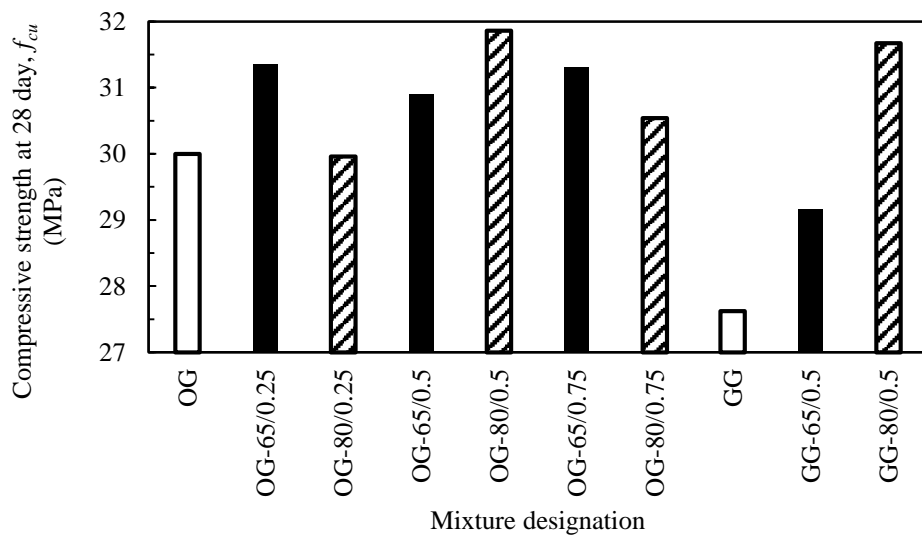


Figure 4.23: 28-day compressive strength

The slight difference of compressive strength was observed due to the different volume of steel fibres and aspect ratio. An insignificant change in the compressive strength at 28-day age was noticed for AR65; while AR80 shows a reduction of compressive strength due to addition of more steel fibre for 0.75%. AR80 for 0.5% volume of steel fibre shows

better performance than AR65 with same % volume of steel fibre. Previous research works (Gao et al., 1997; Neves and Almeida, 2005) also show that higher AR provides better performance. Mo et al. (2014a) related the occurrence of micro-crack in the lightweight aggregate during loading as an explanation of how the steel fibre help improving compressive strength. It is known that lightweight aggregate has less aggregate crushing value than normal weight aggregate. Therefore, crack may occur in the coarse aggregate before extending into the binding material and bonds.

The steel fibre may take a role in this part to enhance the strength of the concrete by controlling the propagation of crack in the lightweight aggregate. A sufficient good bonding between steel fibre and binding material increases the compressive strength of light weight concrete (Gao et al., 1997). The larger surface area of steel fibre may enhance the possibility of good bonding and this is the reason why higher AR performs better than lower AR. The previous research findings (Neves and Almeida, 2005) claims this reason that higher AR control the crack propagation due to the stiffness of fibre.

The mix with AR of 80 was found to produce higher compressive strength between 3-6% than the mix with AR of 65; however, for the FNWGC, the effect was slightly higher than that of FOPSGC as the strength increase was found between 5-14% for similar addition volume of steel fibre.

4.5.3 Flexural strength

The steel fibre has an important role in the development of flexural strength and its significance is more than that in the development of compressive strength. The experimental value of flexural strength for different volume proportion of steel fibre with AR 65 and 80 is shown in Table 4.18. The increment of flexural strength due to the addition of steel fibre was noticed in the range of 5 to 12%. The highest flexural strength

of 5.14 MPa was achieved for the OG-80/0.75. The pattern of loading tension and compression may not comparable for the effect of steel fibres in concrete.

Table 4.18: Flexural strength

Mix Designation	28-day Compressive strength (MPa)	Flexural strength (MPa)
OG	30.0	4.33
OG-65/0.25	31.4	4.69
OG-80/0.25	29.9	4.65
OG-65/0.5	30.9	4.72
OG-80/0.5	31.9	4.80
OG-65/0.75	31.3	4.86
OG-80/0.75	30.5	5.14
GG	27.6	3.41
GG-65/0.5	29.2	3.61
GG-80/0.5	31.7	3.67

The effect of fibre volume had direct influence on the flexural strength (Figure 4.24). GG shows the lowest flexural strength among all the mix proportions. OG performed better flexural strength. The improvement of flexural strength due to the OPS is reported by other research work also (Yap et al., 2013). Further, the flexural improvements of 8 to 12% and 7 to 18% were found for AR65 and AR80, respectively using 0.25, 0.5 and 0.75% of steel fibre. The gradient of the dotted line in Figure 4.24 shows higher than the other one.

This reflects the more possibility of improvement of flexural strength using AR80 with higher volume than that of AR65.

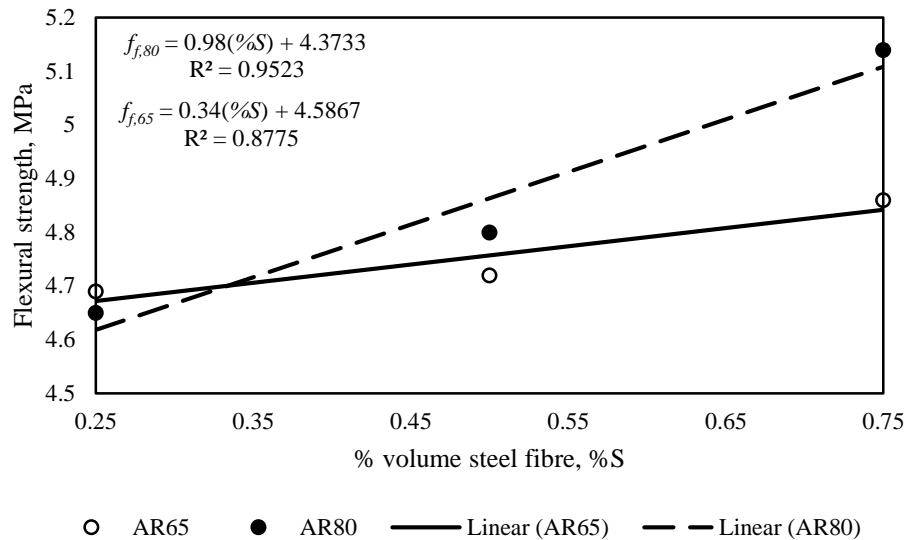


Figure 4.24: Development of flexural strength for different % volume of steel fibre

Other research works (Gao et al., 1997; Köksal et al., 2008) also support this finding. Köksal et al. (2008) studied the reason of effectiveness of higher AR and concluded with the point of length of steel fibre due to the higher capability of delaying crack propagation in concrete.

4.5.4 Indirect tensile strength (Splitting tensile test)

The splitting tensile test, which is known as the indirect tensile strength test, provides information on the maximum tensile load may induce on the concrete member before cracking. The experimental data in this study shows the effect of volume and aspect ratio steel fibre in the development of indirect tensile strength (ITS).

The ITS of the specimens with different volume of steel fibre of AR 65 and 80 are shown in Table 4.19. The 28-day compressive strength of OG is slightly higher than GG and in terms of flexural strength, the performance of OG and GG shows inversely. However, the addition of same volume of steel fibre changes the scenario, i.e. the addition of steel fibre in OPSGC shows better performance than NWGC.

Table 4.19: Indirect tensile strength (Mix design 3)

Mix Designation	28-day Compressive strength (MPa)	Indirect tensile strength (MPa)
OG	30.0	2.22
OG-65/0.25	31.4	2.81
OG-80/0.25	29.9	2.55
OG-65/0.5	30.9	2.88
OG-80/0.5	31.9	2.89
OG-65/0.75	31.3	2.93
OG-80/0.75	30.5	3.07
GG	27.6	2.31
GG-65/0.5	29.2	2.62
GG-80/0.5	31.7	2.60

The development of ITS is similar to flexural strength due to the addition of the steel fibre. The bonding between steel fibre and matrix enhance the capability of reducing the propagation of cracks in concrete. The highest value of ITS was noticed for the OG-80/0.75 as 3.07 MPa. The data in Table 4.19 shows that 12 to 29% increase was noticed for specimens with steel fibre in NWGC and LWGC. AR80 developed more ITS than AR65 with 0.75% volume steel fibre. However, the mixes with AR 65 and 80 give similar ITS for 0.5% volume of steel fibre (Figure 4.25).

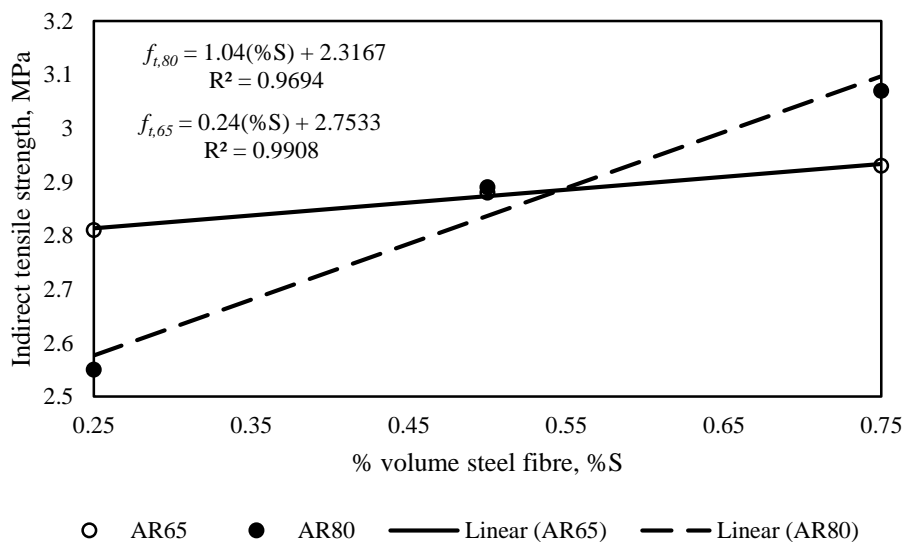


Figure 4.25: Development of flexural strength for different % volume of steel fibre

4.5.5 Static modulus of elasticity

The Young's modulus of elasticity (MoE) is shown in Table 4.20 for the different volume of steel fibre addition in NWGC and LWGC. The MoE of LWGC is 3.5 times less than LWGC. The highest value of MoE in LWGC was found for OG-80/0.75 as 10 GPa. It is noted that flexural and indirect tensile strength also shows the highest result for OG-80/0.75. The addition of steel fibre improves the MoE 4 to 60% and 1 to 4% in LWGC and NWGC, respectively; the higher volume of steel fibre in concrete, higher the MoE. Kurugöl et al. (2008) reported similar outcome that addition of steel fibre increased the MoE.

Table 4.20: Modulus of elasticity

Mix Designation	OG	OG-65/0.25	OG-80/0.25	OG-65/0.5	OG-80/0.5	OG-65/0.75	OG-80/0.75	GG	GG-65/0.5	GG-80/0.5
28-day Density, kg/m ³	1833	1816	1811	1819	1815	1814	1813	2020	2022	2023
28-day compressive strength, MPa	30	31.35	29.96	30.90	31.86	31.30	30.54	27.62	29.17	31.67
Modulus of Elasticity, GPa	6.25	6.56	8.68	8.69	9.10	8.72	10.00	22.35	22.70	23.21
Eq. 4.8	NA	NA	7.64	NA	8.72	NA	7.97	Not Applicable (NA)		

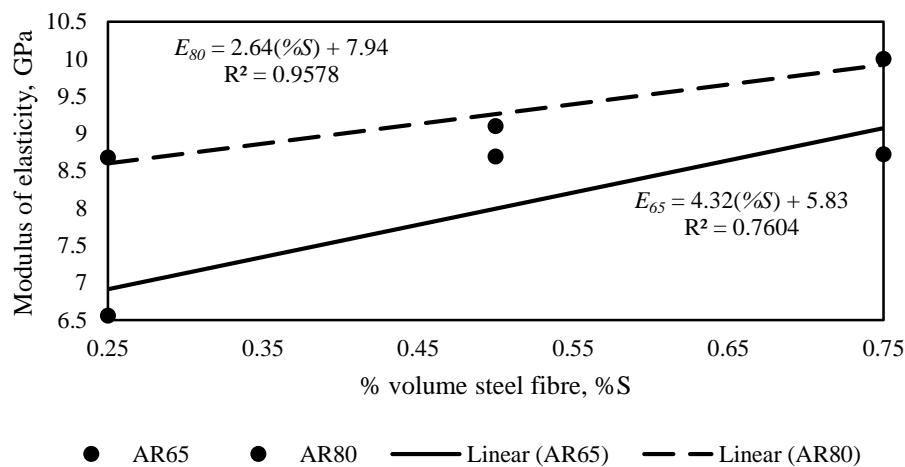


Figure 4.26: Development of MoE for different % volume of steel fibre

A comparison of volume of steel fibre and MoE is shown in Figure 4.26. MoE increases with increment of % volume of steel fibre of both AR65 and 80. Mo et al. (2014a) proposed following Eq. 4.8 to correlate the MoE with the compressive strength of fibre reinforced OPS based lightweight concrete containing steel fibre of AR80.

$$E = 6.31\sqrt{f_{cu}} - 26.90 \quad \text{Eq. 4.8}$$

A comparison is shown for the experimental result and the above equation. The deviation of the estimated result could be due to the usage of different proportion of OPS and binding material.

4.6 Mix design 3: Effect of steel fibres on fracture toughness

4.6.1 Characteristics of fracture toughness

The steel fibres have significant effect on the fracture behaviour of concrete. The fracture failure is shown in Figure 4.27. Table 4.21 shows the characteristic properties of fracture toughness. These properties are derived from the load deflection curve and shown the performance of fibre reinforced concrete. According to ASTM C1609/C1609M-12 (2012), toughness properties are determined in two residual position, as recommended by the deflection limit such as beam span/ 600 and beam span/ 150. The end point deflection which is calculated at beam span/ 150 is a constant value for all types of concrete material and this depends on the span of the beam only which is computed as 2 in this experiment (Table 4.21).

The first peak load (P_1) is the load for the first point of zero slope in the load-deflection curve. The OPS based geopolymer concrete (OPSGC) without fibre (OG) shows the P_1 value as 6.99 kN whereas the gravel based geopolymer concrete without fibre (GG) performed up to 6.09 kN. This could be attributed to the ductility characteristic of OPS. P_1 values were varied from 6.39 to 11.16 kN for the steel fibre of aspect ratio (AR) 65

with different % of volume as 0.25, 0.50 and 0.75. The highest P_1 (11.16 kN) was achieved for the 0.75% volume (OG65/0.75). The bonding effect between the fibre and paste could influence the variation of first peak load (P_1). Similarly, steel fibre with AR 80 has effect on the P_1 . A range of the values of 6.13 to 7.05 kN of P_1 was observed for the volume 0.25, 0.50 and 0.75% steel fibre of AR 80. The deviation in P_1 value for different % volume of AR 80 is insignificant.

The effect of steel fibre in OPSGC was found more significant than NWGC. GG65/0.5 and GG80/0.5, which contained 0.5% of steel fibre of AR 65 and AR80 respectively, achieved P_1 5.85 and 3.22 kN, respectively. It should be noted that GG was designed for the similar compressive strength of OG for a comparison. It was noted that AR80 showed lower P_1 than AR 65 for all mixes. The first peak strength (f_1) and deflection (δ_1) were related to P_1 and have significance in the fracture performance of FOPSGC. A maximum δ_1 of 1.49 mm was noticed for the 0.25% steel fibre of AR 80; the maximum first peak load (11.16 kN) was obtained for mix OG65/0.75 with 0.75% of steel fibre of AR 65. AR80 has longer fibre length than AR 65, which could influence the deflection.



Figure 4.27: Fracture failure

Table 4.21: Fracture characteristics for different mix designs

Fracture characteristics	OG	OG65/0.25	OG80/0.25	OG65/0.50	OG80/0.50	OG65/0.75	OG80/0.75	GG	GG65/0.50	GG80/0.50
End point deflection	-	2.00	2.00	2.00	2.00	2.00	2.00	-	2.00	2.00
First-peak load, P_1 (kN)	6.99	8.05	6.56	6.39	6.13	11.16	7.05	6.05	5.85	3.22
First-peak deflection, δ_1 (mm)	1.14	1.05	1.49	0.86	0.26	1.26	1.07	0.39	0.93	1.35
First-peak strength, f_1 (MPa)	2.61	4.93	3.82	3.54	3.28	6.53	3.84	3.64	3.58	1.97
Peak load, P_p (kN)	6.99	8.05	7.67	6.39	6.13	11.16	7.05	6.05	5.85	3.86
Peak-load deflection, δ_p (mm)	1.14	1.05	3.39	0.86	0.26	1.26	1.07	0.39	0.93	6.32
Peak strength, f_p (Mpa)	2.61	4.93	4.47	3.54	3.28	6.53	3.84	3.64	3.58	2.37
Residual load, P_{600}^D (kN)	1.74	3.09	2.62	3.92	4.31	7.23	0.28	0.04	2.03	1.31
Residual load, P_{150}^D (kN)	6.99	2.09	6.37	0.36	3.03	9.57	2.60	0.18	2.03	3.24
Residual strength, f_{600}^D (MPa)	0.65	1.89	1.53	2.17	2.30	4.23	0.15	0.02	1.24	0.80
Residual strength, f_{150}^D (MPa)	2.61	1.28	3.71	0.20	1.62	5.60	1.42	0.11	1.24	1.99
Specimen toughness, T_{150}^D (Joule)	3.03	9.86	9.20	4.22	7.64	16.27	6.05	0.94	6.80	4.40
Equivalent flexural strength ratio, $R_{T, 150}^D$	0.02	0.06	0.07	0.03	0.06	0.07	0.04	0.01	0.06	0.07

4.6.2 First peak deflection (FPD)

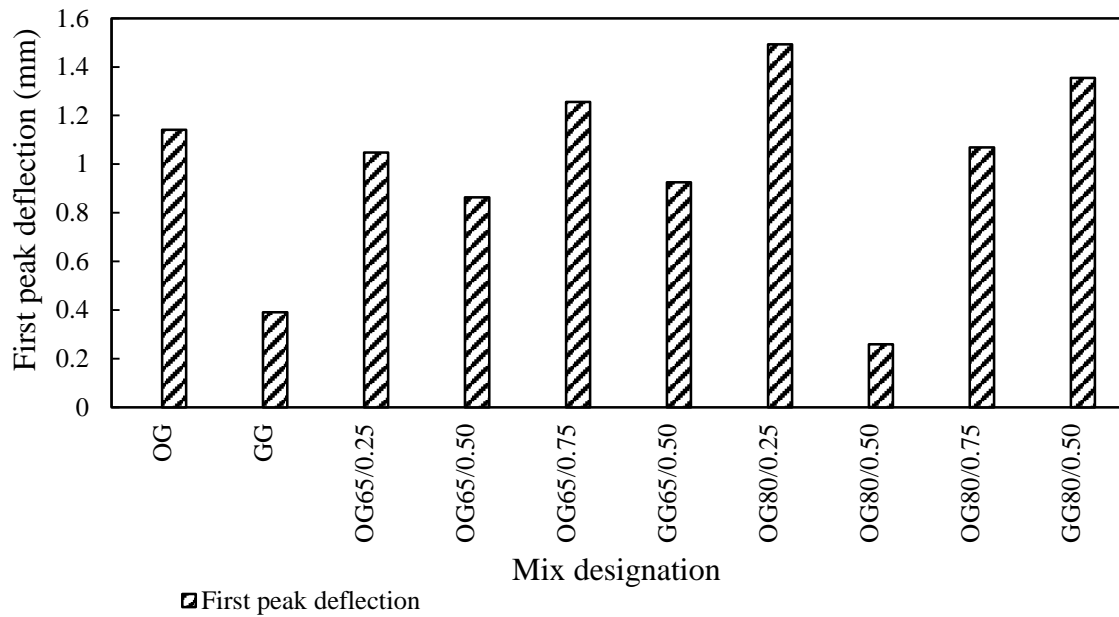


Figure 4.28: First peak deflection for all mix designs

The first peak deflection (FPD) is the measure of the deflection during the first peak load. Figure 4.30 shows a comparison of the first peak deflection of all the mix designs with and without steel fibres of AR65 and 80 in FOPSGC and NWGC. The FPD was measured about 34% higher for OG than GG and this could be due to higher ductility of the former. It should be noted that OG and GG have no steel fibre, therefore, no residual deflection could be found and an immediate failure of the specimens was observed after the first peak load. An addition of 0.25 and 0.5% of steel fibre of AR 65 has insignificant effect and reduces the FPD whereas, 0.75% of steel fibre of AR 65 has slight improvement of FPD. The highest FPD was observed for the addition of 0.25% of steel fibre with AR 80 in OPSGC. The longer fiber size and an appropriate mix proportion of 0.25% of AR 80 in OPSGC could be attributed to the enhanced performance of mix with AR 80. The addition of steel fibre with GG improves FPD and AR 80 has better role than AR 65 in the FPD.

4.6.3 Fracture strength

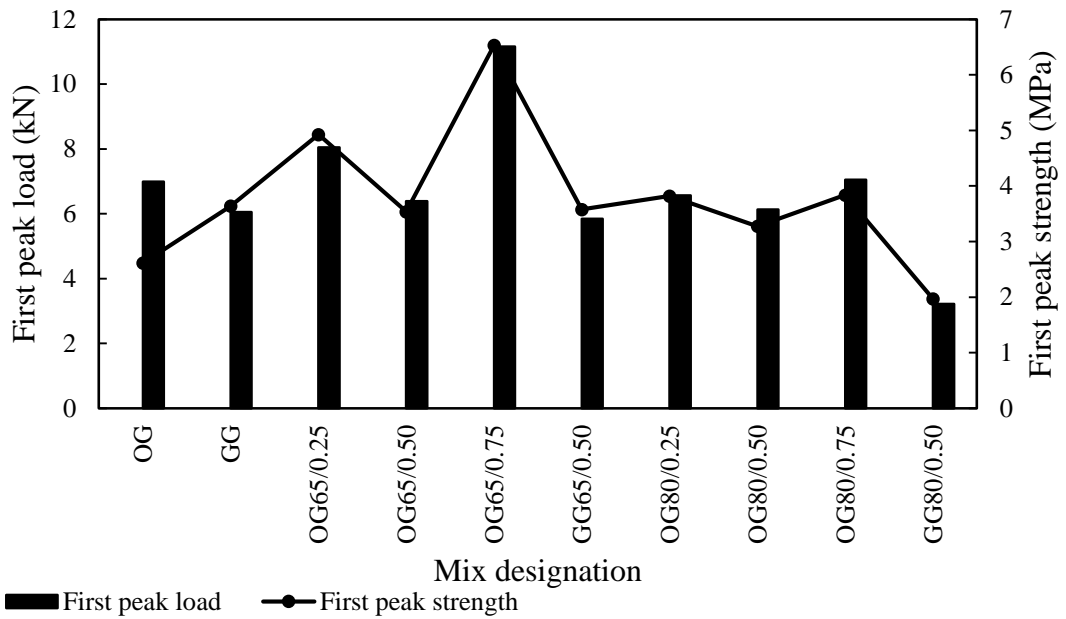


Figure 4.29: First peak load and strength

The first-peak strength (FPS) has the significance on the characterization of the fibre-reinforced concrete (ASTM C1609/C1609M-12, 2012). The behavior of first peak load and the first peak strength of OPSGC and NWGC with and without fibre are shown in Figure 4.29. The FPS in NWGC without fibre is 39% higher than that in OPSGC without fibre. The FPS improved on the addition of steel fibre in both OPSGC and NWGC. The addition of 0.75% steel fibre of AR65 shows the highest FPS. The OPSGC containing 0.75% volume of steel fibre with AR80 produced 41% lower strength than the corresponding volume of fibre with AR 65. The higher FPS of AR65 was found for 0.25% and 0.5% volume of steel fibre. This could be attributed by the total surface area of the steel fibre that has an important role in the development of bond strength. For a given volume of steel fibre, the number of fibres with AR65 is more than that of AR80 and hence in an identical % volume of fibres, AR65 consists of more surface area than AR80.

It is noticed that 0.75% of steel fibre gives the highest FPS among 0.25, 0.5 and 0.75% of volume in both case of AR65 and AR80. A slight reduction of FPS was found for 0.50% volume of steel fibre.

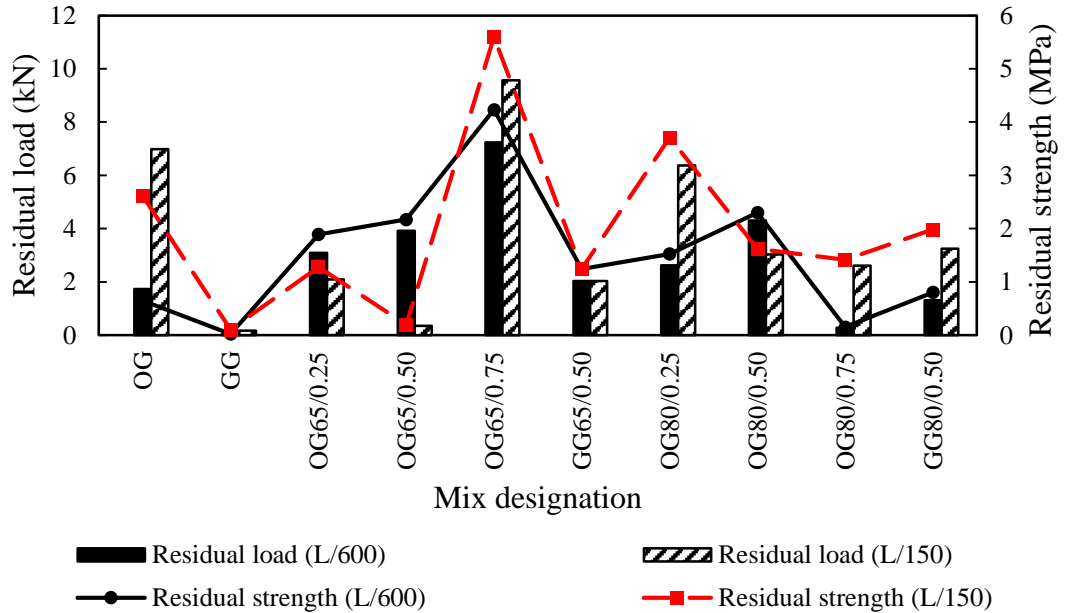


Figure 4.30: Residual load and strength

The residual load (RL) and residual strength (RS) are two important characteristics of fracture behaviour and are determined generally for the limiting deflection of 1/600 and 1/150 of beam span. The RS at specified deflections characterizes the residual capacity of the specimen after cracking. Figure 4.30 shows the RL and RS of all mix proportions of OPSPGC and NWGC with/ without fibre. OG, which contains OPS as aggregate and no fibre, achieved more RL and RD than the NWGC without fibre (GG). The RL (L/150) and RS (L/150) of OG are relatively 62 and 75% higher than the RL (L/600) and RS (L/600); however, this variation was found lower in GG.

The addition of steel fibres influences the RL as explained below. The highest RL (L/150) and RS (L/150) were obtained for 0.75% volume of steel fibre of AR65. The OPSPGC with steel fibre AR65 of 0.75% volume achieved about 74% higher RL (L/150) and RS

(L/150) than that of OG80/0.75. Similar reduction in RL (L/150) and RS (L/150) was also found in OG80/0.25 and OG80/0.50.

The values of RL and RS in two-deflection limit of L/600 and L/150 indicate the progressive failure, which reflects the ductility of the concrete material.

4.6.4 Fracture toughness

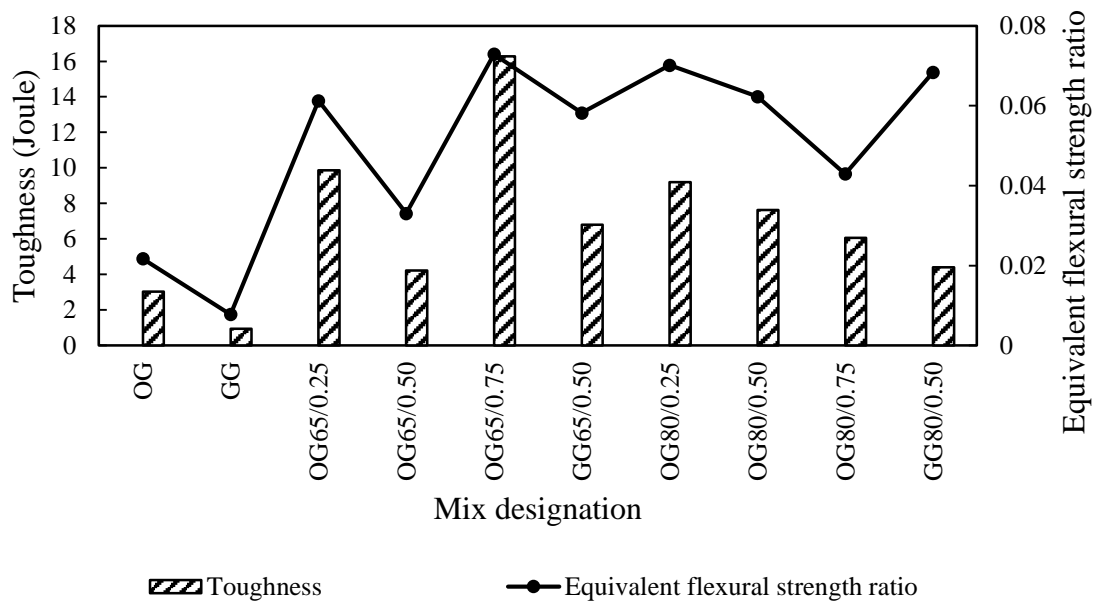


Figure 4.31: Toughness and equivalent flexural strength ratio

The toughness and equivalent flexural strength ratio are shown in Figure 4.31. The toughness determines the capacity of energy absorption of the specimen and is expressed in terms of Joules (J). The higher toughness indicates the better post-cracking response (Mo et al., 2014a) and the better ductility performance of the fibre reinforced concrete. The OPSGC and NWGC without fibre shows the toughness as 3.03 and 0.94 J, respectively (Table 4.21) and it indicates OG as more ductile than GG. Further, the toughness as well as the ductility performance increases by adding steel fibres. Similar findings were reported by Yap et al. (2014) and Mo et al. (2014a).

Steel fibre with AR65 shows more enhancement of toughness than AR80. The highest toughness was recorded among all the mix proportions is 16.27 J for the material OG65/0.75 and this value is 5.5 and 17 times higher than OG and GG, respectively. Mo et al. (2014a) added 0.5, 0.75 and 1% of steel fibre and reported the increment of toughness about 6 to 17 times compared to the control concrete. Şahin and Köksal (2011) used normal weight concrete of grade 45 and steel fibres of aspect ratio of 80, and found the increase of fracture energy by about 2.2 and 3.6 times for the addition of steel fibres from 0.33% to 0.67% and 0.33% to 1.0%, respectively. The equivalent flexural strength ratio (EFSR) was also found the maximum value for OG65/0.75. It is noted from Figure 4.31 that the EFSR changes simultaneously with the change of toughness.

CHAPTER 5 CONCLUSION AND RECOMMENDATION

5.1 Introduction

This chapter contains the conclusions of each experimental findings and recommendation for further research. The conclusions are separated into four clauses based on each objectives.

5.1.1 Development of appropriate mix proportion (objective 1)

This objective was concerned with the investigation on the appropriate mix design using palm oil fuel ash (POFA), fly ash (FA) and metakaolin (MK) as binding material and to investigate the effect of manufactured sand (M-sand) and quarry dust (QD) in geopolymer mortar as a replacement of conventional mining sand as fine aggregate. The conclusions are listed below:

- The M-sand was found to be a potential replacement of conventional mining sand. The mix with 100% replacement of N-sand by QD showed higher compressive strength compared to replacing N-sand by different proportion of M-sand and QD. Though the compressive strength slightly reduces due to the replacement of N-sand or QD by M-sand, the M-sand is considered as a viable alternative to conventional sand due to depletion of natural resources. The slight variation in the compressive strength might be attributed to the aggregate shape and texture.
- The usage of 100% M-Sand in POFA-FA-based geopolymer mortar produced comparable strength as that of 100% N-sand. The use of QD as fine aggregate also reinforces the use of waste material as replacement for conventional N-sand; the high strength of specimens with 100% QD is attributed to the rough surfaces of QD that enhances the bond between the paste and the aggregates.

- The replacement of conventional N-sand with M-sand and QD shows comparable strength as that of N-sand based specimens and the use of M-sand and QD is recommended in geopolymer concrete.
- The high concentration of sodium hydroxide solution increases the compressive strength. The mixes with more fine particles require more past to cover the surface areas; but for the mixes with constant binder content, the influence of the finer particles can't be ignored.
- The failure mode of geopolymer mortar was found similar to that of Portland cement mortar. The density and compressive strength relationship of N-sand/M-sand/QD based geopolymer mortar was also found similar to that of the Portland cement mortar.
- The POFA and MK mix proportions achieve the better mix proportion than POFA, FA and MK. The mix proportion consisting 90% POFA and 10% MK gives the highest strength.
- No significant changes on the compressive strength were observed for the replacement of FA by MK while the proportion of POFA remains constant. This is due to the consistent of silica/ alumina ratio in all proportion of POFA-FA-MK.
- Silica/ alumina ratio has the main role in finding an appropriate mix proportion of raw binding materials. The silica/ alumina ratio of 9.26 contributes in the development of structural grade light weight concrete. The replacement of POFA by MK from 10% to 40% gradually reduces the compressive strength due to the gradual reduction of silica/ alumina ratio from 9.26 to 3.42.

- Heat curing in a temperature of 65⁰C for 48 hours and the alkaline solution with 14 molarity sodium hydroxide are effective to develop about 80% of 28-day compressive strength by the age of 3-day.
- There was no significant detrimental effect detected on the usage of oil palm shell (OPS) in geopolymer concrete.

5.1.2 Investigation on the mechanical properties of OPSGC (objective 2)

The investigation of the fresh and hardened properties of oil palm shell geopolymer concrete (OPSGC) shows following outcomes.

- The fresh density of OPSGC increases with the replacement of POFA/ FA by MK since the specific gravity of MK is higher than POFA and MK.
- The usage of excessive water decreases the strength of OPSGC effecting proper geopolymerization. The usage of minimum required additional water may enhance the compressive strength and reduce the slump value. Proper vibration during casting helps to overcome the workability issue for less water content and no honeycomb was found after demoulding and crushing the concrete specimens.
- The POFA and MK mix proportions achieved higher strength than that of POFA, FA and MK proportions due to the appropriate Silica/ Alumina ratio.
- The mix proportion consisting 80% POFA and 20% MK produced the highest compressive strength (23.6 MPa), however 90% POFA and 10% MK is the considerable mix proportions since the compressive strength (23.2 MPa) is very close to the highest compressive strength and this proportion contains more quantity of industrial by-product POFA and also usable for the preparation of structural grade lightweight concrete.

- The proportion of silica/ alumina has a significant role in the development of flexural and indirect tensile strength. The silica/ alumina ratio of 9.26 shows the highest flexural strength development for 90%POFA and 10% MK.
- The established equations for lightweight concrete in determining the flexural and indirect tensile strength from compressive strength is comparable for lightweight geopolymer concrete with a slight deviation due to the difference in the binding materials.
- The highest flexural and indirect tensile strengths of 3.41 and 2.14 MPa, respectively were obtained for the mix proportion of 90% POFA and 10% MK.
- Both the flexural and indirect tensile strengths were reduced significantly due to the replacement of POFA by MK from the level of 10% to 40%.
- Following recommendation could be provided for the practical uses of OPSGC:

Mix Designation	Cube compressive strength, f_{cu} (MPa), 28-day	Practical use according to the recommendation of ACI 213R-14
P10-F85-M05	17.8	Non-structural lightweight precast geopolymer concrete
P10-F80-M10	14.1	
P10-F75-M15	16.1	
P10-F70-M20	12.3	
P10-F65-M25	14.9	
P90-M10	23.2	Structural lightweight precast geopolymer concrete
P80-M20	23.6	
P70-M30	18.4	Non-structural lightweight precast geopolymer concrete
P60-M40	17.2	

5.1.3 Investigation of Mechanical properties of FOPSGC and FNWGC (Objective 3)

A significant effect volume and aspect ratio (AR) of steel fibre in the development of mechanical properties of OPSGC was found from this research experiment. The ARs used in this investigation were 80 and 65 with % volume of 0.25, 0.5 and 0.75. The main findings are concluded as follows:

- All the FOPSGC produced zero slump due to the addition of fibres and the cohesive nature of the mixes.
- The highest fresh density of 1890 kg/m^3 was observed for OPSGC with 0.75% of steel fibre of AR80 and this is attributed by the specific gravity and % volume of steel fibre in concrete. The lowest fresh density of 1845 kg/m^3 was noted in the fibre reinforced OPSGC for the 0.25% volume of steel fibre of both AR.
- The volume and AR of steel fibre had insignificant effect in the development of strength.
- The different volume and AR of steel fibre in OPSGC had insignificant effect on the compressive strength. The compressive strength was varied in the range of 30.54 to 31.86 MPa for the variation of steel fibres in OPSGC. The highest compressive strength of fibre reinforced OPSGC was achieved with addition of 0.5% of steel fibre of AR80.
- The AR80 has more effect in the development of strength compared to AR65 for the same % volume of steel fibre in OPSGC and this could be due to the capability of fibre in reducing the crack propagation in concrete.
- The contribution of steel fibre in the development of strength was found more in lightweight geopolymer concrete than the normal weight geopolymer concrete.

- The bonding between steel fibre and binding material influences the development of strength and this is related to the surface area of the steel fibre.

5.1.4 Investigation of fracture behaviour of FOPSGC (objective 4)

The fracture behavior of fibre reinforce OPSGC and NWGC were examined and compared. The conclusions on the effect of volume and AR of steel fibres on the characteristics of fracture behavior, i.e. first peak deflection, fracture strength and the fracture toughness are given below:

- The 0.75% volume of steel fibre with AR65 shows the best performance among 0.25, 0.5, 0.75% volumes with AR80 & 65 and this could be attributed to the efficiency of energy absorption of high volume of steel fibre with lower aspect ratio.
- The highest values of fracture toughness, strength and residual strength (L/150) produced by OG96/0.75 are 16.27J, 6.53MPa and 5.60 MPa, respectively.
- OG containing OPS as aggregate without fibre produced higher RL and RD than the corresponding NWGC (GG).
- The highest RL (L/150) and RS (L/150) were obtained for specimens with 0.75% volume of steel fibre of AR65.

5.2 Recommendation for future work

The following recommendations for future research work are made based on the findings from this research work:

- The workability of PMGC is lower or nonexistent and the cohesive mixes require improvement and hence further investigation on this aspect needs to be conducted.
- Microstructure analysis will be beneficial for better understanding of the geopolymeric reaction in the PMGC.
- An investigation on the structural behavior of beam and columns using PMGC is recommended.
- The experiments on the durability and thermal conductivity are required to be investigated to study the properties of PMGC.
- The effect of steel fibres in the development of impact and torsional resistance of structural beam/ slabs of FOPSGC may be examined.
- To investigate a design guideline for the PMGC.
- Special type of mixer machine is necessary for geopolymer concrete for proper mixing with less amount of water.
- Long term properties such as shrinkage, creep and other durability aspects have to be examined.

REFERENCES

- Abdulkareem, O. A., Mustafa Al Bakri, A. M., Kamarudin, H., Khairul Nizar, I., & Saif, A. e. A. (2014). Effects of elevated temperatures on the thermal behavior and mechanical performance of fly ash geopolymer paste, mortar and lightweight concrete. *Construction and Building Materials*, 50(0), 377-387.
- Abdullah, A. A. A. (1996). 10 - Palm oil shell aggregate for lightweight concrete. In S. Chandra (Ed.), *Waste Materials Used in Concrete Manufacturing* (pp. 624-636). Westwood, NJ: William Andrew Publishing.
- ACI 213R-14. (2014). Guide for structural lightweight aggregate concrete: American Concrete Institute.
- Alengaram, U. J., Jumaat, M. Z., & Mahmud, H. (2008). *Influence of sand content and silica fume on mechanical properties of palm kernel shell concrete*. Paper presented at the International conference on construction and building technology ICCBT.
- Alengaram, U. J., Jumaat, M. Z., Mahmud, H., & Fayyadh, M. M. (2011a). Shear behaviour of reinforced palm kernel shell concrete beams. *Construction and Building Materials*, 25(6), 2918-2927.
- Alengaram, U. J., Mahmud, H., & Jumaat, M. Z. (2011b). Enhancement and prediction of modulus of elasticity of palm kernel shell concrete. *Materials and Design*, 32(4), 2143-2148.
- Alengaram, U. J., Muhit, B. A. A., & Jumaat, M. Z. (2013a). Utilization of oil palm kernel shell as lightweight aggregate in concrete – A review. *Construction and Building Materials*, 38, 161-172.
- Alengaram, U. J., Muhit, B. A. A., Jumaat, M. Z., & Jing, M. L. Y. (2013b). A comparison of the thermal conductivity of oil palm shell foamed concrete with conventional materials. *Materials and Design*, 51, 522-529.
- Alexander, M., & Mindess, S. (2005). *Aggregates in concrete*. 2 Park Square, Milton Park, Abingdon, Oxon OX 14 4RN: Taylor & Francis.
- Alida, A., Al Bakri, A. M., Kamarudin, H., Ruzaidi, C., Salleh, M. M., & Chin, K. H. (2013). The Effect of Acidic to the Fly Ash Based Geopolymer Artificial Aggregate. *Australian Journal of Basic and Applied Sciences*, 7(5), 303-307.
- Álvarez-Ayuso, E., Querol, X., Plana, F., Alastuey, A., Moreno, N., Izquierdo, M., . . . Barra, M. (2008). Environmental, physical and structural characterisation of geopolymer matrixes synthesised from coal (co-) combustion fly ashes. *Journal of Hazardous Materials*, 154(1), 175-183.
- Appukutty, P., & Murugesan, R. (2009). Substitution of quarry dust to sand for mortar in brick masonry works. *International Journal on Design and Manufacturing Technologies*, 3(1), 59-63.

- Ashtiani, M. S., Scott, A. N., & Dhakal, R. P. (2013). Mechanical and fresh properties of high-strength self-compacting concrete containing class C fly ash. *Construction and Building Materials*, 47, 1217-1224.
- ASTM C125 - 13b. (2013). Standard Terminology Relating to Concrete and Concrete Aggregates. West Conshohocken, PA: ASTM International.
- ASTM C127-12. (2012). Standard Test Method for Density, Relative Density (Specific Gravity), and Absorption of Coarse Aggregate. West Conshohocken, PA: ASTM International.
- ASTM C128-12. (2012). Standard Test Method for Density, Relative Density (Specific Gravity), and Absorption of Fine Aggregate. West Conshohocken, PA: ASTM International.
- ASTM C131-06. (2006). Standard Test Method for Resistance to Degradation of Small-Size Coarse Aggregate by Abrasion and Impact in the Los Angeles Machine. West Conshohocken, PA: ASTM International.
- ASTM C136-06. (2006). Standard Test Method for Sieve Analysis of Fine and Coarse Aggregates. West Conshohocken, PA: ASTM International.
- ASTM C143/C143M-12. (2012). Standard Test Method for Slump of Hydraulic-Cement Concrete. West Conshohocken, PA: ASTM International.
- ASTM C188-09. (2009). Standard test method for density of hydraulic cement. West Conshohocken, PA: ASTM International.
- ASTM C469 - 14. Standard Test Method for Static Modulus of Elasticity and Poisson's Ratio of Concrete in Compression. West Conshohocken, PA, 2003: ASTM International.
- ASTM C618-12a. (2012). Standard Specification for Coal Fly Ash and Raw or Calcined Natural Pozzolan for Use in Concrete. West Conshohocken, PA: ASTM International.
- ASTM C1018-97. (1997). ASTM C1018-97 Standard Test Method for Flexural Toughness and First-Crack Strength of Fiber-Reinforced Concrete (Using Beam With Third-Point Loading). West Conshohocken, PA: ASTM International.
- ASTM C1609/C1609M-12. (2012). Standard Test Method for Flexural Performance of Fiber-Reinforced Concrete (Using Beam With Third-Point Loading). West Conshohocken, PA: ASTM International.
- ASTM C1688/C1688M-13. (2013). Standard Test Method for Density and Void Content of Freshly Mixed Pervious Concrete. West Conshohocken, PA: ASTM International.
- Atiş, C. D., & Karahan, O. (2009). Properties of steel fiber reinforced fly ash concrete. *Construction and Building Materials*, 23(1), 392-399.
- Autef, A., Joussein, E., Gasgnier, G., & Rossignol, S. (2013a). Role of the silica source on the geopolymerization rate: A thermal analysis study. *Journal of Non-Crystalline Solids*, 366, 13-21.

- Autef, A., Joussein, E., Poulesquen, A., Gasgnier, G., Pronier, S., Sobrados, I., . . . Rossignol, S. (2013b). Influence of metakaolin purities on potassium geopolymer formulation: the existence of several networks. *Journal of Colloid and Interface Science*(0).
- Awal, A. S. M. A., & Hussin, M. W. (1997). The effectiveness of palm oil fuel ash in preventing expansion due to alkali-silica reaction. *Cement and Concrete Composites*, 19(4), 367-372.
- Bagheri, A., & Nazari, A. (2014). Compressive strength of high strength class C fly ash-based geopolymers with reactive granulated blast furnace slag aggregates designed by Taguchi method. *Materials & Design*, 54(0), 483-490.
- Bakharev, T. (2005). Geopolymeric materials prepared using Class F fly ash and elevated temperature curing. *Cement and Concrete Research*, 35(6), 1224-1232.
- Bakharev, T. (2006). Thermal behaviour of geopolymers prepared using class F fly ash and elevated temperature curing. *Cement and Concrete Research*, 36, 1134-1147.
- Balamurugan, G., & Perumal, P. (2013). Use of Quarry Dust to Replace Sand in Concrete—An Experimental Study. *International Journal of Scientific and Research Publications*, 3(12).
- Barbosa, V. F. F., MacKenzie, K. J. D., & Thaumaturgo, C. (2000). Synthesis and characterisation of materials based on inorganic polymers of alumina and silica: sodium polysialate polymers. *International Journal of Inorganic Materials*, 2(4), 309-317.
- BS EN 12390-3:2009. (2009). Testing hardened concrete Compressive strength of test specimens: BSI.
- BS EN 12390-5:2009. (2009). Testing hardened concrete Flexural strength of test specimens: BSI.
- BS EN 12390-6:2009. (2009). Testing hardened concrete tensile splitting strength of test specimens: BSI.
- Chandra, S., & Berntsson, L. (2002). *Light weight aggregate concrete*. 13 Eaton Avenue, Norwich, NY 13815: Noyels publications.
- Chindaprasirt, P., Jaturapitakkul, C., Chalee, W., & Rattanasak, U. (2009). Comparative study on the characteristics of fly ash and bottom ash geopolymers. *Waste Management*, 29(2), 539-543.
- Chindaprasirt, P., Jaturapitakkul, C., & Sinsiri, T. (2007). Effect of fly ash fineness on microstructure of blended cement paste. *Construction and Building Materials*, 21(7), 1534-1541.
- Chow, R. K. K., Yip, S. W. S., & Kwan, A. K. H. (2013). Processing crushed rock fine to produce manufactured sand for improving overall performance of concrete. *HKIE Transactions*, 1-10.
- Davidovits, J. (1979). Synthesis of new high-temperature geo-polymers for reinforced plastics/composites.

- Davidovits, J. (1991). Geopolymers. *Journal of Thermal Analysis and calorimetry*, 37(8), 1633-1656.
- Davidovits, J. (1994a). High-alkali cements for 21st century concretes. *ACI Special Publication*, 144.
- Davidovits, J. (1994b). *Properties of geopolymer cements*. Paper presented at the First International Conference on Alkaline Cements and Concretes.
- Davidovits, J. (2008). *Geopolymer chemistry & application* (3rd ed.). 16 rule Galilee, F-02100 Saint-Quentin, France: Institute Géopolymère.
- Dhir, R. K. (1986). Pulverized-fuel ash. *Cement Replacement Materials* (Ed. RN Swamy), Survey University Pres, London.
- Dumitru, I., Zdrilic, T., & Smorchevsky, G. (1999). *The use of manufactured quarry fines in concrete*. Paper presented at the Proc. 7 th Annual Symposium on Aggregates-Concrete, Bases and Fines, Austin.
- Duxson, P., Provis, J. L., Lukey, G. C., Mallicoat, S. W., Kriven, W. M., & Van Deventer, J. S. (2005). Understanding the relationship between geopolymer composition, microstructure and mechanical properties. *Colloids and Surfaces A: Physicochemical and Engineering Aspects*, 269(1), 47-58.
- Fernández-Jiménez, A., Palomo, A., & Criado, M. (2005). Microstructure development of alkali-activated fly ash cement: a descriptive model. *Cement and Concrete Research*, 35(6), 1204-1209.
- Fernandez-Jimenez, A. M., Palomo, A., & Lopez-Hombrados, C. (2006). Engineering properties of alkali-activated fly ash concrete. *ACI Materials Journal*, 103(2).
- Fung, W. W. S., Kwan, A. K. H., & Wong, H. H. C. (2009). Wet packing of crushed rock fine aggregate. *Materials and structures*, 42(5), 631-643.
- Galloway, J. E. (1994). *Grading, Shape and Surface Properties* (Vol. 169C): ASTM International.
- Gao, J., Sun, W., & Morino, K. (1997). Mechanical properties of steel fiber-reinforced, high-strength, lightweight concrete. *Cement and Concrete Composites*, 19(4), 307-313.
- Guo, X., Shi, H., & Dick, W. A. (2010). Compressive strength and microstructural characteristics of class C fly ash geopolymer. *Cement and Concrete Composites*, 32(2), 142-147.
- Hamid, A., Azlina, N., Thamrin, R., & Ibrahim, A. (2013). Shear capacity of non-metallic (FRP) reinforced concrete beams with stirrups. *Unpublished* (<http://eprints.uthm.edu.my/view/creators/Thamrin=3ARendy=3A=3A.html>).
- Hardjito, D., Cheak, C. C., & Ing, C. H. L. (2009). Strength and setting times of low calcium fly ash-based geopolymer mortar. *Modern Applied Science*, 2(4), 3-11.

- Hardjito, D., & Rangan, B. V. (2005). Development and properties of low-calcium fly-ash based geopolymer concrete *Research Report GC 1*. Engineering Faculty, Curtin University of Technology, Perth, Australia.
- Hardjito, D., Wallah, S. E., Sumajouw, D. M., & Rangan, B. V. (2005). Fly ash-based geopolymer concrete. *Australian Journal of Structural Engineering*, 6(1), 77-84.
- He, C., Osbaeck, B., & Makovicky, E. (1995). Pozzolanic reactions of six principal clay minerals: activation, reactivity assessments and technological effects. *Cement and Concrete Research*, 25(8), 1691-1702.
- Hudson, B. P. (1999a). Concrete workability with high fines content sands. *Quarry*, 7(2), 22-25.
- Hudson, B. P. (1999b). *Modification to the fine aggregate angularity test*. Paper presented at the Seventh Annual Symposium Austin, TX.
- Hussin, M. W., & Awal, A. S. M. A. (1996). *Influence of palm oil fuel ash on strength and durability of concrete*. Paper presented at the Proc., 7th Int. Conf. on Durability of Building Materials and Components.
- İpek, M., Yilmaz, K., & Uysal, M. (2012). The effect of pre-setting pressure applied flexural strength and fracture toughness of reactive powder concrete during the setting phase. *Construction and Building Materials*, 26(1), 459-465.
- Isabella, C., Lukey, G. C., Xu, H., & Deventer, J. S. J. v. (2003, 7-12 September 2003). *The effect of aggregate particle size on formation of geopolymeric gel*. Paper presented at the Advanced materials for construction of bridges, buildings and other structures III, Davos, Switzerland.
- Jarrige, A. (1971). Les Cendres Volantes properties - Applications Industrielles. from <http://trid.trb.org/view.aspx?id=1080769>
- Ji, T., Chen, C.-Y., Zhuang, Y.-Z., & Chen, J.-F. (2013). A mix proportion design method of manufactured sand concrete based on minimum paste theory. *Construction and Building Materials*, 44(0), 422-426.
- Jumaat, Z. (2010). Comparison of mechanical and bond properties of oil palm kernel shell concrete with normal weight concrete. *International Journal of the Physical Sciences*, 5(8), 1231-1239-1231-1239.
- Kaplan, M. (1960). The Flexural and Compressive Strength of Concrete as Affected by the Properties of Coarse Aggregates: National Building Research Institute, Council for Scientific and Industrial Research (CSIR).
- Khale, D., & Chaudhary, R. (2007). Mechanism of geopolymerization and factors influencing its development: a review. *Journal of materials science*, 42(3), 729-746.
- Köksal, F., Altun, F., Yiğit, İ., & Şahin, Y. (2008). Combined effect of silica fume and steel fiber on the mechanical properties of high strength concretes. *Construction and Building Materials*, 22(8), 1874-1880.

- Kong, D. L., & Sanjayan, J. G. (2008). Damage behavior of geopolymer composites exposed to elevated temperatures. *Cement and Concrete Composites*, 30(10), 986-991.
- Kovalchuk, G., Fernández-Jiménez, A., & Palomo, A. (2007). Alkali-activated fly ash: Effect of thermal curing conditions on mechanical and microstructural development—Part II. *Fuel*, 86(3), 315-322.
- Kurugöl, S., Tanaçan, L., & Ersoy, H. Y. (2008). Young's modulus of fiber-reinforced and polymer-modified lightweight concrete composites. *Construction and Building Materials*, 22(6), 1019-1028.
- Lee, W. K. W., & van Deventer, J. S. J. (2007). Chemical interactions between siliceous aggregates and low-Ca alkali-activated cements. *Cement and Concrete Research*, 37(6), 844-855.
- Li, Q., Sun, Z., Tao, D., Xu, Y., Li, P., Cui, H., & Zhai, J. (2013). Immobilization of simulated radionuclide $^{137}\text{Cs}^+$ by fly ash-based geopolymer. *Journal of Hazardous Materials*, 262(0), 325-331.
- Liu, M. Y. J., Alengaram, U. J., Jumaat, M. Z., & Mo, K. H. (2014). Evaluation of thermal conductivity, mechanical and transport properties of lightweight aggregate foamed geopolymer concrete. *Energy and Buildings*, 72(0), 238-245.
- Lloyd, N., & Rangan, V. (2009). Geopolymer Concrete-Sustainable Cementless Concrete. *ACI Special Publication*, 261(3), 33-54.
- McDonald, M., & Thompson, J. (2003). Sodium silicate a binder for the 21st century. *Industrial Chemicals Division. The PQ Corporation*.
- Mehta, P. K., & Monteiro, P. J. M. (2006). *Concrete - Microstructure, Properties, and Materials* (3rd ed.): McGraw-Hill Companies, Inc.
- Memon, F. A., Nuruddin, M. F., Khan, S., Shafiq, N., & Ayub, T. (2013). Effect of Sodium Hydroxide concentration on fresh properties and compressive strength of self-compacting geopolymer concrete. *Journal of Engineering Science and Technology*, 8(1), 44-56.
- Mijarsh, M. J. A., Johari, M. A. M., & Ahmad, Z. A. (2014). Synthesis of geopolymer from large amounts of treated palm oil fuel ash: Application of the Taguchi method in investigating the main parameters affecting compressive strength. *Construction and Building Materials*, 52(0), 473-481.
- Mo, K. H., Yap, K. K. Q., Alengaram, U. J., & Jumaat, M. Z. (2014a). The effect of steel fibres on the enhancement of flexural and compressive toughness and fracture characteristics of oil palm shell concrete. *Construction and Building Materials*, 55(0), 20-28.
- Mo, K. H., Yap, S. P., Alengaram, U. J., Jumaat, M. Z., & Bu, C. H. (2014b). Impact resistance of hybrid fibre-reinforced oil palm shell concrete. *Construction and Building Materials*, 50(0), 499-507.
- Neves, R. D., & Almeida, J. F. d. (2005). Compressive behaviour of steel fibre reinforced concrete. *structural concrete*, 6(1), 1-8.

- Noorvand, H., Ali, A. A. A., Demirboga, R., Noorvand, H., & Farzadnia, N. (2013). Physical and chemical characteristics of unground palm oil fuel ash cement mortars with nanosilica. *Construction and Building Materials*, 48(0), 1104-1113.
- Okpala, D. C. (1990). Palm kernel shell as a lightweight aggregate in concrete. *Building and Environment*, 25(4), 291-296.
- P.Sravana, S. K. T. C. S. R. (2013). Effect of Manufacture sand on Strength Characteristics of Roller Compacted Concrete. *International Journal of Engineering Research & Technology (IJERT)*, 2(2).
- Pacheco-Torgal, F., Castro-Gomes, J., & Jalali, S. (2008). Alkali-activated binders: A review: Part 1. Historical background, terminology, reaction mechanisms and hydration products. *Construction and Building Materials*, 22(7), 1305-1314.
- Palomo, A., Grutzeck, M. W., & Blanco, M. T. (1999). Alkali-activated fly ashes: a cement for the future. *Cement and Concrete Research*, 29(8), 1323-1329.
- Pangdaeng, S., Phoo-ngernkham, T., Sata, V., & Chindapasirt, P. (2013). Influence of curing conditions on properties of high calcium fly ash geopolymer containing Portland cement as additive. *Materials and Design*.
- Phoo-ngernkham, T., Chindapasirt, P., Sata, V., Hanjitsuwan, S., & Hatanaka, S. (2014). The effect of adding nano-SiO₂ and nano-Al₂O₃ on properties of high calcium fly ash geopolymer cured at ambient temperature. *Materials and Design*, 55, 58-65.
- Powers, T. C. (1969). The properties of fresh concrete (W. D. Transportation Research Board, Trans.). 111 River Street, Hoboken, NJ 07030-6000 USA: Road Research Laboratory, UK.
- Puertas, F., Martínez-Ramírez, S., Alonso, S., & Vazquez, T. (2000). Alkali-activated fly ash/slag cement Strength behaviour and hydration products. *Cement and Concrete Research*, 30(10), 1625-1632.
- Quiroga, P. N., & Fowler, D. W. (2004). The effects of aggregates characteristics on the performance of Portland cement concrete. 1 University Station C1755, Austin, TX 78712-0277: International Centre for Aggregates Research (ICAR), The University of Texas at Austin.
- Raman, S. N., Ngo, T., Mendis, P., & Mahmud, H. B. (2011). High-strength rice husk ash concrete incorporating quarry dust as a partial substitute for sand. *Construction and Building Materials*, 25(7), 3123-3130.
- Rangan, B. V. (2008). Fly ash-based geopolymer concrete *Research Report GC 4*. Engineering Faculty, Curtin University of Technology, Perth, Australia.
- Rashad, A. M. (2014). A comprehensive overview about the influence of different admixtures and additives on the properties of alkali-activated fly ash. *Materials & Design*, 53(0), 1005-1025.
- Rovnaník, P. (2010). Effect of curing temperature on the development of hard structure of metakaolin-based geopolymer. *Construction and Building Materials*, 24(7), 1176-1183.

- Roy, D. M. (1999). Alkali-activated cements opportunities and challenges. *Cement and Concrete Research*, 29(2), 249-254.
- Rukzon, S., & Chindaprasirt, P. (2009). Use of disposed waste ash from landfills to replace Portland cement. *Waste Management & Research*, 27(6), 588-594.
- Ryu, G. S., Lee, Y. B., Koh, K. T., & Chung, Y. S. (2013). The mechanical properties of fly ash-based geopolymer concrete with alkaline activators. *Construction and Building Materials*, 47(0), 409-418.
- Sabir, B., Wild, S., & Bai, J. (2001). Metakaolin and calcined clays as pozzolans for concrete: a review. *Cement & Concrete Composites*, 23(6), 441-454.
- Saeed, A., Hammons, M. I., & Petermann, J. C. (2010). Alkali-Activated Geopolymers: A Literature Review: Applied RESEARCH ASSOCIATES INC PANAMA CITY FL.
- Safiuddin, M., Abdus Salam, M., & Jumaat, M. Z. (2011a). Utilization of palm oil fuel ash in concrete: a review. *Journal of Civil Engineering and Management*, 17(2), 234-247.
- Safiuddin, M., Alengaram, U. J., Salam, M. A., Jumaat, M. Z., Jaafar, F. F., & Saad, H. (2011b). Properties of high-workability concrete with recycled concrete aggregate. *Materials Research*, 14(2), 248-255.
- Şahin, Y., & Köksal, F. (2011). The influences of matrix and steel fibre tensile strengths on the fracture energy of high-strength concrete. *Construction and Building Materials*, 25(4), 1801-1806.
- Shafiqh, P., Alengaram, U. J., Mahmud, H., & Jumaat, M. Z. (2013a). Engineering properties of oil palm shell lightweight concrete containing fly ash. *Materials and Design*, 49, 613-621.
- Shafiqh, P., Jumaat, M. Z., Mahmud, H., & Alengaram, U. J. (2013b). Oil palm shell lightweight concrete containing high volume ground granulated blast furnace slag. *Construction and Building Materials*, 40, 231-238.
- Shilstone, J. M. (1999). *The Aggregate: The most important value-adding component in concrete*. Paper presented at the Seventh Annual Symposium Austin, Texas.
- Short, A., & Kinniburgh, W. (1978). *Lightweight concrete* (3rd ed.): Applied Science Publishers London.
- Sivakumar, A., & Santhanam, M. (2007). Mechanical properties of high strength concrete reinforced with metallic and non-metallic fibres. *Cement and Concrete Composites*, 29(8), 603-608.
- Škvára, F., Jílek, T., & Kopecký, L. (2005). Geopolymer materials based on fly ash. *Ceram.-Silik*, 49(3), 195-204.
- Somna, K., Jaturapitakkul, C., Kajitvichyanukul, P., & Chindaprasirt, P. (2011). NaOH-activated ground fly ash geopolymer cured at ambient temperature. *Fuel*, 90(6), 2118-2124.

- Sumadi, S. R., & Hussin, M. W. (1995). Palm oil fuel ash (POFA) as a future partial cement replacement material in housing construction. *Journal of Ferrocement*, 25(1), 25-34.
- Sumajouw, D., Hardjito, D., Wallah, S., & Rangan, B. (2004). *Geopolymer concrete for a sustainable future*. Paper presented at the Proceedings of the second international conference on sustainable processing of minerals and metals, green processing.
- Sumajouw, M. D. J., & Rangan, B. V. (2006). Low-calcium fly ash-based geopolymer concrete: Reinforced beams and columns *Research Report GC 3*. Engineering Faculty, Curtin University of Technology, Perth, Australia.
- Tan, K. H., & Du, H. (2013). Sandless concrete with fly ash as supplementary cementing material. *Journal of Sustainable Cement-Based Materials*(ahead-of-print), 1-12.
- Tasong, W. A., Cripps, J. C., & Lynsdale, C. J. (1998). Aggregate-cement chemical interactions. *Cement and Concrete Research*, 28(7), 1037-1048.
- Van Jaarsveld, J. G. S., Van Deventer, J. S. J., & Lukey, G. C. (2002). The effect of composition and temperature on the properties of fly ash-and kaolinite-based geopolymers. *Chemical Engineering Journal*, 89(1), 63-73.
- Venkatarayanan, H. K., & Rangaraju, P. R. (2013). Decoupling the effects of chemical composition and fineness of fly ash in mitigating alkali-silica reaction. *Cement and Concrete Composites*(0).
- Wallah, S. E., & Rangan, B. V. (2006). Low-calcium fly ash-based geopolymer concrete: Long-term properties *Research Report GC 2*. Engineering Faculty, Curtin University of Technology, Perth, Australia.
- Wang, B., Han, Y., & Liu, S. (2013). Effect of highly dispersed carbon nanotubes on the flexural toughness of cement-based composites. *Construction and Building Materials*, 46(0), 8-12.
- Westerholm, M., Lagerblad, B., Silfwerbrand, J., & Forssberg, E. (2008). Influence of fine aggregate characteristics on the rheological properties of mortar. *Cement and Concrete Composites*, 30(4), 274-282.
- Wu, H.-C., & Sun, P. (2010). Effect of Mixture Compositions on Workability and Strength of Fly Ash-Based Inorganic Polymer Mortar. *ACI Materials Journal*, 107(6).
- Xu, H., & Van Deventer, J. S. J. (2000). The geopolymerisation of alumino-silicate minerals. *International Journal of Mineral Processing*, 59(3), 247-266.
- Yap, S. P., Alengaram, U. J., & Jumaat, M. Z. (2013). Enhancement of mechanical properties in polypropylene- and nylon-fibre reinforced oil palm shell concrete. *Materials and Design*, 49, 1034-1041.
- Yap, S. P., Bu, C. H., Alengaram, U. J., Mo, K. H., & Jumaat, M. Z. (2014). Flexural toughness characteristics of steel-polypropylene hybrid fibre-reinforced oil palm shell concrete. *Materials and Design*, 57, 652-659.

- Yew, M. K., Mahmud, H., Ang, B. C., & Yew, M. C. (2014). Effects of heat treatment on oil palm shell coarse aggregates for high strength lightweight concrete. *Materials and Design*, 54, 702-707.
- Yost, J. R., Radlińska, A., Ernst, S., & Salera, M. (2013). Structural behavior of alkali activated fly ash concrete. Part 1: mixture design, material properties and sample fabrication. *Materials and structures*, 46(3), 435-447.
- Yusuf, M. O., Johari, M. A. M., Ahmad, Z. A., & Maslehuudin, M. (2013). Evolution of Alkaline Activated Ground Blast Furnace-Ultrafine Palm Oil Fuel Ash Based Concrete. *Materials and Design*.
- Yusuf, M. O., Johari, M. A. M., Ahmad, Z. A., & Maslehuudin, M. (2014). Effects of addition of Al(OH)₃ on the strength of alkaline activated ground blast furnace slag-ultrafine palm oil fuel ash (AAGU) based binder. *Construction and Building Materials*, 50(0), 361-367.
- Zhang, M., & Malhotra, V. (1995). Characteristics of a thermally activated aluminosilicate pozzolanic material and its use in concrete. *Cement and Concrete Research*, 25(8), 1713-1725.
- Zhang, Z.-h., Yao, X., Zhu, H.-j., Hua, S.-d., & Chen, Y. (2009). Preparation and mechanical properties of polypropylene fiber reinforced calcined kaolin-fly ash based geopolymer. *Journal of Central South University of Technology*, 16(1), 49-52.
- Žvironaitė, J., Pundienė, I., Gaidučis, S., & Kiziniavič, V. (2012). Effect of different pozzolana on hardening process and properties of hydraulic binder based on natural anhydrite. *Journal of Civil Engineering and Management*, 18(4), 530-536.

LIST OF PUBLICATIONS

Journal articles

Bashar, I. I., Alengaram, U. J., Jumaat, M. Z., & Islam, A. (2014). The effect of variation of molarity of alkali activator and fine aggregate content on the compressive strength of the fly ash – palm oil fuel ash based geopolymer mortar. *Advances of Materials Science and Engineering* (Under review)

Islam, A., Alengaram, U. J., Jumaat, M. Z., & **Bashar, I. I.** (2014). The development of compressive strength of ground granulated blast furnace slag-palm oil fuel ash-fly ash based geopolymer mortar. *Materials and Design*, 56, 833-841. doi: <http://dx.doi.org/10.1016/j.matdes.2013.11.080> (Published)

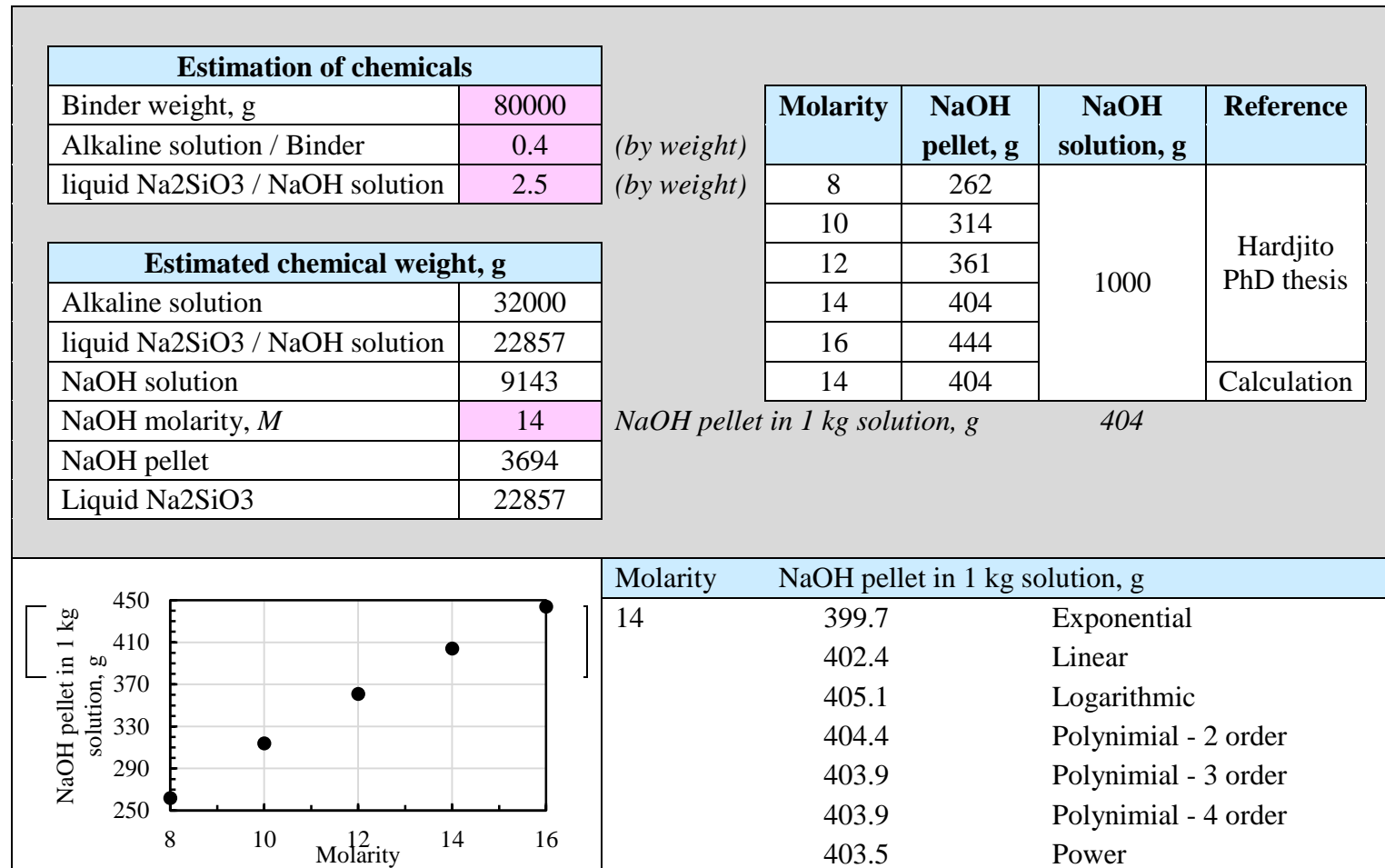
Conference papers

Bashar, I. I., Alengaram, U. J., Jumaat, M. Z., & Islam, A. (2014, 24th - 26th November 2014). The development of sustainable geopolymer mortar from fly ash-palm oil fuel ash based binder and manufactured sand. Paper will be presented at the **International Conference on Construction Materials and Structures (ICCMATS)**, Johannesburg, South Africa. (Accepted abstract)

Islam, A., Alengaram, U. J., Jumaat, M. Z., & **Bashar, I. I.** (2014, 24th - 26th November 2014). Development of structural grade geopolymer concrete using palm oil fuel ash and blast furnace slag as binders. Paper will be presented at the **International Conference on Construction Materials and Structures (ICCMATS)**, Johannesburg, South Africa.

APPENDIX A

Calculation of Alkaline solution



Calculation for Mix design 1

Material	POFA	FA	Sand	M-sand	QD	Alkaline solution	Water
Specific gravity	2.2	2.4	2.77	1.97	2.09	1.18	1
density (kg/m ³)	2200	2400	2770	1970	2090	1180	1000

Mix ID	Binder		Fine Aggregate			Alkaline solution	Water	Total
	POFA	FA	Sand	M-Sand	Q-Dust			
Proportion by weight (g)								
N100	720	720	2160	0	0	576	288	4464
N75-M25	720	720	1620	540	0	576	288	4464
N25-M75	720	720	540	1620	0	576	288	4464
M100	720	720	0	2160	0	576	288	4464
M75-Q25	720	720	0	540	1620	576	288	4464
M25-Q75	720	720	0	1620	540	576	288	4464
Q100	720	720	0	0	2160	576	288	4464
N25-Q75	720	720	540	0	1620	576	288	4464
N75-Q25	720	720	1620	0	540	576	288	4464
N50-M25-Q25	720	720	1080	540	540	576	288	4464
N25-M50-Q25	720	720	540	1080	540	576	288	4464
N25-M25-Q50	720	720	540	540	1080	576	288	4464

Mix ID	Volume	Binder		Fine Aggregate			Alkaline solution	Water	Total
		POFA	FA	Sand	M-Sand	Q-Dust			
	cm ³	Proportion by (kg/m ³)							
N100	2100	343	343	1029	0	0	274	137	2126
N75-M25	2100	343	343	771	257	0	274	137	2126
N25-M75	2100	343	343	257	771	0	274	137	2126
M100	2100	343	343	0	1029	0	274	137	2126
M75-Q25	2100	343	343	0	257	771	274	137	2126
M25-Q75	2100	343	343	0	771	257	274	137	2126
Q100	2100	343	343	0	0	1029	274	137	2126
N25-Q75	2100	343	343	257	0	771	274	137	2126
N75-Q25	2100	343	343	771	0	257	274	137	2126
N50-M25-Q25	2100	343	343	514	257	257	274	137	2126
N25-M50-Q25	2100	343	343	257	514	257	274	137	2126
N25-M25-Q50	2100	343	343	257	257	514	274	137	2126

Calculation for Mix design 2

Material	POFA	FA	MK	M-sand	COPS	Alk. Sol.	Water
S.G.	2.2	2.34	2.5	2.67	1.33	1.15	1
Density (kg/m3)	2200	2340	2500	2670	1330	1150	1000

Mixture ID	Binder			Binder			Aggregate		Alkaline solution	Water
	POFA	FA	MK	POFA	FA	MK	M-sand	COPS		
	Proportion of Binders (%)			Proportion by weight (kg)						
P10-F85-M05	10	85	5	4	34	2	45	15	16	7.2
P10-F80-M10	10	80	10	4	32	4	45	15	16	7.2
P10-F75-M15	10	75	15	4	30	6	45	15	16	7.2
P10-F70-M20	10	70	20	4	28	8	45	15	16	7.2
P10-F65-M25	10	65	25	4	26	10	45	15	16	7.2
P90-M10	90	0	10	36	-	4	45	15	16	7.2
P80-M20	80	0	20	32	-	8	45	15	16	7.2
P70-M30	70	0	30	28	-	12	45	15	16	7.2
P60-M40	60	0	40	24	-	16	45	15	16	7.2

Mixture ID	Binder			Aggregate				Water	Total
------------	--------	--	--	-----------	--	--	--	-------	-------

	POFA	FA	MK	M-sand	COPS	Alkaline solution		
	Proportion by (kg/m³)							
C 1	60	507	30	672	224	239	107	1839
C 2	60	478	60	672	224	239	107	1839
C 3	60	448	90	672	224	239	107	1839
C 4	60	418	119	672	224	239	107	1839
C 5	60	388	149	672	224	239	107	1839
C 6	537	-	60	672	224	239	107	1839
C 7	478	-	119	672	224	239	107	1839
C 8	418	-	179	672	224	239	107	1839
C 9	358	-	239	672	224	239	107	1839

Calculation for Mix design 3

Binder	1				
Aggregate	1.5	2			
14 M NaOH sol.		1	Alkaline sol./Binder	0.4	0.5
Liquid Na ₂ SiO ₃		2.5	Water/Binder	0.111	0.2

Mix ID	POFA	MK	Msand	COPS	Gravel	Steel Fibre-65/35	Steel fibre-80/60	Water	Alkamline Sol.
Proportion by weight (kg)									
OG	66.10	7.34	82.62	27.54	-	-	-	8.15	36.72
OG-65/0.25	66.10	7.34	82.62	27.54	-	2.47 (0.25%)	-	8.15	36.72
OG-80/0.25	66.10	7.34	82.62	27.54	-	-	2.47 (0.25%)	8.15	36.72
OG-65/0.5	66.10	7.34	82.62	27.54	-	4.93 (0.50%)	-	8.15	36.72
OG-80/0.5	66.10	7.34	82.62	27.54	-	-	4.93 (0.50%)	8.15	36.72
OG-65/0.75	66.10	7.34	82.62	27.54	-	7.40 (0.75%)	-	8.15	36.72
OG-80/0.75	66.10	7.34	82.62	27.54	-	-	7.40 (0.75%)	8.15	36.72
GG	61.20	6.80	45.33	-	90.67	-	-	13.60	27.20
GG-65/0.5	61.20	6.80	45.33	-	90.67	4.73 (0.50%)	-	13.60	27.20
GG-80/0.5	61.20	6.80	45.33	-	90.67	-	4.73 (0.50%)	13.60	27.20

Mix ID	POFA	MK	Msand	COPS	Gravel	Steel Fibre- 65/35	Steel fibre- 80/60	Water	Alkamline Sol.
Proportion by weight (kg/m³)									
OG	529	59	662	221	-	-	-	65	294
OG-65/0.25	528	59	660	220	-	19.75	-	65	293
OG-80/0.25	528	59	660	220	-	-	19.75	65	293
OG-65/0.5	527	59	658	219	-	39.50	-	65	293
OG-80/0.5	527	59	658	219	-	-	39.50	65	293
OG-65/0.75	525	58	657	219	-	59.25	-	65	292
OG-80/0.75	525	58	657	219	-	-	59.25	65	292
GG	512	57	379	-	758	-	-	114	227
GG-65/0.5	512	57	379	-	758	39.50	-	113	226
GG-80/0.5	512	57	379	-	758	-	39.50	113	226

APPENDIX B



Photo B.1: Palm oil bunch



Photo B.2: Palm oil fibre and shell before burning



Photo B.3: Processing of separating shell



Photo B.4: Collection of POFA



Photo B.5: Preparation of NaOH solution for trial

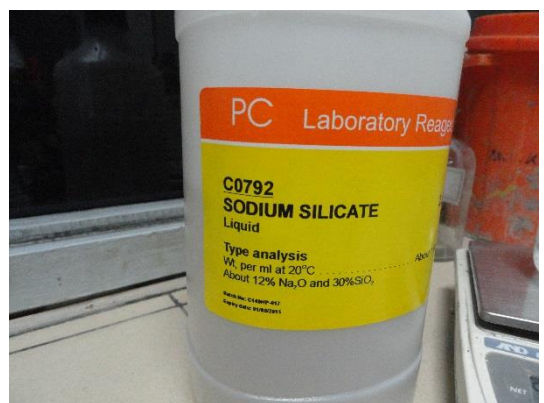


Photo B.6: Liquid sodium silicate



Photo B.7: Curing oven



Photo B.8: Liquid sodium silicate



Photo B.9: Outer surface of OPS



Photo B.10: Inner surface of OPS



Photo B.11: Broken prisms after flexure test



Photo B.12: Broken cylinder after splitting test



Photo B.13: Preparation of moulds for casting



Photo B.14: OPSGC for casting



Photo B.15: Casting completed, specimen after vibration



Photo B.16: Preparation for fracture test



Photo B.17: Arrangement of fracture test